UNIVERSITY OF SOUTH ALABAMA

ALDOT Research Project 930-917

Verification of WBUZPILE Design Methodology and the Development of a LRFD Driven Pile Resistance Factor Calibration for Alabama Soils

A Final Report Submitted by:

Eric J. Steward, Ph. D.
John Cleary, Ph.D.
Associate Professors, Department of Civil Engineering
University of South Alabama
Mobile, AL 36688
esteward@southalabama.edu or cleary@southalabama.edu
251-460-6174

Co-Authored by Graduate Students:
Axel Arnold Yarahuaman Chamorro
Benjamin John Pement

May 2020

SOUTH ALABAMA JAGUARS

DISCLAIMER

The contents of this report reflect the views of the authors who are responsible for the facts and accuracy of the data herein. The contents do not necessarily reflect the official views or policies of the Alabama DOT or The University of South Alabama. This report does not constitute a standard, specification, or regulation. Comments contained in this paper related to the specific testing equipment and materials should not be considered an endorsement of any commercial product or service, no such endorsement is tended or implied.

TABLE OF CONTENTS

Page

LIST OF TABLES

Page

LIST OF FIGURES

Page

LIST OF SYMBOLS

cdf, CDF =	Cumulative Distribution Function
COV_Q =	Coefficient of variation of loads or coefficient of variation of the bias values for the loads.
COV_{QD} =	Coefficient of variation of dead load or coefficient of variation of the bias values for the dead load.
COV_{QL} =	Coefficient of variation of live load or coefficient of variation of the bias values for the live load.
COV_R =	Coefficient of variation of the resistance or coefficient of variation of the bias values for the resistance.
COV_x =	Coefficient of variation of loads or coefficient of variation of random variable X.
$E[Q]$ =	Expected value of the load random variable
$E[Q_N]$ =	Expected equivalent normal random variable for the load.
$E[R]$ =	Expected value of the resistance random variable
$E[R_N]$ =	Expected equivalent normal random variable for the resistance.
$F_x(X)$ =	Cumulative Distribution Function of the normal random variable X.
$f_x(X)$ =	Probability Distribution Function of the normal random variable X.
F_z =	Cumulative Distribution Function of the standard normal random variable Z.
f_z =	Probability Distribution Function of the standard normal random variable Z.
G =	Limit state equation function
g_i =	Limit state function of value i

n = Number of failures

N = Number of simulations for Monte Carlo simulation.

$NORMSINV$ = A Microsoft Excel function that returns the inverse of the standard normal distribution.

n_σ = Constant representing the number of standard deviations from the mean needed to obtain the desired probability of exceedance.

pdf, PDF = Probability Distribution Function

$P_{f\,true}$ = True probability of failure

P_f: = Probability of failure

q^* = Trial Load standard normal space design point

Q = Load random variable

q = Standard normal space design point for the load

Qc = Cone penetration Bearing Resistance

q_D = Predicted (nominal) value of dead load.

QD_i, $\lambda_{QD,i}$ = Simulated dead load value i

Q_i, $\lambda_{Q,I}$ = Simulated load value i

q_L = Predicted (nominal) value of live load.

QL_i, $\lambda_{QL,I}$ = Simulated live load value i

Q_n = Nominal load.

r^* = Trial Resistance standard normal space design point

R = Resistance random variable

r = Standard normal space design point for the resistance.

R_{EOID} = Nominal EOID resistance.

R_i, $\lambda_{R,I}$ = Simulated resistance value i

r_n, R_n = Nominal resistance

R_{setup} = Nominal setup resistance increase

V_p = Coefficient of variation of the estimated probability established

x, X = Random variable X

z, Z = Standard normal random variable Z

$Z_{i\text{-}Q}$ = The value of the standard normal variable corresponding to the i'th value of the load random variable.

$Z_{i\text{-}QD}$ = The value of the standard normal variable corresponding to the i'th value of the dead load random variable.

$Z_{i\text{-}QL}$ = The value of the standard normal variable corresponding to the i'th value of the live load random variable.

$Z_{i\text{-}R}$ = The value of the standard normal variable corresponding to the i'th value of the resistance random variable.

β = Reliability index

β_T = Target reliability index.

γ_{avg} = Average load factor

γ_Q = Load factor for loads.

γ_{QD} = Load factor for dead load.

γ_{QL} = Load factor for live load.

η = Dead-to-live ratio (Q_D/Q_L)

λ_Q = Normal mean of the bias values for the loads.

λ_{QD} = Normal mean of the bias values for the dead load.

λ_{QL} = Normal mean of the bias values for the live load.

λ_R = Normal mean of the bias values for the resistance.

$\mu_{ln\text{-}Q}$ = Lognormal mean of loads

$\mu_{ln\text{-}QD}$ = Lognormal mean of dead load

$\mu_{ln\text{-}QL}$ = Lognormal mean of live load

$\mu_{ln\text{-}R}$ = Lognormal mean of dead load

μ_X = Normal mean of population random variable X.

$\widehat{\mu_X}$ = Normal mean of sample random variable X.

$\sigma_{ln\text{-}Q}$ = Lognormal standard deviation of loads

$\sigma_{ln\text{-}QD}$ = Lognormal standard deviation of dead load

$\sigma_{ln\text{-}QL}$ = Lognormal standard deviation of live load

$\sigma_{ln\text{-}R}$ = Lognormal standard deviation of resistance

$\sigma_{ln\text{-}x}$ = Lognormal standard deviation of the random variable X.

σ_Q = Standard deviation for the load Q or the measured load $Q_{measured}$.

σ_{QN} = The normal standard deviation for the load Q.

σ_R = Standard deviation for the resistance R or the measured resistance $R_{measured}$.

σ_{RN} = The normal standard deviation for the resistance R.

$\sigma_{\lambda D}$ = Standard deviation of the dead load dataset.

$\sigma_{\lambda L}$ = Standard deviation of the live load dataset.

$\sigma_{\lambda R}$ = Standard deviation of the resistance dataset.

σ_X = Standard deviation value of population random variable X.

$\widehat{\sigma_X}$ = Standard deviation value of sample random variable X.

$\Phi(X)$ = Cumulative Distribution Function of the random variable X.

$\phi(X)$ = Probability Distribution Function of the random variable X.

ϕ_{EOID} = Resistance Factor for EOID nominal resistance

$\phi_{R,}\phi$ = Resistance Factor

ϕ_R/λ = Bias Efficiency factor

ϕ_{setup} = Resistance Factor for setup nominal resistance.

ABSTRACT

In 2007, the American Association of State Highway and Transportation Officials published a new policy requiring the application of the Load and Resistance Factor Design (LRFD) methodology for pile foundations. The Alabama Department of Transportation (ALDOT) currently uses LRFD, however, the LRFD resistance factor used is not based on reliability theory and does not necessarily represent the Alabama soils. A pair of authors calibrated LRFD resistance factors for Alabama soils using First Order Second Moment (FOSM). However, FOSM leads to over-conservatism. Thus, this study calibrated LRFD resistance factors using the First Order Reliability Method and Monte Carlo Simulation (MCS) besides FOSM. MCS was found to be the most efficient method. Moreover, pile setup was incorporated into the LRFD resistance factor calibration and generated a reasonable increase on the resistance factors at 30, 45, 60, and 90 days after the end of initial driving. Finally, the calibrated resistance factors are compared to similar resistance factors calibrated within the United States to evaluate the performance of the prediction methods used in Alabama. The results generate a variety of reliability-based resistance factors that are recommended for use depending on the standard ALDOT design methodology and the field test procedures used.

CHAPTER I – INTRODUCTION

1.1 Research Objectives

Pile foundations are used extensively as support for high-rise buildings, bridges and other heavy structures, and to safely transfer the structural loads and moments to the ground. Piles are also used to avoid excess settlement or lateral movement. The most common type of piles utilized in the state of Alabama are driven piles. Piles are designed to carry the structural loads and maintain construction costs as low as possible at the same time. Nevertheless, the design of pile foundations involves a significant number of uncertainties which can be translated generally to over-conservatism. One way to decrease the construction costs is to develop more accurate prediction methods through static analysis methods, design programs, dynamic analysis methods, and pile setup consideration. If the anticipated pile resistance is more accurately estimated before its driving, pile lengths and sizes can be reduced and, hence, cost savings are achieved. Therefore, it is clear that managing uncertainty is largely important to use resources, time, and money efficiently.

The basic pile design starts with static analysis methods or design programs. Both are related since design programs incorporate one or more static analysis methods to estimate the pile capacity. The static analysis methods allow engineers to estimate the pile length and pile size prior to installation. Several static analysis methods are available and each one of them has specific applications, limitations, and soil parameters required. In the same way, several design programs have become more popular due to their time efficiency. The federal government developed its own design program DRIVEN through the Federal Highway Administration. On the other hand, Alabama also developed a design program called WBUZPILE to be applied for pile designing in Alabama soils.

Once the pile length, pile size, and nominal resistance are estimated through static analysis methods or design programs, the designs are confirmed during construction by

field control determination tests or methods. The most accurate method to verify the pile capacity is through static load testing. Static load tests consist of loading the pile using a load cell attached to a reaction system that keeps the load cell fixed. The load increases gradually until failure. Another method to verify or revise design is through dynamic load testing based on dynamic analysis and wave propagation theory. Dynamic tests consist of a hammer hitting the head of a pile during and after installation. The compression wave data during hammer blows is obtained and processed through a Pile Driving Analyzer (PDA*),* which can incorporate signal matching (iCAP or CAPWAP). Dynamic load testing can be considered as an economically efficient method to determine the capacity of a pile compared to the significant cost of static load testing.

Another aspect of design capable of producing cost-savings for pile design is the phenomenon named pile setup, which consists of a pile resistance or capacity increase over some time interval after installation. When the pile is being driven, the surrounding soil is disturbed and losses strength. Once the installation has finished, the same soil starts a process to attempt to recover lost strength, which contributes to an increase in the pile capacity. If the pile capacity increase is accurately anticipated, the pile length, sizes and quantity can be decreased, hence lower costs would be required. Pile setup capacity increase can be measured immediately or some time interval after installation through dynamic load tests. Several prediction models to predict this capacity increase are available, but the most popular is the Skov and Denver [1] model.

Driven piles have been designed following the Allowable Stress Design (ASD) methodology for years. ASD represents the construction uncertainties and safety margin typically through a single factor of safety (FS). For ASD, the pile capacity is reduced by dividing the nominal pile capacity by the FS. Nonetheless, the limitations of ASD were recognized in the 1990s [2]. Consequently, an alternative design methodology known as Load and Resistance Factor Design (LRFD) has been developed since the mid-1980 [3] and is becoming more popular due its reliability basis. For LRFD, loads and resistance have different sources and levels of uncertainty. Thus, each one (loads and resistances) is modified by partial factors. The loads are affected by load factors that are larger or equal to 1. The resistance is affected by resistance factors that are smaller or equal to 1. In other

words, if LRFD is employed, the loads are amplified while the resistance is underestimated. In this way, LRFD generates a design with more consistency and uniform level of safety [2]. Consequently, more economically efficient and repeatable designs are possible compared to ASD methodology [3].

Under LRFD, the resistance is reduced by multiplying the nominal capacity by a resistance factor (ϕ). This resistance factor can be lower or equal to 1 and can be calibrated for a specified regional soil if enough statistical data is available. The calibration depends on significant data sizes and is based on probability theory. The most widely probability-based methods used to calibrate a resistance factor are the First Order Second Method (FOSM), the First Order Reliability Method (FORM), and Monte Carlo Simulation (MCS). The three methods require a resistance bias factor (λ_R) obtained from the ratio between a set of measured capacity data and a set of predicted capacity data. The measured capacity is obtained from field test such as dynamic and static load testing, while the predicted capacity is obtained from static analysis method or design programs.

Over some decades ago, several efforts have been made to implement and develop LRFD resistance factors for deep foundations for bridges. Nonetheless, the transition has been relatively slow [4] due to the large quantity and quality of data required, as well as deficiencies included in the early development of LRFD specifications. The American Association of State Highway and Transportation Officials (AASHTO) and the Federal Highway Administration (FHWA) published a policy that turned into an obligation for the usage of LRFD for all new bridges initiated after October 1st, 2007. Therefore, AASHTO also provided some recommended resistance factors for various design methods along with the policy. Nevertheless, several Departments of Transportation (DOTs) expressed their concern about the accuracy and over-conservatism of these resistance factors when applied to specific regions [3]. Consequently, AASHTO and FHWA allowed the state Department of Transportations to develop their regionally calibrated LRFD resistance factors for bridge foundations using statistical and reliability theory using existing databases. Since then, several DOTs started working on the composition of adequate databases and the development of their own LRFD resistance

factors to eliminate over-conservative designs and generate cost savings to the state and taxpayers.

While states such as Florida, Illinois, Louisiana, Wisconsin, Iowa, and Arkansas have published studies where LRFD resistance factors are recommended to be used for bridge foundations within their respective states, Alabama is still transitioning from ASD to LRFD. Currently, there are two studies about region-specific resistance factors for Alabama, Prado [5] and Pement [2]. However, both studies calibrated the LRFD resistance factors using only FOSM and not FORM or MCS. Studies conducted by NCHRP 507 [6], Styler [7], Haque and Abu-Farsakh [8] revealed that FOSM tends to lead to some over-conservatism. For instance, NCHRP 507 [6] found that FOSM provides resistance factors 10% lower than FORM. Moreover, Styler [7] contends that FORM resistance factors tend to be 8%-23% larger than FOSM resistance factors. Also, Allen et al. [9] suggests that MCS is more adaptable and rigorous method than FOSM and provides resistance factors consistent with FORM. Consequently, the main objective of this study is to develop LRFD resistance factors unique to Alabama soils using FOSM, FORM, and MCS, in order to enhance accuracy and efficiency of pile design. Through this calibration, the reliability, consistency and efficiency of WBUZPILE and DRIVEN are evaluated. The second objective is to evaluate the performance of WBUZPILE and DRIVEN for pile design according to the relationships of the predicted capacity and the measured capacity. The third objective is to evaluate the performance of the Skov and Denver model for Alabama soils. The fourth objective is to evaluate the effect of pile setup on the calibrated LRFD resistance factors. Finally, the fifth objective is to compare the calibrated resistance factors with the recommended resistance factors from published studies from the federal government and other states in terms of reliability, consistency and efficiency.

CHAPTER II - LITERATURE REVIEW

This chapter attempts to describe and explain the basic concepts applied to the subsequent chapters of this study. The main conceptual sections included are (1) driven piles, (2) basic pile design, (3) Allowable Stress Design methodology, (4) Load and Resistance Factor Design methodology, (5) pile load testing, and (6) pile setup. Some sentences, tables, figures, graphs, and equations will be referenced in the following chapters of the study.

2.1 Driven Piles

The first problem for a foundation designer is to establish whether the soil conditions are suitable to support the structure using shallow foundations or deep foundations (such us piles). Vesic [10] says *that piles are used where upper soil strata are compressible or weak; where footings cannot transmit inclined, horizontal, or uplift forces; where scour is likely to occur; where future excavation may be adjacent to the structure; and where expansive collapsible soils extend for a considerable depth*. The Federal Highway Administration (FHWA) [11] adds that pile foundations are used extensively to support buildings, bridges, and other heavy structures, to safely transfer structural loads to the ground, and to avoid excess settlement or lateral movement. According to Pement [2], driven piles and drilled shaft are the most common deep foundations. Nevertheless, driven piles are more widely implemented in the state of Alabama.

Driven piles can be installed by impact driving or vibrating. There are two types of driven piles: End-bearing piles and friction piles. On one hand, End-bearing piles resist loads through the interaction of the cross-sectional area of its tip and the hard layer beneath. Although a minimal friction resistance is developed, this is usually ignored. On the other hand, friction piles resist loads through the interaction and friction of the perimetrical pile area and the soil around it. When bedrock is not encountered at a

reasonable depth below the ground surface, piles can resist loads through both end-bearing and frictional resistance for economic efficiency [2].

2.2 Basic pile design

One of the most important challenges for foundation engineering, especially for pile design, is to develop a safe and cost-effective foundation system. National committees such us Federal Highway Administration (FHWA), American Concrete Institute (ACI), American Institute of Steel Construction (AISC), and the American Association of State Highway and Transportation officials (AASHTO) are deeply involved in the updating of design requirements. However, in the geotechnical field, several variables affect the soil conditions and its interaction with a structure. Therefore, *the soil conditions can be estimated, but cannot be determined with complete accuracy* [2]. Generally, the required capacity and depth shall be estimated before driving the pile,. Thus, it is vital to predict the amount of nominal resistance of the pile with a reasonable accuracy despite the complex nature of the soils. This prediction or design can be performed through static analysis or design programs, which can implement several design methods.

2.2.1 Static Analysis methods

The most basic way to estimate the nominal capacity of the pile is through static analysis methods. FHWA [13] indicates that static analysis methods assume the pile as a geomaterial and are used to estimate required pile length for a given nominal resistance in the contract documents. Many methods of estimating pile lengths and axial capacity of driven piles have been developed based on the types of soils encountered by the pile. Once the pile lengths and nominal resistances are estimated, they are confirmed during construction by field control determination tests or methods. Each method has specific a application, limitations, and required soil parameters. Table 1 compares the static analysis

methods presented in AASHTO [14] design specifications and GEC-12 [13] manual, where shaded methods are the ones that are present in both documents.

Table 1: Summary of Static Analysis Methods in GEC-12 and AASHTO (2014) for Determination of Nominal Resistance.

Analysis method	Soil Type	Soil Information Required	Presented in GEC-12	Presented in 2014 AASHTO code
Meyerhof (1976)	Cohesionless	SPT N	No	Yes
Nordlund (1963)	Cohesionless	ϕ'	Yes	Yes
α-method	Cohesive	S_u	Yes	Yes
β-method (1951) (1979) *	Cohesive	S_u	No	Yes
λ-method (1972)	Cohesive	S_u	No	Yes
API RP2A (1993)	Mixed	S_u, ϕ'	Yes	No
β-method (1991) **	Mixed	ϕ'	Yes	No
Brown (2001)	Mixed	SPT N	Yes	No
Elsami & Fellenius (1997)	Mixed	CPTu	Yes	No
Schmertmann (1975)	Mixed	CPT	Yes	Yes

Notes:

ϕ' = effective stress friction angle.
S_u = Undrained shear strength.
SPT = Standard penetration test.
CPT = Cone penetration test.
* = β-method in AASHTO is based on Skempton (1951) and Ersig and Kirby (1979).
** = β-method in GEC-12 is based on Fellenius (1991)

FHWA [13] recommends the use of the Nordlund method for cohesionless soils, and the α-method for cohesive soils, and the API method for large diameter pipe piles. However, FHWA [13] also states that *regional geologic settings or construction control techniques may offer unique conditions not accounted for in these provided methods, therefore reliability calibrations for design methods and resistance factors are encouraged, and may supersede the presented guidelines herein if justified*.

2.2.2 Software Program Analysis.

Due to its time efficiency, software program analysis is becoming more popular for engineering purposes. As indicated by Pement [2], Software Program Analysis are mainly used for axial loaded single piles or pile groups. These programs can include one or several static analysis design methods. Also, they incorporate different soil layers, soil types, soil characteristics, which are used to estimate the pile capacity according to a specific depth. Table 2 summarizes some of the available commercial programs including the static analysis programs that they are based on.

Table 2: Summary of Computer Analysis Software for Axial Single Pile Analysis (FHWA, 2016).

Computer Program	Static Analysis Methods In Program	Method Presented in GEC-12 (2016)	Method Presented in AASHTO 7th edition (2014)
AllPile	Navfac DM-7	No	No
A-Pile	API-RP2A	Yes	No
A-Pile	US Army COE	No	No
A-Pile	FHWA (Alpha / Nordlund)	Yes	Yes
A-Pile	Lambda Method	No	Yes
A-Pile	NGI (CPT)	No	No
A-Pile	ICP (CPT)	No	No
DrivenPiles	Alpha Method	Yes	Yes
DrivenPiles	Nordlund Method	Yes	Yes
FB-Deep	FDOT SPT Method	No	No
FB-Deep	Schmertmann (CPT)	Yes	Yes
FB-Deep	UF (CPT)	No	No
FB-Deep	LCPC (CPT)	No	No
Unipile	Alpha Method	Yes	Yes
Unipile	Beta Method	Yes	Yes, but differs
Unipile	Elsame and Fellenious (CPT)	Yes	No
Unipile	Schmertmann (CPT)	Yes	Yes
Unipile	LCPC (CPT)	No	No
Unipile	Meyerhof (SPT)	No	Yes

It should be noted that the software "DrivenPiles" shown in table 2 is an updated version of the software DRIVEN, which will be explained in the following sections. In addition, Alabama Department of Transportation (ALDOT) developed a software named WBUZPILE for pile design in soils within the state of Alabama. This software is also explained in the following sections.

2.2.2.1 WBUZPILE software.

ALDOT uses the program WBUZPILE for pile design. This software was developed in the 1980s and as a result of field and test data from piles driven in coastal Mobile County over several years of experience [15]. The program allows the user to input variables such as soil description, the ground elevation, pile type, pile tip elevation, groundwater elevation, soil classification (sand or clay), strata thickness, and SPT blow count numbers for each soil strata [2], as well as to choose between a ASD or LRFD design methodology. WBUZPILE uses empirical equations following four soil models: Silt, Sand, Clay, and Weathered Rock.

For silt soils, by using D50, WBUZPILE converts the SPT-N values to the CPT bearing resistance (q_c) according to the correlation presented by Kulhawy and Mayne [16]. Then, the friction ratio (R_f)(%) and adhesion are calculated using the following equations:

$$R_f(\%) = [\ln(q_c) - 2.58]/0.742 \text{ (For sandy silt)}, \quad (1)$$

$$R_f(\%) = [\ln(q_c) - 1.894]/0.547 \text{ (For clavey silt)}, \quad (2)$$

$$R_f(\%) = [\ln(q_c) - 0.817]/0.36 \text{ (For silty clay), and} \quad (3)$$

$$Adhesion = R_f * q_c \quad (4)$$

where q_c is the pile bearing resistance. In addition, WBUZPILE uses the Caquot's relationship [17] to calculate the silt effective angle of internal friction [18]. The pile resistance can be calculated as follows:

$$Pile\ tip\ (base) resistance = q_c * Area_{pile\ tip}, \quad (5)$$

For sand, WBUZPILE uses the following empirical equations:

$$Fricition\ angle\ (\varphi) = 27.9877 + (0.0951663 * N) + (0.0137846 * N^2) - (0.000354596 * N^3) + (0.00000290751 * N^4), \quad (6)$$

$$Bearing\ factor = 76103.3 - 11496.7 * \phi + 691.929 * \varphi^2 - 20.7312 * \varphi^3 + 0.309012 * \varphi^4 - 0.00183079 * \varphi^5 \quad (7)$$

For clay, WBUZPILE uses the following empirical equations:

$$Cohesion\ (C) = 125 * N\ (psf) (\text{if N} < 100), \quad (8)$$

$$Cohesion\ (C) = 0.375 * 144 * N\ (psf) (\text{if N} > 100), \quad (9)$$

$$Bearing\ factor = 9 * C\ (psf) \quad (10)$$

Finally, for weathered Rock, WBUZPILE uses equations developed by O'Neill and Reese [19]:

$$Bearing\ factor = 0.59 * (N_{60})^{0.8} \overline{\sigma_{vo}}\ (psf), \quad (11)$$

where N_{60} is the N corrected for the Hammer efficiency, and $\overline{\sigma_{vo}}$ is the effective stress at the pile tip.

As a result, the software provides the nominal pile capacity per linear foot of pile [2]. The shaft resistance typically shows a linear increase while the tip resistance remains constant along the corresponding strata. Some concerns have been raised about the reliability accuracy, and limitations of WBUZPILE since it uses fully empirical equations and does not consider conventional static analysis methods [2]. Consequently, ALDOT is currently using it just for sand and clay models.

2.2.2.2 DRIVEN software.

DRIVEN is a software program used developed by the federal government and has been used by some DOTs for decades. According to Pement [2], the FHWA developed DRIVEN in 1998 for static pile capacity calculation in either SI or imperial units. DRIVEN allows the user to consider open and closed end pipe piles, H-piles, circular or square solid concrete piles, timber piles, and monotube piles. The user inputs the soil profile based on strength parameters, strength loss during driving, and unit weights. Basically, DRIVEN uses the Nordlund method for cohesionless soils, and the α-method for cohesive soils [2].

For cohesionless soils, *the Nordlund method is mostly influenced by the soil friction angle, which is an indicator of the soil shear strength* [2]. Moreover, the Nordlund method considers factors such as pile tapering, soil displacement, different grades of soil-pile friction (for different pile materials) and it is based on results of load tests in cohesionless soils [20]. In the same way as WBUZPILE, DRIVEN estimates soil properties for cohesionless soil layers using SPT data.

For cohesive soils, DRIVEN requires cohesion and adhesion values for each layer. Nevertheless, DRIVEN is also capable of estimating the cohesion based on SPT data, if available. It should be noted that *the adhesion factor is dependent upon the strength and nature of the clay, pile dimension, method of installation, and time effects* [2]. In addition, DRIVEN allows the user to consider five different adhesion factors for each cohesive soil stratum, including a general adhesion value for cohesive soils and customized adhesion values [2].

As output, DRIVEN generates results of pile capacity versus pile depth for the whole soil profile. Furthermore, for cohesive and cohesionless soils, the software considers the effects of soft compressible soils, pile plugging, and potential scour [2]. As stated before, DRIVEN has recently been updated to a windows-based, commercially available program called “DrivenPiles”.

2.3 Allowable Stress Design (ASD) method

ASD design methodology has been used for decades in the Geotechnical engineering field as a way to incorporate uncertainties into a design. This method consists of utilizing a limit equilibrium analysis by keeping the anticipated loads lower than the capacity or resistances. In ASD, the uncertainties in the loads and resistances are expressed in an incorporated value named “Factor of Safety” (FS). Pement [2] suggests that the uncertainties from a design method are most likely due to (1) *variability of engineering properties and load predictions*, (2) *errors in measuring material resistance*, (3) *errors in*

prediction models used, and (4) *sufficiency and applicability of sampling and testing methods*. The ASD design equation used is the following:

$$\frac{R_n}{FS} \geq \sum Q_i \tag{12}$$

where R_n is the nominal resistance (capacity), *FS* is the Factor of Safety, and $\sum Q_i$ is the sum of load effects (dead, live, and environmental) applied on a pile [21]. Nevertheless, ASD is becoming less popular due to the following limitations. (1) The Factor of Safety (FS) is a subjective value that is not based of probability of failure. The FS just depends on the design models and material parameters selected [2]. (2) ASD assumes similar uncertainties for load and resistance variables. (3) ASD is based only on experience and engineering judgment, which can lead to over conservatism [20]. Even though several sources of uncertainties can be considered by the designer when using ASD, their consideration is mainly qualitative rather than quantitative [21].

Figure 1 shows the way ASD reduces the probability of failure when probability density functions are evaluated. Failure is defined as loads exceeding the resistance, which graphically represented by the area formed by the load curve overlapping the resistance curve. The graph on the left shows when load and resistance are unmodified, hence, they are similar theoretically. The graph on the right shows when the resistance has been modified by the FS. The displacement of the resistance probability density function curve, due to the FS, reduces the probability of failure by decreasing the overlapped area. The new failure area is represented in orange color.

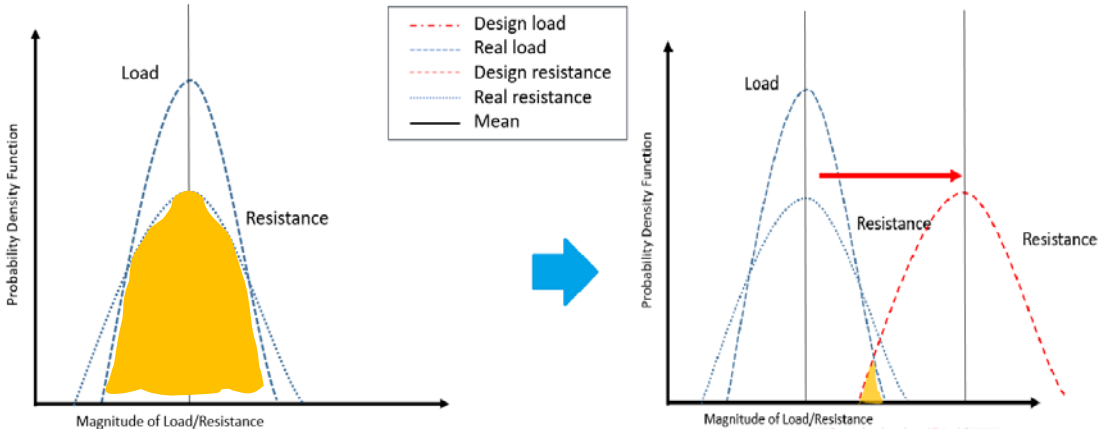

Figure 1: Probability density function for load and resistance when ASD is used (Cleary, 2019).

When designing driven piles, ALDOT has followed an Allowable Stress Design (ASD) methodology and divides the resistance by a Factor of Safety (FS) of 2 and check if the loads are smaller than the allowable resistance.

2.4 Load and Resistance Factor Design (LRFD) method

Load and Resistance Factor Design (LRFD) is an alternative design methodology specifically and progressively developed for bridges since the mid-1980s [3]. LRFD originated due to the limitations of ASD methodology recognized in the 1990s [2]. Moreover, AASHTO required the LRFD method to design deep foundations supporting bridges in 2007. The LRFD design equation is the following:

$$\phi R_n \geq \sum \gamma_i Q_i, \tag{13}$$

where ϕ is the resistance factor, R_n is the nominal resistance or capacity, γ_i is the load factor, Q_i is the nominal load value.

Under LRFD, both loads and resistance have different sources and levels of uncertainty. These uncertainties can be quantified using probability-based procedures to satisfy engineered design with consistent and specific levels of reliability. Paikowsky et al. [6] says that *The principal difference between Reliability Based Design and the traditional or partial factors of safety design approaches lies in the application of reliability theory, which allows uncertainties to be quantified and manipulated consistently in a manner that is free from self-contradiction*. In other words, the implementation of LRFD allows the separation of uncertainties from loads and resistances and, then, to use methods based on probability theory to satisfy a prescribed margin of safety [6]. It should be noted that since loads are better known than resistances, the load effect usually has smaller variability than the resistance effect.

Figure 2 shows the way LRFD reduces the probability of failure when probability density functions are evaluated. Failure is defined as loads exceeding the resistance. This failure is graphically translated to point where the load curve overlaps the resistance curve. The graph on the left shows when load and resistance are unmodified, hence, they are similar theoretically. The graph on the right shows when the loads have been factored (increased) by the load factors and the resistance has been factored (decreased) by the resistance factor. The displacement of the load and resistance probability density function curve to opposite directions reduces the probability of failure by decreasing the overlapped area. The new failure area is represented in orange color.

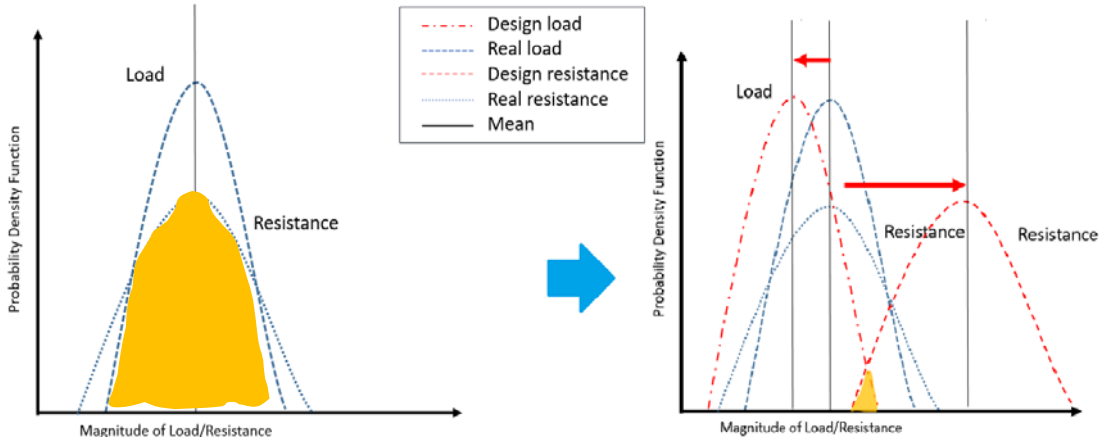

Figure 2: Probability density function for load and resistance when LRFD is used (Cleary, 2019).

As mentioned by Paikowsky et al [6], some of the specific benefits of implementing LRFD for pile design include the following:

- Cost savings and improved reliability due to more efficiently balanced design.
- More rational and rigorous treatment of uncertainties in the design.
- Enhanced perspective on the overall design and construction processes.
- Development of probability-based design method capable of stimulating advances in pile analysis and design.
- Conversion of the codes into living and easier to revise documents.
- The factors of safety previously used provide a framework to extrapolate existing design procedures into newer foundation concepts and materials.

As mentioned before, ALDOT has used ASD design methodology with a FS of 2. Recently, ALDOT has begun to design using LRFD methods as Ashour et al [14] suggests using a resistance factor ϕ of 0.71 obtained by calibration by fitting FS.

2.5 Pile Axial Load Testing

Load testing is the most accurate way to determine the nominal capacity of a pile [23]. Due to the high uncertainty of soils involve, it is imperative to perform actual load tests before or during construction to verify the preliminary design. The load tests are best known as field control methods. AASHTO states that when axial nominal resistance is determined by using actual load testing, the uncertainty in the axial nominal resistance is solely due to the reliability of the field determination method. They are mainly classified in two axial field control methods: Dynamic Load Test (DLT) and Static Load Test (SLT).

2.5.1 Static Load Test.

Static Load Test is the most accurate method to determine the pile load capacity. FHWA [24] says that *depending upon the size of the project and other project variables, static load tests may be performed either during the design stage or construction stage*. Usually, a SLT is performed inside or close to the site of the final pile installation. Once a pile is installed, a waiting period is required before the pile can be tested. ALDOT states that the waiting period shall be no less than 36 hours after EOID for H-Piles, and no less than 7 days for concrete piles [24]. This waiting period allows the disturbed soil to return to a more stable condition.

The axial Static Load Test is regulated by ASTM D 1143-07 [27]. A system of reaction beams is attached to the load cell to assure minimum displacement as shown in Figure 3. Generally, the reaction beams are connected to reaction piles. ASTM D 1143-07 [25] mentions several loading methods. However, the Quick Maintained (QM) Testing Method is the fastest and most efficient when determining the pile capacity [22]. In this method, the load is applied in increments of 5% of the anticipated nominal resistance. Load can be incremented until pile failure. The load gradient shall be composed by at least 20 points before reaching the geotechnical nominal resistance in order to generate a load-displacement curve [2]. The test shall not last more than one hour as cited by

Hannigan et al [19]. Once the load-displacement curve is plotted, several determination methods or acceptance criteria can be performed, such as the Davisson's Methods, the Shape of Curvature Methods, the Limited Total Settlement Method, the De Beer's Method, the Chin's methods, and the Iowa DOT method. However, the Davisson's Criterion is the most popular method and works better with QM test data [26].

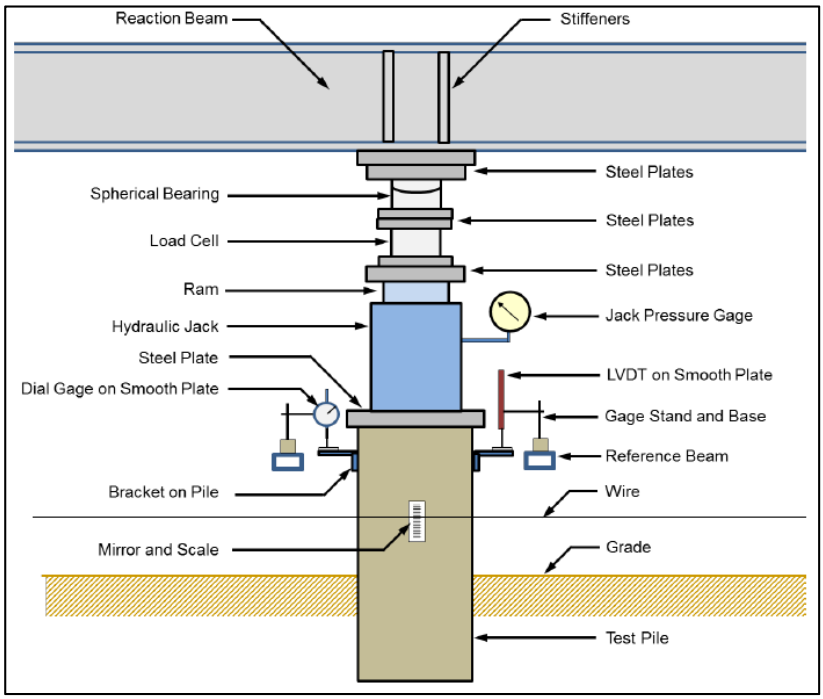

Figure 3: Static load test diagram (FHWA, 2016)

The Davisson method is used to determine the load at which the pile fails and is based on the deformation of the pile head. The Davisson method uses a drawn line parallel to the elastic compression line (base line), which is offset by a specified amount of displacement depending on the pile size [22]. The parallel line is known as Offset Limit Line or Davisson Line. As shown on figure 4, the point of intersection between the Offset Limit Line and the load-displacement curve is considered to the pile nominal capacity.

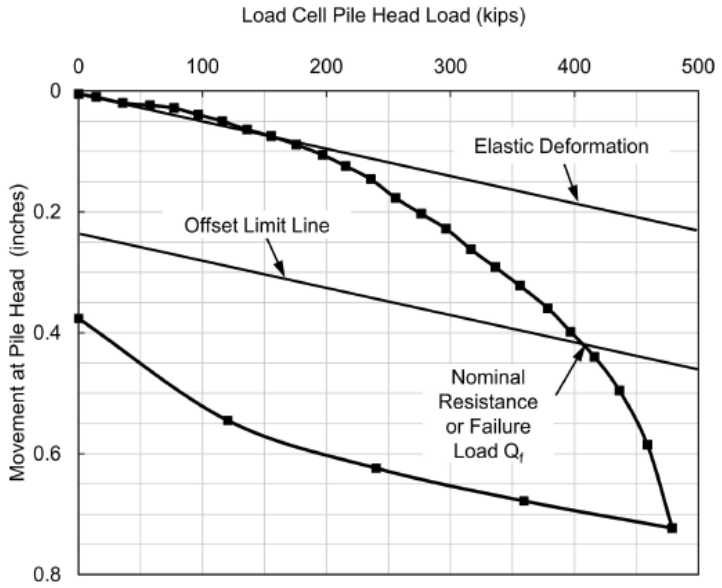

Figure 4: Load-Displacement Curve and The Davisson offset method (Hannigan et al, 2016)

The Elastic Deformation Line or Base Line can be plotted considering the following equation:

$$\Delta = \frac{Q_{va}L}{AE}, \tag{14}$$

where Δ is the elastic movement of the base line, Q_{va} is the applied load, A is the cross sectional are of the pile, E is the modulus of elasticity of the pile material, and L is the embedded length of the pile. In addition, to draw the Offset Limit Line or Davisson Line, the following expression can be used:

$$X = 0.15 + \frac{D}{120}, \tag{15}$$

where X is the offset displacement from the base line (inches), and D is the pile diameter (inches).

2.5.2 Dynamic Load Test.

Dynamic Load Testing is an economically efficient method to test a pile because the time involving the setup of testing equipment is low and simple. Dynamic Load Tests

are performed typically during pile installation and a short time after the end of initial driving (EOID) and consists of obtaining compression wave data during hammer blows onto the pile head [2]. Basically, when the hammer strikes the top of the pile, a compressed stressed zone travels along the shaft of the pile at a constant wave speed. The speed depends mainly on the pile material. When the wave hits the pile toe, its amplitude is reduced by the action of static and dynamic soil resistance forces. Depending on the magnitude of the soil resistance, the wave will return to the top of the pile as a tensile (reflective) or compressive (incident) force [20]. Figure 5 shows this procedure.

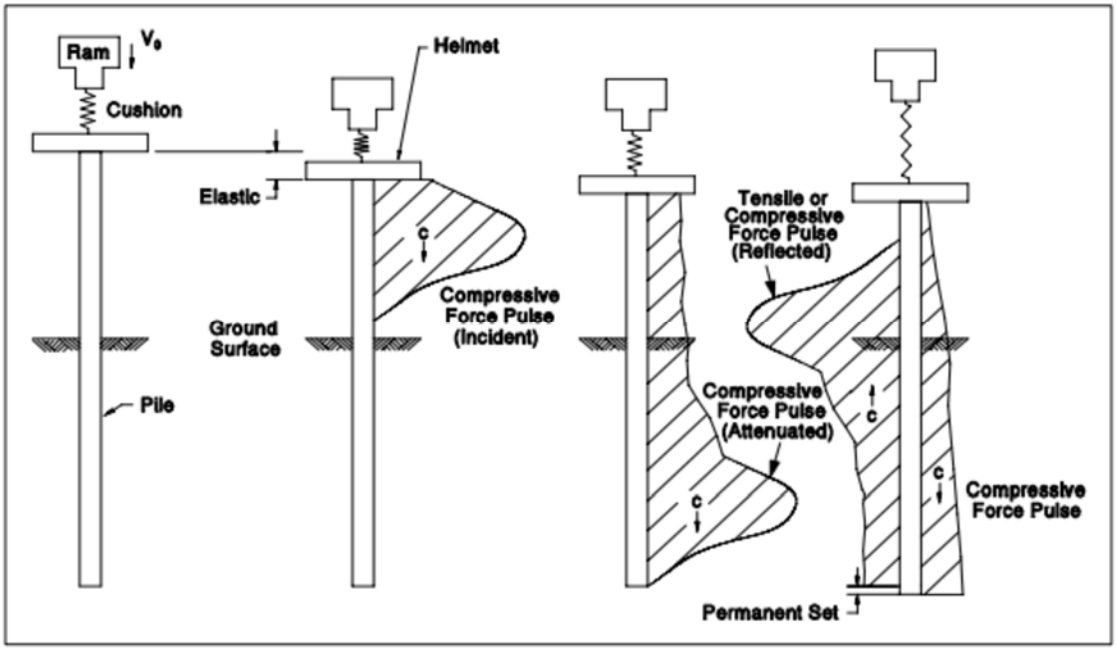

Figure 5: Wave propagation in a pile (Hannigan et al, 2016).

According to FHWA [24], Dynamic Load Tests use measurements of strain and acceleration taken near the pile head as a pile is driven or restruck with a pile driving hammer. *These dynamic measurements can be used to determine the performance of the pile driving system, calculate pile installation stresses, assess pile integrity, and evaluate the nominal geotechnical resistance* [23]. However, Pement [2] says that when the pile is driven into the soil, the soil beneath behaves dynamically. Thus, it resists the pile in a

dynamic manner. Consequently, it is not accurate to assume that the Dynamic resistance is equal to the Static resistance.

As mentioned by Pement [2], to perform a DLT, the pile has usually two or more transducers and accelerometer attached during pile installation. The gauges are connected to a computerized device called Pile Driving Analyzer (PDA), which receives the wave and energy data coming from the pile in real time. *The PDA provides force and acceleration data, which is used to establish force and motion within the pile* [2]. FHWA [24] adds that test results shall be better evaluated using signal matching techniques to determine the relative soil distribution on the pile and the dynamic soil properties to use in wave equation analyses.

There are several wave equations to determine the pile capacity such as dynamic formulas, wave equations, Case Pile Wave Analysis Program (CAPWAP), and iCAP. The last two methods are the most popular since they are programs that incorporate wave equations. Firstly, CAPWAP adopted the Smith [28] soil-pile model *using the wave equation algorithm in the analysis to perform a signals-matching process with the combination of several analytical techniques* [22]. CAPWAP basically partitions the pile into lumped masses linked with linear elastic springs and viscous dampers [23]. Second, iCAP is an automated version of CAPWAP designed to adjust for soil damping. Likins et al [28] mentions that iCAP results match very well with CAPWAP results for several types of piles and soils encountered.

The two ways to control the pile capacity through dynamic testing are through End of Initial Driving (EOID) and Beginning of Restrike (BOR). EOID is performed usually immediately after the pile has been installed and consists of restriking the pile head few times to get dynamic data. BOR analysis can be performed after one- or several-time intervals after EOID and requires few restrikes on the pile head as well. BOR is usually necessary when the pile capacity was not reached at EOID or past BOR tests. Dynamic Load Testing allows a comparison of EOID resistance and BOR resistance. In this way, setup can be quantified. Pement [2] states that ALDOT executes DLTs during the initial pile installation so the operators can obtain the EOID data. ALDOT also performs a “setcheck” analysis, in which the pile is struck several more

times with the driving hammer. If the required pile capacity is not reached at EOID or setcheck analysis, ALDOT requires a 12-hour or 24-hour restrike, where the pile is struck again allowing setup to occur.

In summary, dynamic testing is based on wave propagation principles and uses wave equations to determine the nominal pile capacity. The most popular methods are CAPWAP and ICAP, which are software that incorporate several wave equations. Although DLTs are not as accurate as SLTs, they are useful to perform EOID and BOR analysis and so it is possible to quantify the pile setup.

2.6 Pile setup

Pile setup is defined as the pile capacity increase over time and might generate significant cost savings. Haque et al [8] defined pile setup as *the increase in axial resistance of driven piles after end of initial driving (EOID).* According to Haque and Steward [29], the incorporation of pile setup in the design stage would produce meaningful construction cost savings because the increase in pile capacity can translate into smaller pile elements or shorter embedment lengths. Pile setup phenomenon is mainly a product of three mechanisms: (1) Increase of soil effective stress due to the dissipation of excess pore water pressure, (2) thixotropic effect, and (3) stress independent increase or "aging" effect.

Firstly, during pile driving, the soil is displaced principally radially along the shaft and vertically below the toe. In the course of the driving process, the soil surrounding the pile loses strength due to an excessive increase of pore water pressure and distribution of soil pressure heavily disturbing the soil [30]. Immediately following EOID, this pore water excess begins to dissipate similarly to a consolidation process. Over time, the soil around the pile attempts to recover its original strength, which contributes to an increase in axial resistance of the pile [29]. Second, the phenomenon known was thixotropy also produces a regain of strength of the disturbed soil [31]. Thirdly, Schmertmann [32] indicates that even after the dissipation of excess pore water pressure is completed, pile

setup can continue due to aging mechanism. Haque and Steward [29] state that aging effects increases the shear modulus, stiffness, dilatancy, friction angle of the soil and, also, reduces the soil's compressibility.

Several empirical models have been developed to predict pile setup behavior. However, the most popular is the one developed by Skov and Denver [1] due to its simplicity. This model uses the following equation:

$$\frac{R_t}{R_{to}} = A\ log_{10}\frac{t}{t_o} + 1, \tag{16}$$

where R_t is the total pile capacity at time t, R_{to} is the total pile capacity at reference time t_o, t is the time elapsed since end of initial pile driving, t_o is the initial reference time (usually time at EOID), and A is the setup parameter (log-linear). The parameter A depends on the soil type, pile material, pile type, pile size, and pile capacity [30]. Skov and Denver [1] suggest using A = 0.2 for sand and A = 0.6 for clay. However, Haque and Steward [29] reported an average value of A = 0.2 for soils in Alabama. They concluded to use this value after evaluation the pile setup of 18 axially loaded driven test piles (Steel-H and concrete piles) provided by ALDOT

The incorporation of setup into the calibration of LRFD resistance factors has been studied by Yang and Liang [33] and Haque et al. [8]. They take as basis the limit equation the same used by AASHTO [34], which does not incorporate setup:

$$\phi_R R_n = \gamma_{QD} q_D + \gamma_{QL} q_L, \tag{17}$$

where R_n is the predicted resistance, ϕ_R is the resistance factor for Rn, q_D and q_L are the predicted dead and live loads, respectively; and γ_{QD} and γ_{QL} are the load factors for q_D and q_L, respectively. In this way, Yang and Liang [33] proposes the setup effect of driven piles in the following equation:

$$\phi_{EOID} R_{EOID} + \phi_{setup} R_{setup} = \gamma_{QD} q_D + \gamma_{QL} q_L, \tag{18}$$

where ϕ_{EOID} and ϕ_{setup} are the resistance factors for reference resistance at t_{EOID} and setup resistance, respectively. R_{EOID} is the nominal resistance at end of initial driving, and R_{setup} is the nominal setup resistance increase. Haque and Abu-Farsakh [8] evaluated the resistance factors for setup at time intervals of 30, 45, 60 and 90 days after EOD. Their

final recommendation is using a setup resistance factor ϕ_{setup} of 0.35 at any time after the 14 days.

2.7 Summary of Literature Review

This chapter describes the basic concepts required to understand the following chapters of this study. Essentially, pile foundations consist of deep foundations used to safely transfer structural loads to the ground and to avoid excess settlement or lateral movement. The most common type of pile foundations in Alabama are driven piles. Usually, the nominal pile capacity and depth must be estimated before driving the pile into the ground. Therefore, the basic pile design includes two types of methods. (1) Static analysis method and (2) Software program analysis. The first group assumes the pile as a geomaterial and are based mainly on empirical equations. The second group involves software programs that include one or several static analysis design methods. Two software programs are considered in this study. The first one is WBUZPILE, which is the software used by ALDOT for pile design. This program is based on SPT values and fully empirical equations. The second program is DRIVEN, which is the software used by FHWA. Basically, this software uses the Nordlund method for cohesionless soils and the α-method for cohesive soils.

The geotechnical engineering department from ALDOT currently designs driven piles using WBUZPILE with a LRFD resistance factor of 0.71. This resistance factor was calibrated by ASD fitting from the previous FS of 2. Nonetheless, ALDOT desires to improve and update their pile design through considering a resistance factor calibrated by reliability of structures theory. In this way, the department assembled a 53 piles data base, which contains static load testing and soil boring logs information for each pile. In addition, 18 piles out of the 53 piles contain dynamic load testing information. While Prado [5] and Pement [2] performed calibrations using First Order Second Moment (FOSM), NCHRP 507 [6] reports that FOSM is over-conservative. In addition, Allen et al. [9] and Styler [7] suggest using Monte Carlo Simulation (MCS) and First Order

Reliability Method (FORM), respectively, for being more efficient and rigorous methods. Consequently, the primary objective of this study is to develop LRFD resistance factors unique to Alabama soils using FOSM, FORM, and MCS, in order to enhance accuracy and efficiency of pile design. Through this calibration, the reliability, consistency and efficiency of WBUZPILE and DRIVEN are evaluated. The second objective is to evaluate the effect of pile setup on the calibrated LRFD resistance factors. Finally, the third objective is to compare the calibrated resistance factors with the recommended resistance factors from published studies from the federal government and other states in terms of reliability, consistency and efficiency.

CHAPTER III - PILE ORGANIZATION AND RESEARCH DATABASE.

This chapter shows and describes the database used for the statistical evaluation of resistance factors for the design and construction of driven piles in Alabama Soils. The data assembled by The Alabama Department of Transportation (ALDOT) is composed by 53 piles installed and tested to failure. While all of these were tested using the static load testing, just 18 piles out of the initial 53 were also dynamically tested. Figure 6 shows the location of the piles utilized for this study.

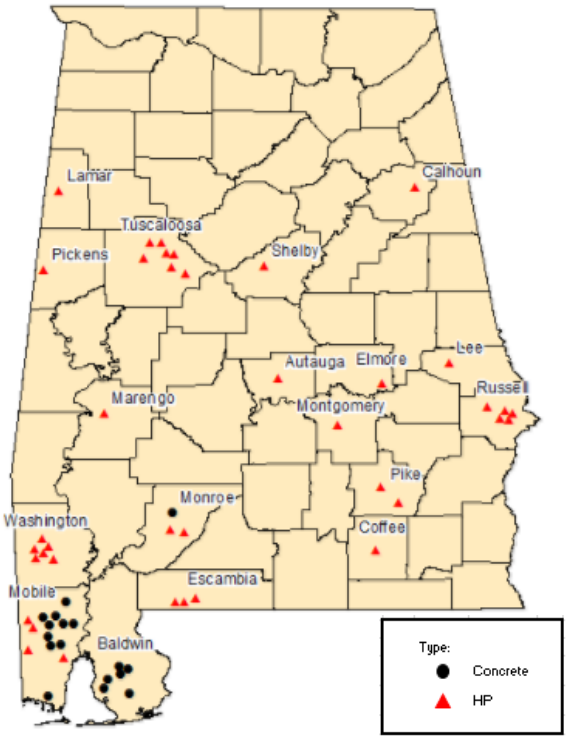

Figure 6: Test Pile locations in the State of Alabama (Pement, 2017)

According to Haque and Steward [30] and as shown in figure 6, the near-surface soils of the Northern 1/3 portion of the state is composed by Limestone uplift, Appalachian Plateau, and Piedmont Plateau, which consist of a hard layer of bedrock

proximate to the surface. Therefore, driven piles used in these areas are toe-bearing piles usually driven to refusal and are not included in this study. The remaining areas are composed of interbedded layers of sand, clay, or silty sands. Thus, driven piles are the typical foundation method for highway structures. Haque and Steward [29] add that *the standard types of piles used by ALDOT for bridge construction are steel H-Piles or square precast, prestressed concrete (PPC) piles*.

3.1 Driven Pile Database -Static Analysis.

The data provided by The Alabama Department of Transportation (ALDOT) consists of 17 concrete piles and 36 steel H-Piles, which sum a total database of 53 piles. For this entire amount, the information available consists of boring logs, pile installation logs, and load test documents. The piles used for this study were specifically chosen because each one was statically load tested using ASTM D1143 [25] standard.

3.1.1 Organization by Pile Material.

Generally, it is suggested to organize the pile database into categories based on the pile material, soil type along the shaft, soil type beneath the toe, length, and geological regions. However, due to the few tests available, the pile database is categorized by pile material into three categories: All Piles, Steel H-Piles only, and Concrete Piles only. The full data base is shown in Table 3. Table 3 displays the pile ID, type (according to the material), size, time from EOID to SLT, SLT measured capacity, DRIVEN predicted capacity, and WBUZPILE predicted capacity. It should be noted that the “time from EOID to SLT” value represents the amount of time that lapsed since EOID finishes until the Static Load Test starts. This time is important for the pile setup evaluation.

Table 3: Pile Database provided by ALDOT for Static Analysis method evaluation (Pement, 2017)

Pile ID	Type	Size	Time from EOID to SLT (days)	SLT measured capacity (Ton-f)	DRIVEN predicted capacity (Ton-f)	WBUZPILE predicted capacity (Ton-f)
210	HP	12x53	13	114	50	118
3002	HP	14x89	2	171	205	154
3003	HP	12x53	2	97	52	98
4301	HP	12x53	2	48	59	131
4601	HP	14x73	2	155	126	206
6503	HP	14x73	3	152	481	294
Celeste Rd Bent 2	HP	12x63	9	162	468	427
Moores Mill Rd	HP	12x53	7	135	26	109
5702	HP	12x53	2	55	107	161
6502	HP	12x53	3	113	107	74
Celeste RD A1	HP	12x63	9	108	186	177
SR 41	HP	12x53	3	54	255	243
212	HP	10x42	4	89	149	171
1901	HP	14x89	7	201	93	135
5502	HP	12x53	2	81	37	62
6504	HP	10x42	2	124	206	193
213	HP	12x53	6	175	155	65
214	HP	14x73	5	114	60	56
301	HP	12x53	3	87	109	55
1101 (pre-splice)	HP	12x84	7	400	305	152
5501	HP	10x42	6	111	185	140
5703	HP	12x53	3	65	114	98
5704	HP	14x102	2	126	116	113
5705	HP	14x89	4	123	156	143
5801	HP	12x53	2	142	95	77
6303	HP	14x73	2	90	151	77
6501	HP	14x73	5	153	148	114
6506	HP	14x73	7	178	138	116
CBD Bridge A1	HP	14x89	2	158	66	99
CBD 7A Bent 2	HP	12x53	3	135	122	59
3001	HP	12x53	2	71	111	108
4001	HP	14x73	8	103	103	110
4801	HP	10x42	14	123	73	47

Table 3, cont.

Pile ID	Type	Size	Time from EOID to SLT (days)	SLT measured capacity (Ton-f)	DRIVEN predicted capacity (Ton-f)	WBUZPILE predicted capacity (Ton-f)
6301	HP	14x73	7	102	85	127
6302	HP	14x89	2	180	130	160
6304	HP	12x53	4	210	133	204
201	Concrete	14"x14"	7	102	149	163
202	Concrete	24"x24"	6	200	191	235
206	Concrete	16"x16"	7	120	1099	274
207	Concrete	14"x14"	26	133	157	223
211	Concrete	14"x14"	12	109	293	447
501	Concrete	16"x16"	7	126	262	178
502	Concrete	16"x16"	11	68	149	107
503	Concrete	16"x16"	7	87	114	123
504	Concrete	14"x14"	7	115	370	495
505	Concrete	14"x14"	28	84	154	199
5103	Concrete	16"x16"	2	125	184	187
204	Concrete	16"x16"	8	176	114	216
205	Concrete	20"x20"	15	180	371	596
506	Concrete	14"x14"	25	112	207	228
203	Concrete	24"x24"	7	270	582	1227
208	Concrete	30"x30"	10	178	149	139
209	Concrete	30"x30"	21	199	261	562

As shown in Table 3, the steel H-Piles database is composed by 36 elements, which are widely spread around the state of Alabama as shown in figure 6. On other hand, the concrete piles database is composed by 17 piles, which were mainly within Mobile and Baldwin county areas along the coast.

3.2 Driven Piles Database – Dynamic analysis.

Eighteen of these piles were also tested dynamically by The Alabama Department of Transportation (ALDOT) consisting of 11 steel H-Piles and 7 concrete. The piles used in this section were specifically chosen because each one was dynamically load tested using PDA and iCAP as signal matching software to adjust the data until a matching quality number of less than 5 was obtained. The remaining 35 piles do not have EOID data, hence they are not considered in this section. Table 4 displays the data for dynamic analysis evaluation.

Table 4: Pile Database provided by ALDOT for Dynamic Analysis method evaluation (Pement, 2017)

Pile ID	Type	Size	EOID measured capacity (Ton-f)	Time from EOID to SLT (days)	SLT measured capacity (Ton-f)
Celeste Rd Bent 2	HP	12x63	112	9	162
Moores Mill Rd	HP	12x53	78	7	135
6502	HP	12x53	70	3	113
Celeste RD A1	HP	12x63	54	9	108
SR 41	HP	12x53	53	3	54
1901	HP	14x89	107	7	201
213	HP	12x53	102	6	175
1101 (pre-splice)	HP	12x84	173	7	400
6501	HP	14x73	126	5	153
CBD Bridge A1	HP	14x89	137	2	158
CBD 7A Bent 2	HP	12x53	43	3	135
202	Concrete	24"x24"	144	6	200
207	Concrete	14"x14"	112	26	133
501	Concrete	16"x16"	55	7	126
502	Concrete	16"x16"	49	11	68
503	Concrete	16"x16"	68	7	87
204	Concrete	16"x16"	201	8	176
205	Concrete	20"x20"	157	15	180

As shown in Table 4, if the data is separated by pile type, the data sizes would be too small (11 for steel H-Piles and 7 piles for concrete piles) for LRFD calibration purposes. Consequently, this data is not categorized and will be evaluated entirely as a single data set.

3.3 Summary of Pile organization and research database.

The database used in this study is the one provided by ALDOT. The data base consists of 53 piles, which have information of boring logs, pile installation logs, and all load test documents. The static analysis methods evaluation includes the 53 piles composed by 36 steel H-piles and 17 concrete piles. For calibration purposes, the SLT database is organized in three pile groups. (1) All piles group, (2) steel H-Piles group, and (3) concrete piles group. The Dynamic analysis method evaluation involves 18 piles out of the 53 piles data base because these 18 piles have EOID information based on PDA test with iCAP as signal matching software. Out of the 18 piles, 11 are steel H-Piles and 7 are concrete piles. For calibration purposes, the DLT database is organized as a single generic group.

CHAPTER IV - PILE CAPACITY DESIGN USING WBUZPILE AND DRIVEN DESIGN PROGRAMS

The objective of this chapter is to evaluate the performance of WBUZPILE and DRIVEN for pile design according to the relationships of the predicted capacity and the measured capacity. The predicted resistance is obtained from WBUZPILE or DRIVEN, and the measured resistance is obtained from SLT test and Davisson criterion.

Exclusively for this chapter, the piles are grouped into 6 categories based on the soil type along the shaft and at the tip of the pile. The purpose of creating the categories was to potentially observe any tendencies of WBUZPILE or DRIVEN, with regards to how these programs estimate pile capacities with respect to the soil types (i.e. over-estimate capacities for piles in only sand or only clay). Even if the number of data points for some soil categories is small, the results are relevant since this chapter does not involve calibration. Each category is based. The soil types are shown in Table 5. The predominant soil type along the shaft was determined by a 35% - 65% criteria. If there was 65% or more of either sand or clay along the shaft of the pile, that soil type was listed as the predominant soil type. If the soil was between 35% and 65% of the pile shaft length, the soil was considered mixed. The soil type that the pile was embedded into was taken as the soil at the tip. This information was obtained from the provided boring logs closest to the test pile location on each site. Only sand and clay were considered, because WBUZPILE data input is restricted to those two soil types. Similarly, DRIVEN data input requires the user to define the soil in each layer as either cohesionless or cohesive.

Table 5: Pile categories according to soil types encountered

Pile Category	**1**	**2**	**3**	**4**	**5**	**6**
Soil at Tip	Sand	Sand	Sand	Clay	Clay	Clay
Soil along Shaft	Sand	Clay	Mixed	Sand	Clay	Mixed

4.1 WBUZPILE Analysis

For this section, the predicted data analysis was begun by designing each pile (using the WBUZPILE design program) as if it were not already installed. The goal of this analysis was to acquire pile capacities based on the WBUZPILE method of analysis, while attempting to simulate the conditions at the time of the static load test, to establish consistency and therefore accurate comparisons. First, the relevant information such as pile type, groundwater elevation, and elevation of zero depth was entered into the necessary fields. This information was obtained from the pile loading documents that were provided for each pile. Next, the boring logs were referenced, and the soil layer information was entered into the program appropriately (see Figure 7). It was assumed that the boring logs provided were indicative of the soils at the load test site. If multiple boring logs were provided, the boring closest to that of the load test site were used. WBUZPILE requires SPT N-values in addition to the soil type, in order to run the analysis. The boring logs displayed N-values throughout the soil profile, and these values were entered into the program. The N-values were multiplied by 1.33 to mimic ALDOTs design procedures, which account for hammer efficiency [35]. Additionally, ALDOT uses the N-values to determine when one soil layer has ended and another has begun. If the N-value changed by more than five blow counts within the same soil layer, a new soil layer was added in WBUZPILE with the same soil classification as the previous layer. Also, a new soil layer was added when the classification changed between sand and clay according to the boring logs. Since ALDOT only uses two soil layer types in their pile design (sand and clay), all silts and clays were entered as clay into WBUZPILE, and all other soils were entered as sand. Sand was the predominant soil type encountered at each pile, however rock-like material was occasionally encountered at some sites and was entered as sand into the program.

Once the soil profiles were entered for each pile, capacity results were displayed through the program. WBUZPILE generates results in kips per linear foot of pile, as shown in Figure 8. To determine accurate capacities, it was important to establish accurate ground

elevations at the pile. The ground elevation at the pile was determined from the static load test documents, however the soil profiles were entered from the boring logs. The boring logs did not always have the same ground elevations as the SLT documents. Therefore, if the boring log elevation was higher than the actual ground elevation at the SLT site, the side resistance was subtracted from the difference in elevation. For example, if the ground elevation at the boring was 23 ft. as shown in Figure 8, and the ground elevation at the pile during the SLT was 10 ft., the side resistance at 10 ft. (34.3 kips) would be subtracted from the total capacity. The tip resistance would not be subtracted because it changes for each soil layer; that is, it does not continuously increase like the side resistance. The tip resistance was taken at the pile tip elevation, which was provided by the load test documents. In some cases, the boring elevation was lower than the actual elevation. If this was the case, a sandy clay layer with an N-value of 10 was added at the top of the boring layers. The total capacity was taken at the pile tip elevation, which was specified in the SLT documents. For example, in Figure 8, if the pile tip elevation was specified as -5.00 ft., the total capacity would be 194.80 kips.

.

Project Number: BR-0213(501)
County Name: Mobile
Description: Abut. 1, Pile 1
Pile type: 14 inch Solid Concrete Pile
Elevation at beginning of driving = 24 ft
Pile tip embedment = 74.5 ft
Elevation at desired pile tip = Every 1 ft
Water table depth = 11.5 ft
LRFD resistance factor = 0.71

Soil Layer Number	Soil Description	Soil Depth (ft) From	To	Soil Total Unit Weight (pcf)	Blow-Counts (N per ft)
1.	Firm Clayey Sand	0.00	1.00	125.00	25.00
2.	Firm Clayey Sand	1.00	2.50	120.00	17.00
3.	Firm Clayey Sand	2.50	3.50	115.00	6.00
4.	Silty Sand w/ Organics	3.50	9.50	125.00	26.00
5.	Silty Sand w/ Organics	9.50	14.50	115.00	4.00
6.	Loose Silty Sand	14.50	19.50	120.00	12.00
7.	Loose Clayey Sand	19.50	24.50	115.00	5.00
8.	Firm Silty Sand	24.50	34.50	125.00	27.00
9.	Firm to Dense Sand	34.50	39.50	130.00	45.00
10.	Firm Silty Sand	39.50	44.50	125.00	29.00
11.	Dense Sand w/ Silt	44.50	49.50	125.00	40.00
12.	Dense Sand w/ Silt	49.50	54.50	130.00	83.00
13.	Dense Sand w/ Silt	54.50	59.50	130.00	64.00
14.	Dense Sand w/ Silt	59.50	64.50	130.00	98.00
15.	Dense Sand w/ Silt	64.50	69.50	130.00	98.00
16.	Very Stiff to Hard Sandy Clay	69.50	74.50	125.00	31.00

Figure 7: WBUZPILE soil/pile data input.

********** OUTPUT DATA **********

Pile Tip Elev. (ft)	Pile embedment in Ground (ft)	Pile Capacity (kips)	Pile Tip Resistance (kips)	Pile Side Resistance (kips)
23.00	1.00	4.90	4.71	0.20
22.00	2.00	5.50	4.71	0.80
21.00	3.00	3.90	2.33	1.60
20.00	4.00	41.20	37.86	3.40
19.00	5.00	43.80	37.86	6.00
18.00	6.00	46.40	37.86	8.60
17.00	7.00	49.00	37.86	11.10
16.00	8.00	51.60	37.86	13.70
15.00	9.00	54.20	37.86	16.30
14.00	10.00	27.70	8.24	19.50
13.00	11.00	31.40	8.24	23.20
12.00	12.00	35.10	8.24	26.90
11.00	13.00	38.80	8.24	30.60
10.00	14.00	42.50	8.24	34.30
9.00	15.00	63.30	24.57	38.70
8.00	16.00	68.50	24.57	44.00
7.00	17.00	73.70	24.57	49.20
6.00	18.00	78.90	24.57	54.40
5.00	19.00	84.10	24.57	59.60
4.00	20.00	77.80	12.88	65.00
3.00	21.00	83.40	12.88	70.50
2.00	22.00	88.90	12.88	76.10
1.00	23.00	94.50	12.88	81.60
0.00	24.00	100.00	12.88	87.20
-1.00	25.00	166.20	72.71	93.50
-2.00	26.00	173.40	72.71	100.70
-3.00	27.00	180.50	72.71	107.80
-4.00	28.00	187.70	72.71	115.00
-5.00	29.00	194.80	72.71	122.10

Figure 8: WBUZPILE output data.

4.2 DRIVEN Analysis

A DRIVEN analysis was performed in similar fashion to the WBUZPILE analysis, where the predicted capacities came from the DRIVEN program. The purpose of this analysis was two-fold: a.) to develop additional resistance factors specifically for DRIVEN, and b.) to directly compare WBUZPILE with a well-established and widely used design program.

DRIVEN is similar to WBUZPILE in that, it uses the same site information as WBUZPILE to determine capacities. However, DRIVEN allows the user to define more

detailed site characteristics. For instance, there is an option to specify soft compressible soils and/or scourable soils overlying the bearing strata, however these options were not specified for any of the piles. For each soil layer, there is an option to specify a percent driving strength loss. Similarly, this remained unspecified for each pile. For steel H-piles, the user may specify an H-pile or box tip, and an H-pile or box perimeter for the analysis. In this study, the H-pile tip and H-pile perimeter were selected for the H-piles. For cohesionless soil layers, the N-values were entered (up to five values per layer) in the program. The N-values were not multiplied by 1.33 during the DRIVEN analysis, as was done for the WBUZPILE analysis. However, DRIVEN allows the user to correct the N-values for the influence of the effective overburden pressure, and this correction was chosen for all piles in this study. Finally, for cohesive soils, DRIVEN requires an adhesion value to be selected. In all cases, the general adhesion value was selected for cohesive soils.

The capacity results provided by DRIVEN are provided at depth intervals, but are not displayed per linear foot of pile, as detailed in Figure 9. Therefore, the capacities obtained from DRIVEN often required interpolation. Since pile tip resistance does not linearly increase with depth, the tip resistance was taken for the layer that the pile tip was in. However, the skin resistance was linearly interpolated if the value was between output result depths. For example, in Figure 9, if the tip was at a depth of 15 m, the tip resistance would be taken as 424.74 kN, while the skin resistance would be interpolated between 919.97 KN and 1168.84 KN (the values between 14.01 m and 17.01 m respectively), as highlighted in Figure 9. Similarly, if soil near the surface of the pile needed to be subtracted to match the elevations at the load test site, the amount of skin resistance to subtract would be interpolated as well.

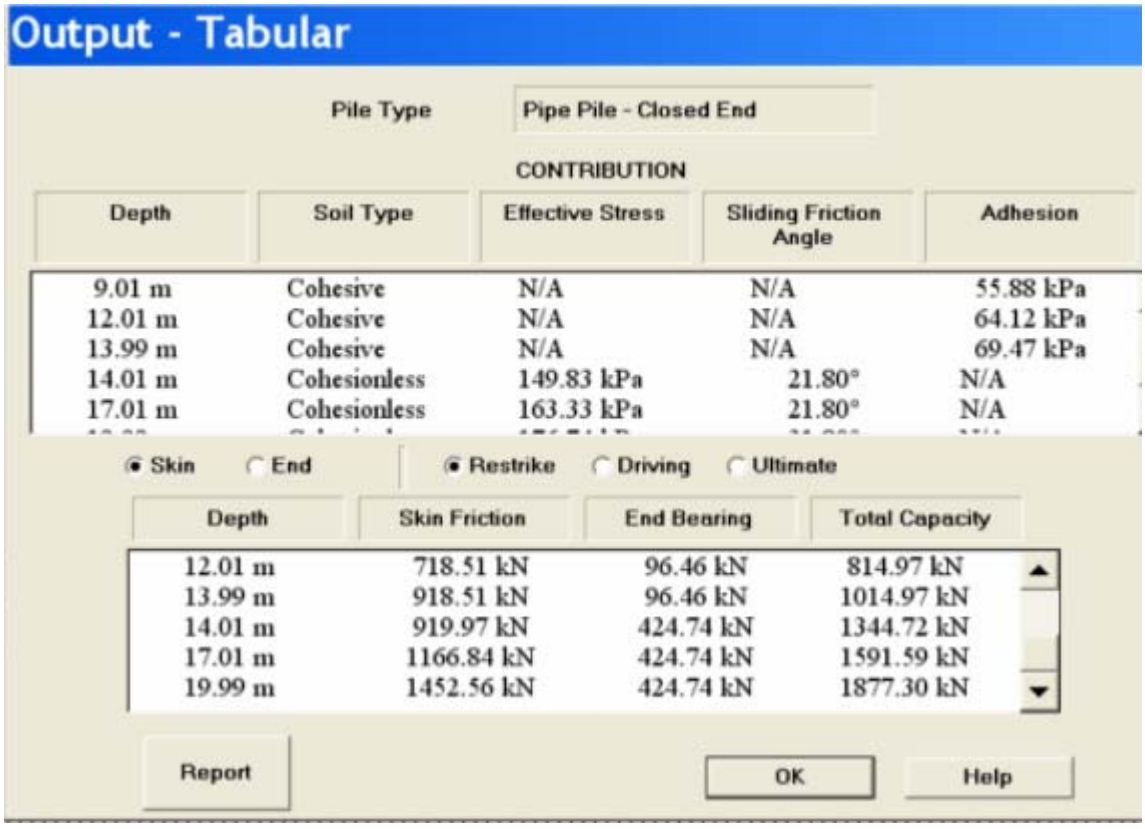

Figure 9: DRIVEN output results and subsequent skin resistance interpolation (Hannigan et al., 2006).

4.3 Comparison between WBUZPILE and DRIVEN

Since WBUZPILE is an internally designed program used exclusively within the ALDOT geotechnical engineering department, a comparison was made between WBUZPILE and DRIVEN, which is a widely used program that uses well-known design methods. WBUZPILE was directly compared to DRIVEN. This comparison was performed to verify the tendencies of WBUZPILE compared to a well-established and widely used design program. When WBUZPILE is directly compared to DRIVEN, it can

be seen in Figure 10 that, on average, WBUZPILE produces a 13% higher capacity than DRIVEN. As shown in Figures 11 and 12, WBUZPILE produces a 6% higher capacity than DRIVEN for H-piles, and 26% higher capacity for concrete piles, respectively.

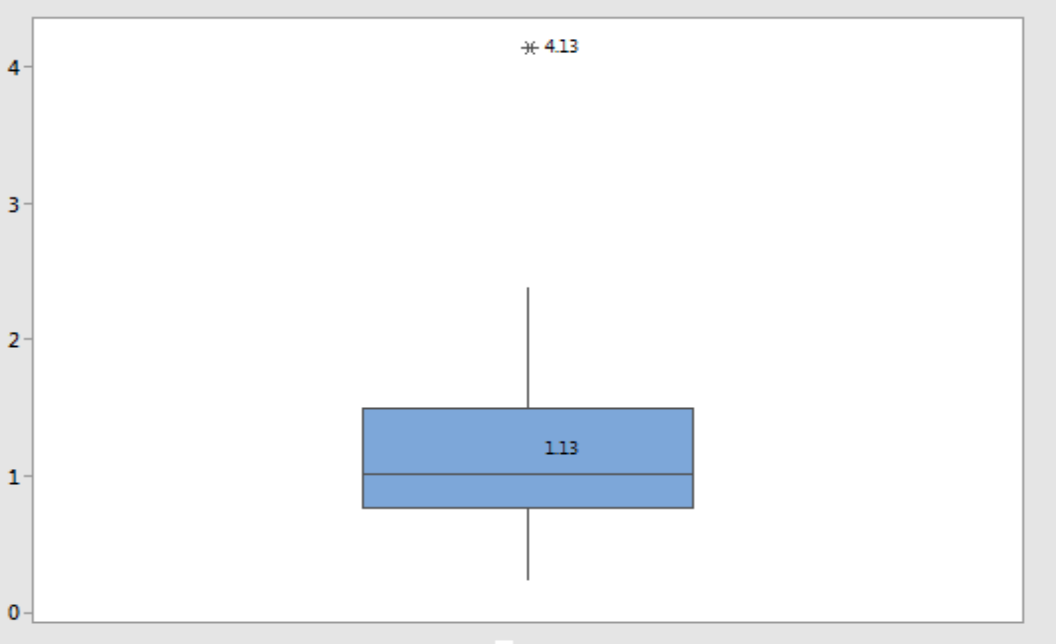

Figure 10: Boxplot of capacity comparison between WBUZPILE and DRIVEN for the entire pile database.

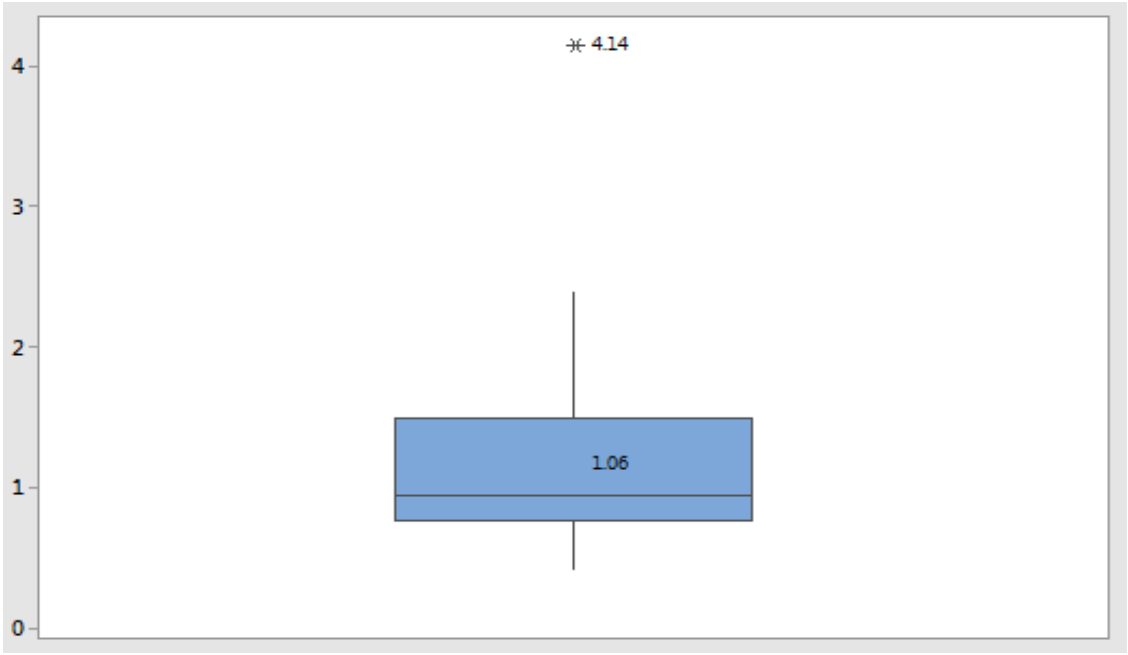

Figure 11: Boxplot of capacity comparison between WBUZPILE and DRIVEN for H-piles.

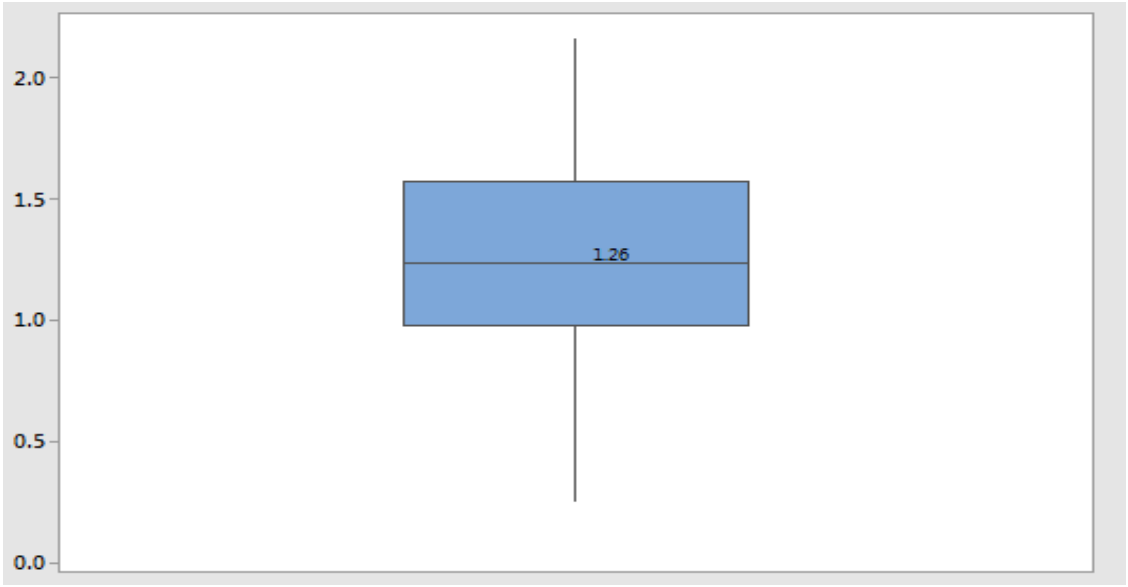

Figure 12: Boxplot of capacity comparison between WBUZPILE and DRIVEN for concrete piles.

4.4 Predicted Results Compared to Static Load Tests

This section involves a comparison of WBUZPILE and DRIVEN with the results from the static load tests. In this study, the corresponding evaluation is performed using the variable named as *error,* which.is obtained from the overall results from Table 3 and by calculating the ratio of the predicted resistance (R_p) to the measured resistance (R_m).

The error value is calculated and shown in Table 6 as (R_p/R_m). An error value of one indicates zero error, meaning the predicted value matched the measured value.

Table 6: Error values for WBUZPILE and DRIVEN

Pile	Type	Soil Category	Rp/Rm DRIVEN	Rp/Rm WBUZPILE
210	HP	1	0.436	1.037
3002	HP	1	1.201	0.901
3003	HP	1	0.537	1.009
4301	HP	1	1.224	2.711
4601	HP	1	0.812	1.328
6503	HP	1	3.167	1.931
Celeste Rd Bent 2	HP	1	2.890	2.638
Moores Mill Rd	HP	1	0.195	0.807
5702	HP	3	1.944	2.930
6502	HP	3	0.946	0.655
Celeste RD A1	HP	3	1.726	1.636
SR 41	HP	3	4.773	4.542
212	HP	4	1.669	1.919
1901	HP	4	0.464	0.673
5502	HP	4	0.457	0.767
6504	HP	4	1.660	1.559
213	HP	5	0.883	0.371
214	HP	5	0.526	0.491
301	HP	5	1.257	0.635
1101 (pre-splice)	HP	5	0.761	0.380
5501	HP	5	1.667	1.264
5703	HP	5	1.746	1.500
5704	HP	5	0.918	0.897
5705	HP	5	1.270	1.164

Table 6, cont.

Pile	Type	Soil Category	Rp/Rm DRIVEN	Rp/Rm WBUZPILE
5801	HP	5	0.670	0.540
6303	HP	5	1.674	0.853
6501	HP	5	0.968	0.744
6506	HP	5	0.774	0.649
CBD Bridge A1	HP	5	0.420	0.628
CBD 7A Bent 2	HP	5	0.903	0.439
3001	HP	6	1.552	1.517
4001	HP	6	1.007	1.075
4801	HP	6	0.597	0.380
6301	HP	6	0.840	1.247
6302	HP	6	0.723	0.889
6304	HP	6	0.633	0.973
201	Concrete	1	1.456	1.595
202	Concrete	1	0.953	1.177
206	Concrete	1	9.158	2.284
207	Concrete	1	1.178	1.673
211	Concrete	1	2.685	4.098
501	Concrete	1	2.081	1.409
502	Concrete	1	2.214	1.586
503	Concrete	1	1.311	1.408
504	Concrete	1	3.217	4.306
505	Concrete	1	1.833	2.367
5103	Concrete	2	1.474	1.498
204	Concrete	3	0.645	1.226
205	Concrete	3	2.060	3.310
506	Concrete	3	1.850	2.036
203	Concrete	4	2.155	4.544
208	Concrete	4	0.841	0.783
209	Concrete	6	1.312	2.824

Table 7: Average error by soil type (steel H-piles)

Soil Category	Number of Concrete Piles	Mean error (Rp/Rm) DRIVEN	Mean error (Rp/Rm) WBUZPILE
1	8	1.308	1.545
3	4	2.347	2.441
4	4	1.062	1.229
5	14	1.031	0.754
6	6	0.892	1.013

Table 8: Average error by soil type (concrete piles)

Soil Category	Number of Concrete Piles	Mean error (Rp/Rm) DRIVEN	Mean error (Rp/Rm) WBUZPILE
1	10	2.609	2.190
2	1	1.474	1.498
3	3	1.518	2.191
4	2	1.498	2.664
6	1	1.312	2.824

Tables 7 and 8 shows the mean error values with respect to design program and soil type encountered, and also shown are the number of piles for each soil type. As shown in Table 7, the tendency for WBUZPILE and DRIVEN was to over-predict the pile capacity by 21.3% and 21.9% respectively, for steel H-piles. In Table 8, it is shown that WBUZPILE and DRIVEN yield similar tendencies and over-predict the pile capacity by 124.3% and 114.3% respectively, for concrete piles. The values in Tables 7 and 8 are shown graphically in Figures 13 and 14. As shown in the Figures, the tendency for both methods is to over-predict the pile capacity by approximately 53%.

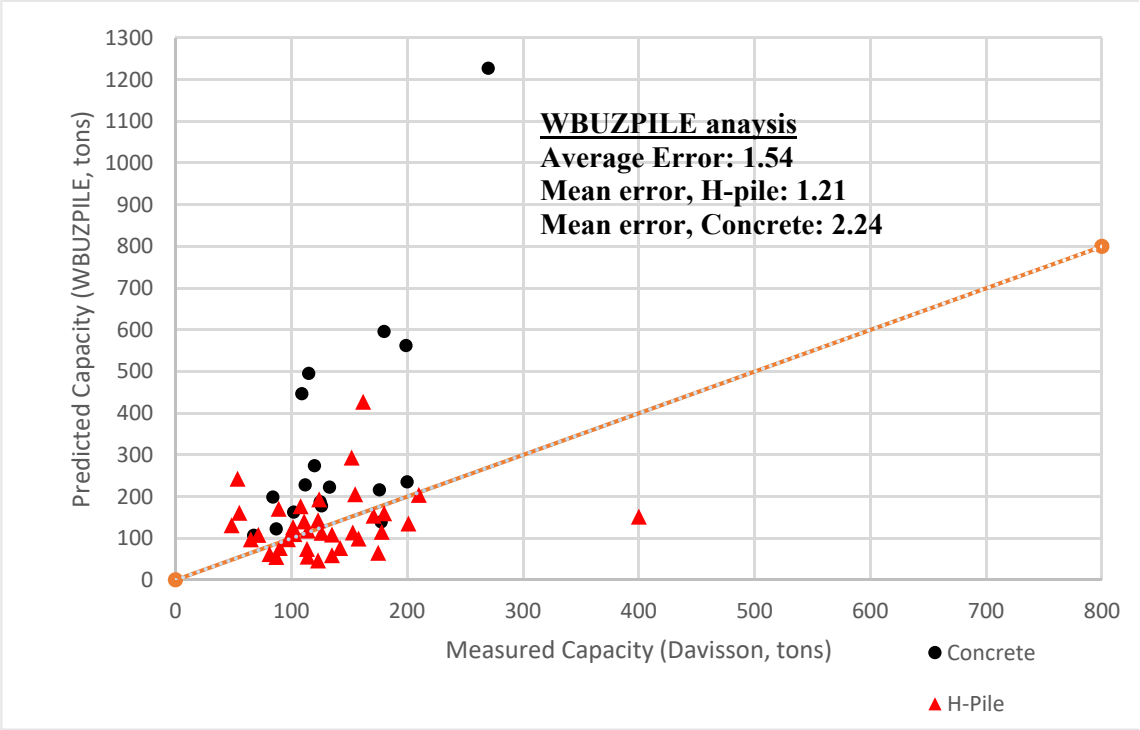

Figure 13: Graphical results for WBUZPILE capacity versus SLT analysis.

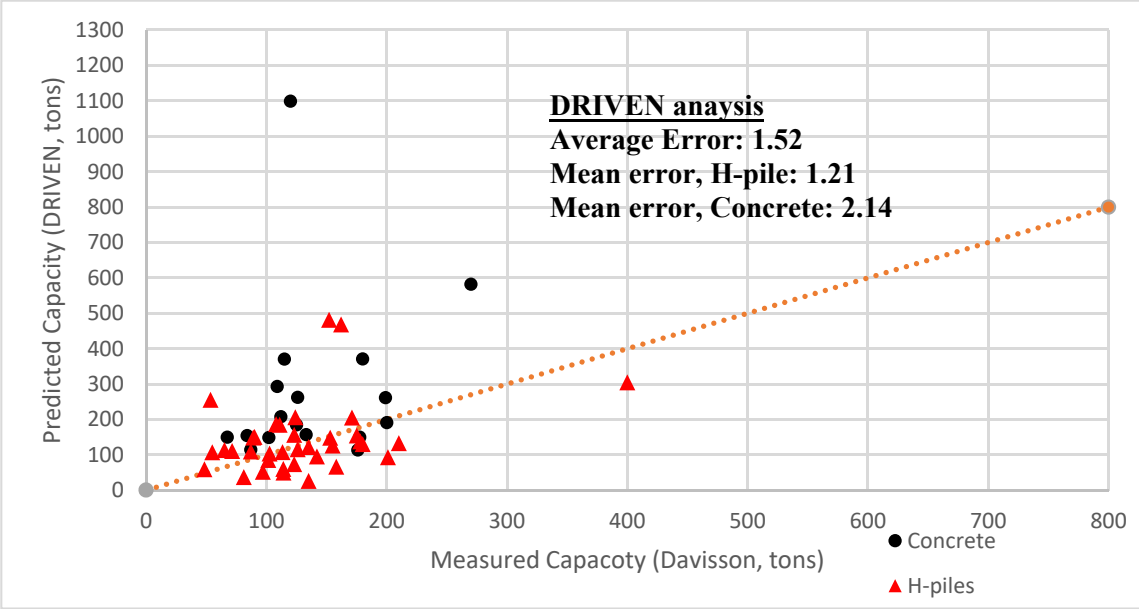

Figure 14: Graphical results for DRIVEN capacity versus SLT analysis.

The results for each separate soil category type encountered are shown graphically for the WBUZPILE analysis in Figures 15 to 20. It is seen that for H-piles, WBUZPILE was least accurate for soil type 3 (sand at tip, mixed along shaft) with a mean error of 2.44, and most accurate for soil type 6 (clay at tip, sand along shaft) with a mean error of 1.01. For concrete piles, WBUZPILE was least accurate for soil type 6 (clay at tip, mixed along shaft) with a mean error of 2.82, and most accurate for soil type 2 (sand at tip, clay along shaft), with a mean error of 1.50. The results for each soil type encountered are not shown graphically for the DRIVEN analysis, however DRIVEN showed similar trends to WBUZPILE.

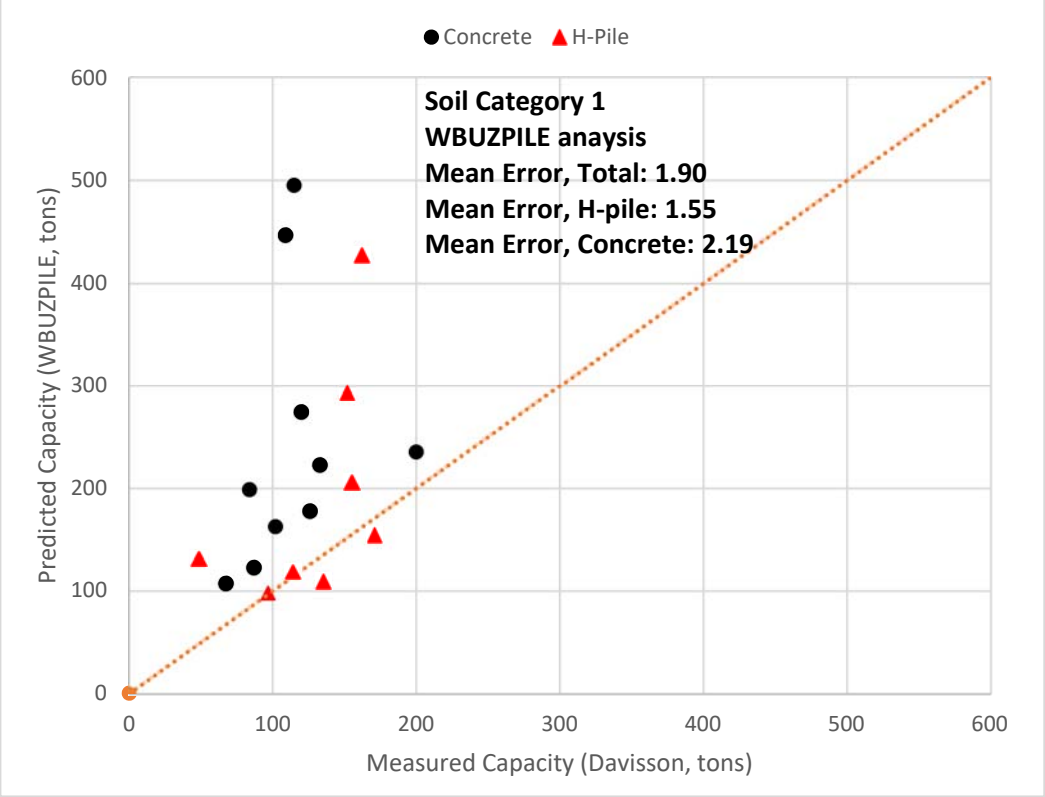

Figure 15: WBUZPILE results for soil type 1 (sand at tip, sand along shaft).

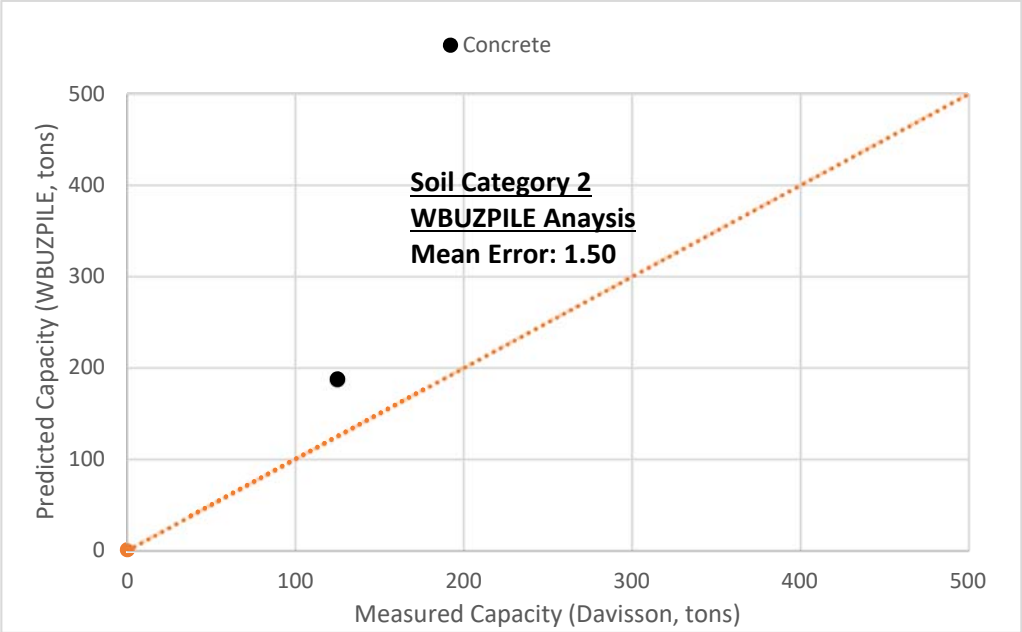

Figure 16: WBUZPILE results for soil type 2 (sand at tip, clay along shaft).

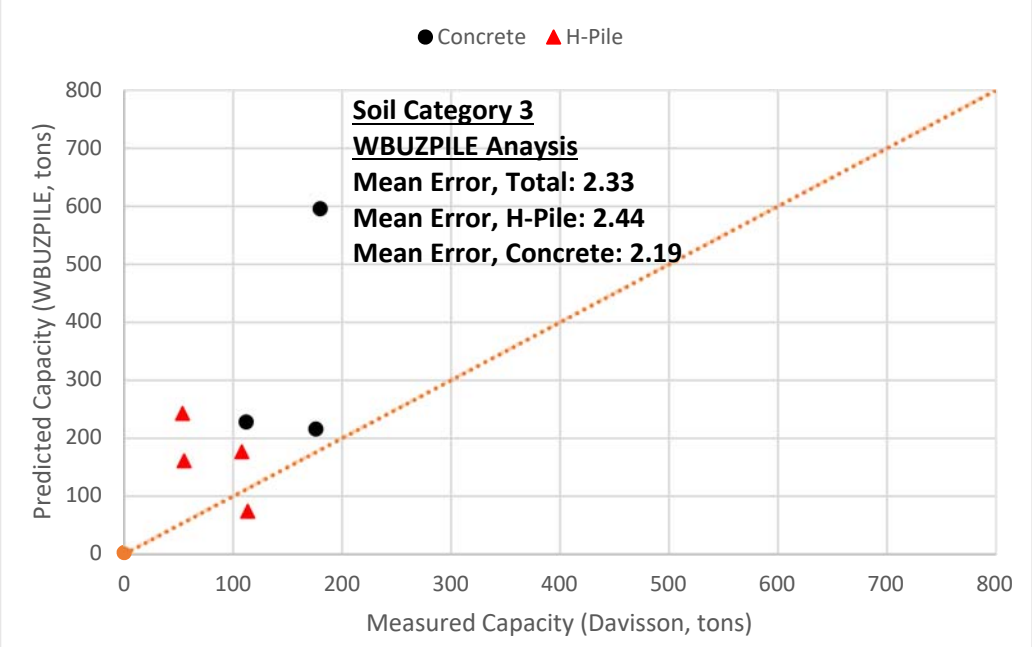

Figure 17: WBUZPILE results for soil type 3 (sand at tip, mixed along shaft).

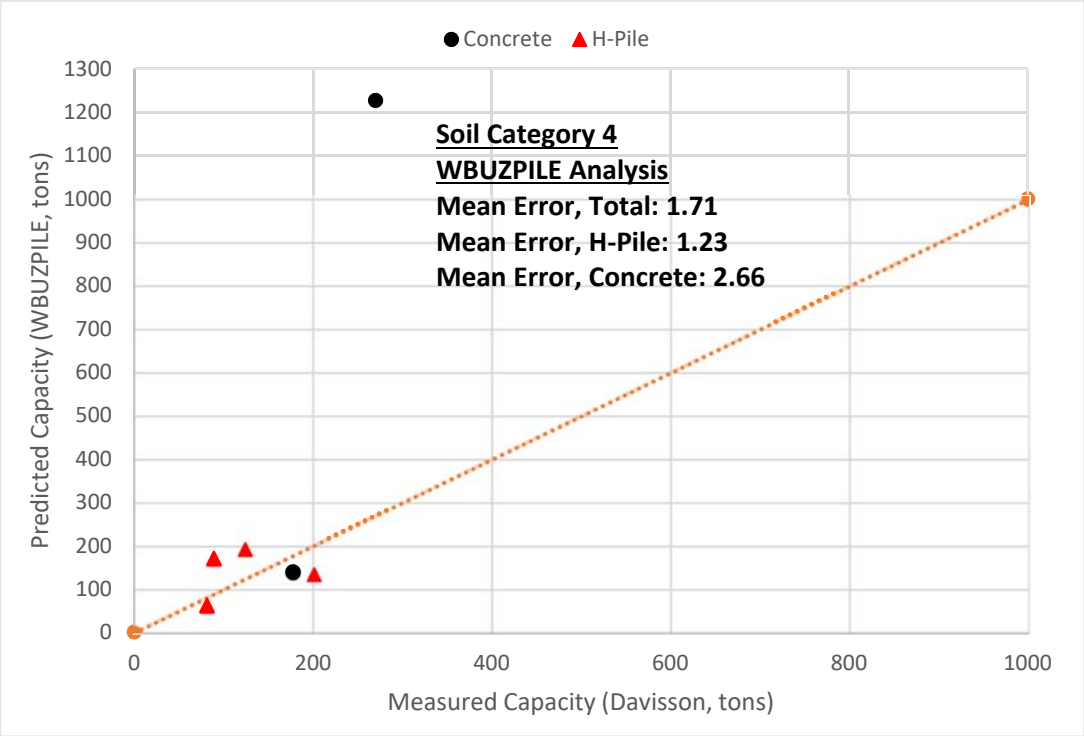

Figure 18: WBUZPILE results for soil type 4 (clay at tip, sand along shaft).

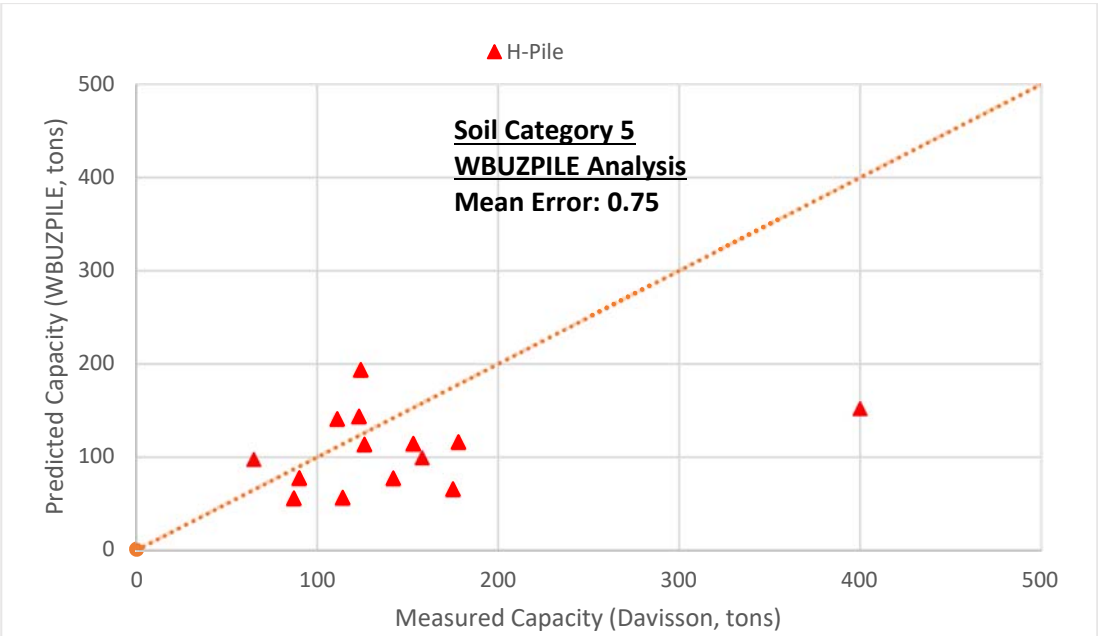

Figure 19: WBUZPILE results for soil type 5 (clay at tip, clay along shaft).

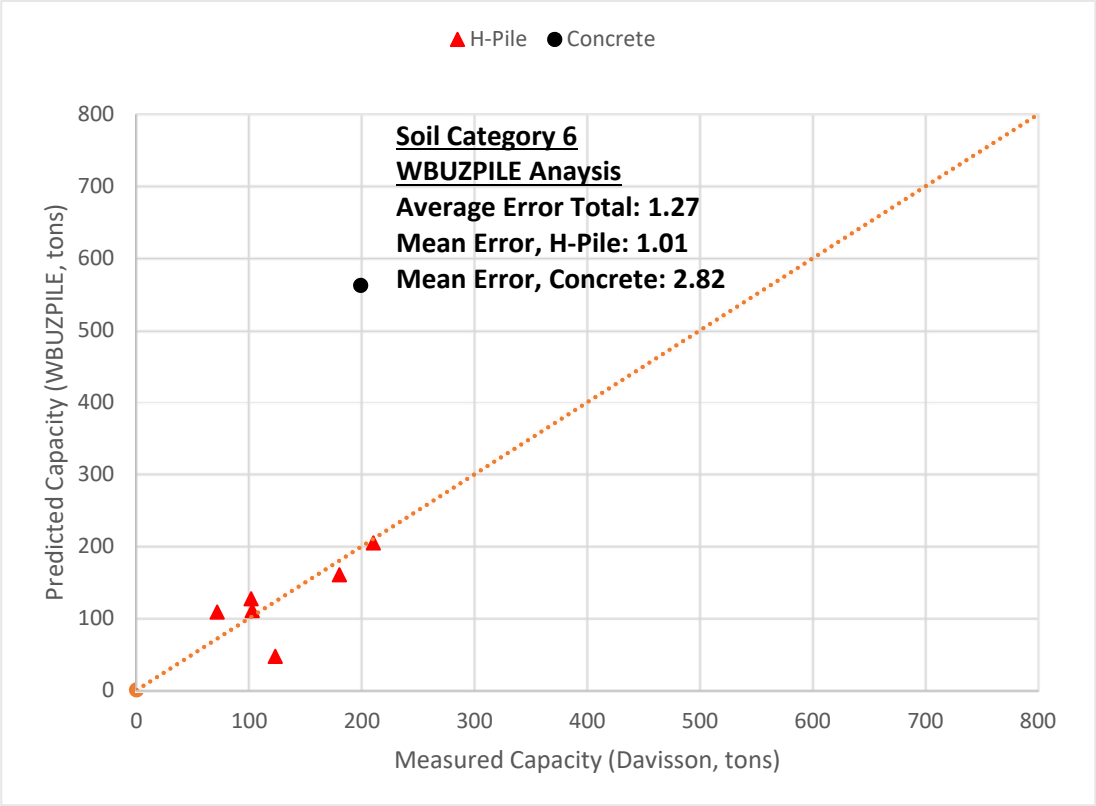

Figure 20: WBUZPILE results for soil type 6 (clay at tip, clay along shaft).

Overall, WBUZPILE performs similarly to DRIVEN. Both DRIVEN and WBUZPILE tend to over-predict the pile capacity for concrete and H-piles. On average, WBUZPILE predicts a 19% higher pile capacity than DRIVEN. Furthermore, WBUZPILE predicts a 11% higher capacity for H-piles and a 3% higher capacity for concrete piles when compared to DRIVEN. Both DRIVEN and WBUZPILE are better at predicting the capacity of H-piles.

It is shown in this study that for H-piles, WBUZPILE was least accurate at predicting the pile capacity for soil type 3, where the tip was in sand, and mixed soils were along the shaft. WBUZPILE was most accurate at predicting the pile capacity for soil type 6, where the tip was embedded in clay, and sand was along the pile shaft.

For concrete piles, WBUZPILE was least accurate at predicting pile capacity for soil type 6, where the tip was embedded in clay, and mixed soils were along the pile shaft. WBUZPILE was most accurate at predicting the pile capacity for soil type 2, where the tip was in sand, and clay was along the shaft – although there are limited data points to confirm these conclusions.

CHAPTER V – EVALUATION OF SKOV AND DENVER MODEL FOR ALABAMS SOILS

As previously stated, pile setup can generate significant cost savings to the government and taxpayers. While there are several models to predict pile setup, one of the most popular methods is the Skov and Denver model [1]. The main objective of this chapter is to evaluate the performance of the Skov and Denver model for pile setup estimation in Alabama soils. This section divided in two parts. The first part considers the Skov and Denver model to estimate a later pile capacity from an earlier known and actually measured pile capacity. The second part considers the Skov and Denver model to estimate an earlier pile capacity from a later known and actually measured pile capacity. In other words, the second part follows a reversal approach from the first part.

The Skov and Denver [1] model suggest using a setup factor of A = 0.2 for sand and A = 0.6 for clay. Nonetheless, Haque and Steward [29] established A = 0.2 for soil in Alabama, hence this value is used in this study. Moreover, EOID capacity is considered to be developed at 15 minutes for every pile, and SLT capacity at the time period from EOID to SLT (which is different for each pile).

The research data base used for this chapter consists of 18 driven piles tested by ALDOT. The rest of piles are not used in this chapter because they do not have dynamic load testing data. Each of the 18 piles contains information about their measured EOID capacity, measured SLT capacity, and time from EOID to SLT.

The variable named error is used to evaluate the performance of the prediction method. The error is calculated from the ratio of the estimated resistance to the measured resistance. The closer the value to 1, the more accurate the model is.

5.1 Evaluation of the Skov and Denver Model for estimating pile setup

The objective of this subsection is to evaluate the performance of the Skov and Denver [1] model for estimating pile setup. The Skov and Denver model is used to estimate a future pile capacity based on an earlier measured pile capacity (EOID for this subsection) and a specific time period. More specifically, this subsection involves comparing a measured SLT capacity and an estimated SLT capacity. The estimated SLT resistance is obtained by incorporating the Skov and Denver model to the results of dynamic load testing at EOID. The error is calculated as the ratio of the predicted SLT capacity to the measured SLT capacity.

5.1.1 Evaluation of Skov and Denver model for the entire data set.

This subsection evaluates the Skov and Denver [1] model using the entire data base with EOID and SLT results. This data base is composed by 11 steel H-piles and 7 concrete piles. The analysis and results are shown in Table 9 and Figure 21, which present the measured SLT capacities, the estimated SLT capacities obtained from the measured EOID capacities, and the error for each pile. It should be noted that for the entire data set, the average time period from EOID to SLT is 7.6 days.

Table 9: Error-values for pile setup estimation for the entire data set.

Pile	Pile Type	EOID measured (Ton-f)	Time from EOID to SLT (Days)	SLT measured (Ton-f)	SLT estimated (Ton-f)	**Error**
205	Concrete	157	15	180	256	**1.420**
501	Concrete	55	7	126	87	**0.687**
503	Concrete	68	7	87	107	**1.226**
6501	H-Pile	126	5	153	193	**1.260**
Celeste Rd Bent 2	H-Pile	112	9	162	178	**1.097**
Celeste RD A1	H-Pile	54	9	108	85	**0.791**
Moores Mill RD	H-Pile	78	7	135	122	**0.904**
CBD 7A Bent 2	H-Pile	43	3	135	65	**0.479**
SR 41	H-Pile	53	3	54	79	**1.479**
202	Concrete	144	6	200	224	**1.119**
204	Concrete	201	8	176	317	**1.803**
207	Concrete	112	26	133	188	**1.416**
502	Concrete	49	11	68	79	**1.170**
213	H-Pile	102	6	181	158	**0.873**
1101	H-Pile	173	7	400	270	**0.676**
1901	H-Pile	107	2	201	156	**0.775**
6502	H-Pile	70	3	113	104	**0.920**
CBD Bridge A1	H-Pile	137	2	158	200	**1.265**

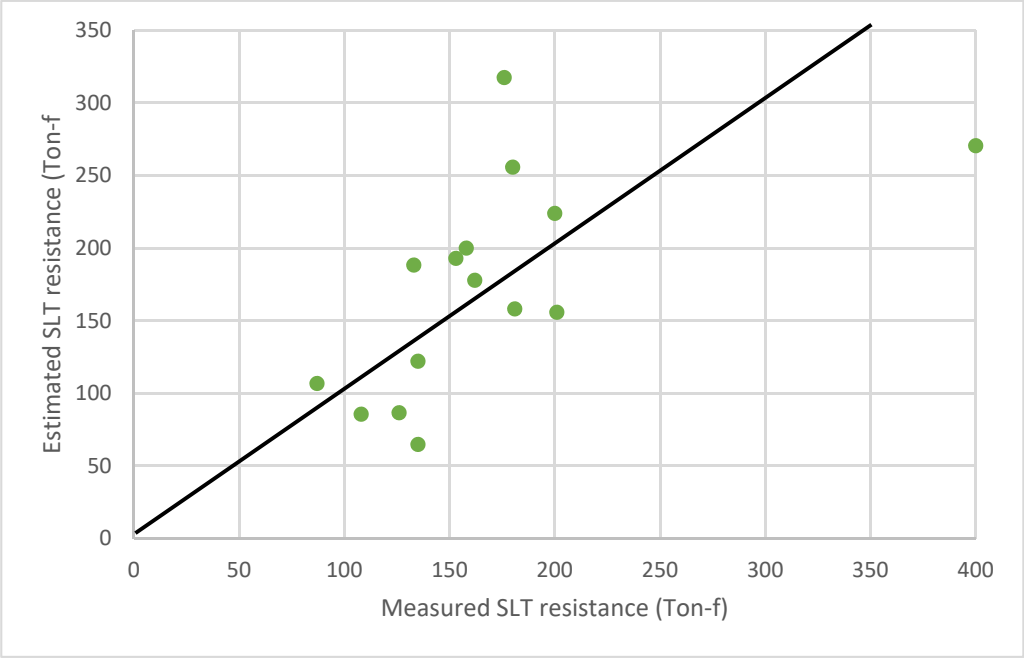

Figure 21: Comparison of estimated SLT and measured SLT for the entire data set.

When comparing the estimated SLT capacity with the measured SLT capacity for the entire pile set, the average error is 1.076, which represents that Skov and Denver model over-estimates the SLT capacity for 7.6%.

5.1.2 Evaluation of Skov and Denver model for the steel H-piles data set.

This subsection evaluates the Skov and Denver model using the only the steel H-piles data base with EOID and SLT results. This data base is composed by 11 steel H-piles. The analysis and results are shown in Table 10 and Figure 22, which present the measured SLT capacities, the estimated SLT capacities obtained from the measured EOID capacities, and the error for each pile. It should be noted that for the entire data set, the average time period from EOID to SLT is 5.1 days.

Table 10: Error-values for pile setup estimation for the steel H-piles data set.

Pile	Pile Type	EOID measured (Ton-f)	Time from EOID to SLT (Days)	SLT measured (Ton-f)	SLT estimated (Ton-f)	**Error**
6501	H-Pile	126	5	153	193	**1.260**
Celeste Rd Bent 2	H-Pile	112	9	162	178	**1.097**
Celeste RD A1	H-Pile	54	9	108	85	**0.791**
Moores Mill RD	H-Pile	78	7	135	122	**0.904**
CBD 7A Bent 2	H-Pile	43	3	135	65	**0.479**
SR 41	H-Pile	53	3	53.5	79	**1.479**
213	H-Pile	102	6	181	158	**0.873**
1101	H-Pile	173	7	400	270	**0.676**
1901	H-Pile	107	2	201	156	**0.775**
6502	H-Pile	70	3	113.4	104	**0.920**
CBD Bridge A1	H-Pile	137	2	158	200	**1.265**

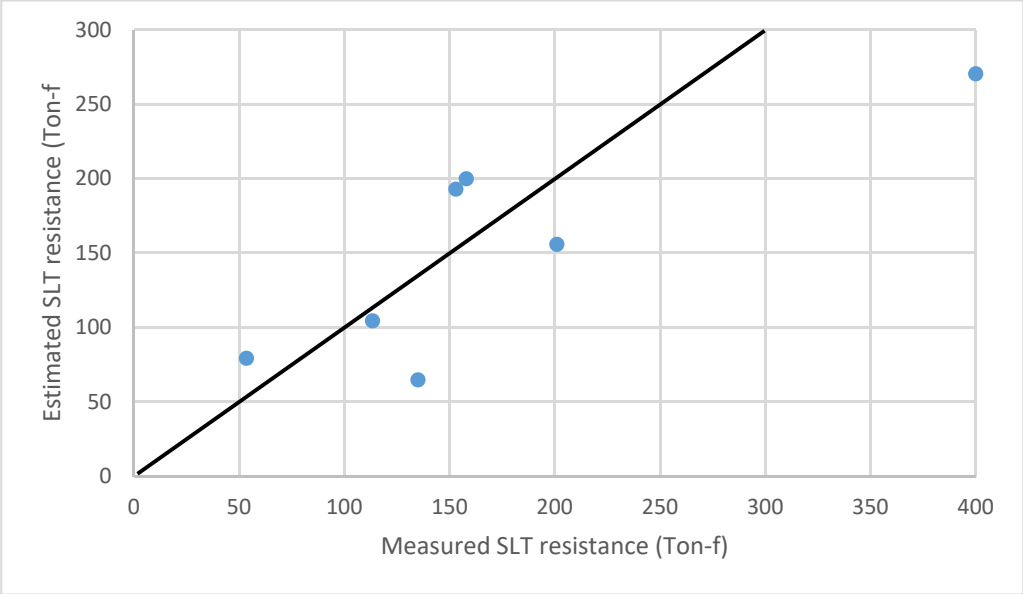

Figure 22: Comparison of estimated SLT and measured SLT for the steel H-piles data set.

When comparing the estimated SLT capacity with the measured SLT capacity for the steel H-piles data set, the average error is 0.956, which represents that Skov and Denver model under-estimates the SLT capacity for 4.4%.

5.1.3 Evaluation of Skov and Denver model direction for the concrete piles data set.

This subsection evaluates the Skov and Denver model using the only the concrete piles data base with EOID and SLT results. This data base is composed by 7 concrete piles. The analysis and results are shown in Table 11 and Figure 23, which present the measured SLT capacities, the estimated SLT capacities obtained from the measured EOID capacities, and the error for each pile. It should be noted that for the entire data set, the average time period from EOID to SLT is 11.4 days.

Table 11: Error-values for pile setup estimation for the concrete piles data set.

Pile	Pile Type	EOID measured (Ton-f)	Time from EOID to SLT (Days)	SLT measured (Ton-f)	SLT estimated (Ton-f)	**Error**
205	Concrete	157	15	180	256	**1.420**
501	Concrete	55	7	126	87	**0.687**
503	Concrete	68	7	87	107	**1.226**
202	Concrete	144	6	200	224	**1.119**
204	Concrete	201	8	176	317	**1.803**
207	Concrete	112	26	133	188	**1.416**
502	Concrete	49	11	67.5	79	**1.170**

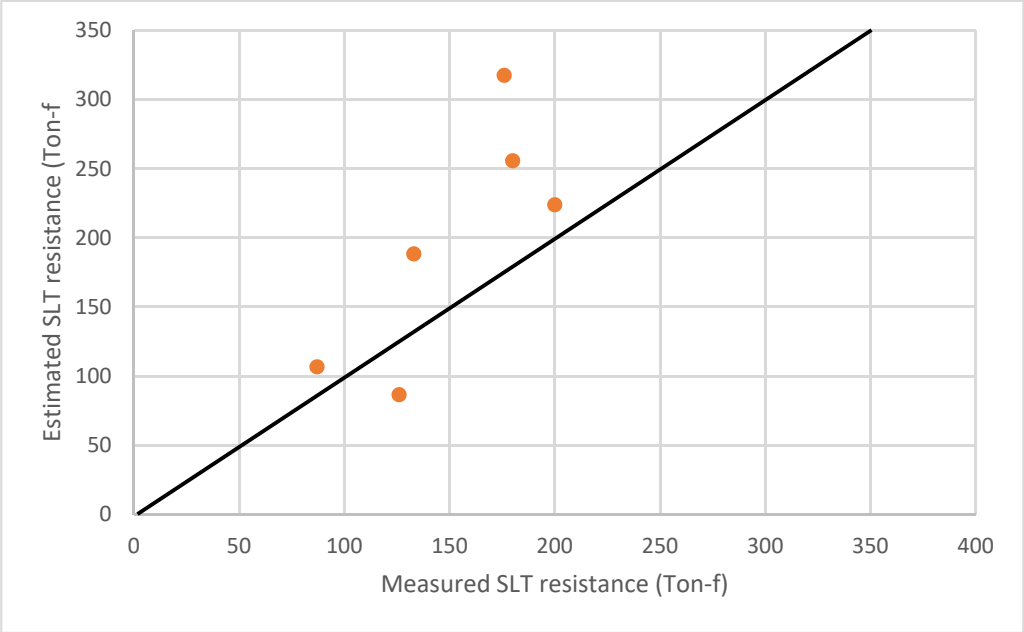

Figure 23: Comparison of estimated SLT and measured SLT for the concrete piles data set.

When comparing the estimated SLT capacity with the measured SLT capacity for the concrete piles data set, the average error is 1.263, which represents that Skov and Denver model over-estimates the SLT capacity for 26.3%.

5.2 Evaluation of the Skov and Denver Model for estimating pile setup in reverse direction

The Skov and Denver model is generally used to estimate the future pile capacity based on an earlier capacity. Nevertheless, this subsection follows a reversal approach by estimating an earlier capacity from a real future capacity. Thus, the objective of this subsection is to establish whether the Skov and Denver model can be used to estimate an earlier resistance based on the results of an actual resistance test performed later. More specifically, this subsection involves comparing a measured EOID capacity and an estimated EOID capacity. The estimated EOID resistance is obtained by incorporating the

Skov and Denver model to the results of static load tests. The error is calculated as the ratio of the predicted EOID capacity to the measured EOID capacity.

5.2.1 Evaluation of Skov and Denver model in reverse direction for the entire data set.

This subsection evaluates the Skov and Denver model in reverse direction using the entire data base with EOID and SLT results. This data base is composed by 11 steel H-piles and 7 concrete piles. The analysis and results are shown in Table 12 and Figure 24, which present the measured EOID capacities, the estimated EOID capacities obtained from the measured SLT capacities, and the error for each pile. It should be noted that for the entire data set, the average time period from EOID to SLT is 7.6 days.

Table 12. Error-values for reverse pile setup estimation for the entire data set.

Pile	Pile Type	EOID measured (Ton-f)	EOID estimated (Ton-f)	**Error**
205	Concrete	157	110	**0.704**
501	Concrete	55	80	**1.455**
503	Concrete	68	56	**0.815**
6501	H-Pile	126	100	**0.794**
Celeste Rd Bent 2	H-Pile	112	102	**0.911**
Celeste RD A1	H-Pile	54	68	**1.264**
Moores Mill RD	H-Pile	78	86	**1.106**
CBD 7A Bent 2	H-Pile	43	90	**2.087**
SR 41	H-Pile	53	36	**0.676**
202	Concrete	144	129	**0.894**
204	Concrete	201	112	**0.555**
207	Concrete	112	79	**0.706**
502	Concrete	49	42	**0.855**
213	H-Pile	102	117	**1.146**
1101	H-Pile	173	256	**1.480**
1901	H-Pile	107	138	**1.291**
6502	H-Pile	70	76	**1.087**
CBD Bridge A1	H-Pile	137	108	**0.791**

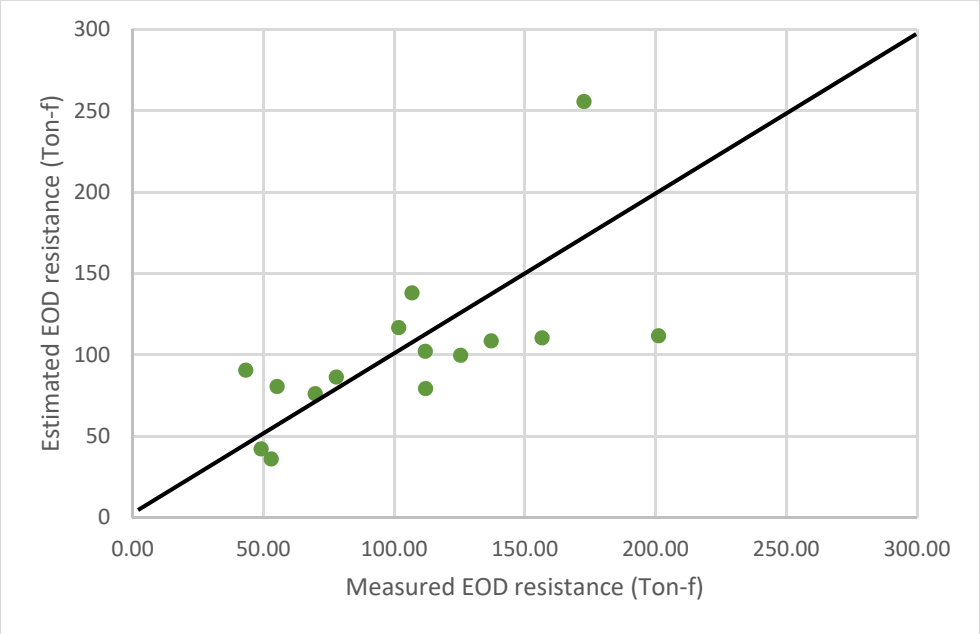

Figure 24. Comparison of estimated EOD and measured EOD for the entire data set.

When comparing the estimated EOID capacity with the measured EOID capacity for the entire pile set, the average error is 1.034, which represents that Skov and Denver model over-estimates the EOID capacity for 3.4%.

5.2.2 Evaluation of Skov and Denver model in reverse direction for the steel H-piles data set.

This subsection evaluates the Skov and Denver model in reverse direction using the only the steel H-piles data base with EOID and SLT results. This data base is composed by 11 steel H-piles. The analysis and results are shown in Table 13 and Figure 25, which present the measured EOID capacities, the estimated EOID capacities obtained from the measured SLT capacities, and the error for each pile. It should be noted that for the steel H-piles data set, the average time period from EOID to SLT is 5.1 days.

Table 13. Error-values for reverse pile setup estimation in reverse for the steel H-piles data set.

Pile	Pile Type	EOID measured (Ton-f)	EOID estimated (Ton-f)	**Error**
6501	H-Pile	126	100	**0.794**
Celeste Rd Bent 2	H-Pile	112	102	**0.911**
Celeste RD A1	H-Pile	54	68	**1.264**
Moores Mill RD	H-Pile	78	86	**1.106**
CBD 7A Bent 2	H-Pile	43	90	**2.087**
SR 41	H-Pile	53	36	**0.676**
213	H-Pile	102	117	**1.146**
1101	H-Pile	173	256	**1.480**
1901	H-Pile	107	138	**1.291**
6502	H-Pile	70	76	**1.087**
CBD Bridge A1	H-Pile	137	108	**0.791**

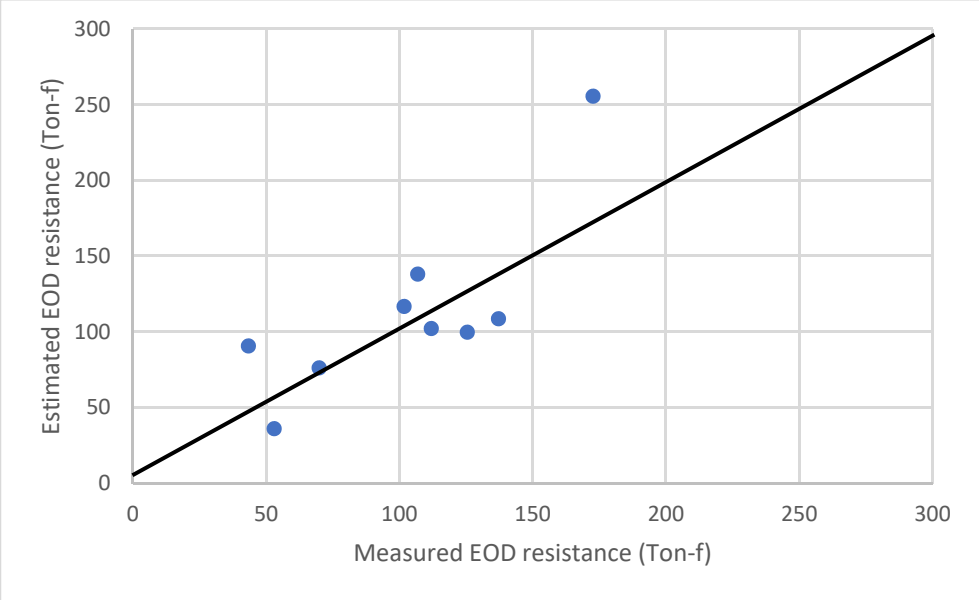

Figure 25. Comparison of estimated EOD and measured EOD for steel H-piles data set.

When comparing the estimated EOID capacity with the measured EOID capacity for the steel H-piles pile set, the average error is 1.148, which represents that Skov and Denver model over-estimates the EOID capacity for 14.8%.

5.2.3 Evaluation of Skov and Denver model in reverse direction for the concrete piles data set.

This subsection evaluates the Skov and Denver model in reverse direction using the only the concrete data base with EOID and SLT results. This data base is composed by 7 concrete piles. The analysis and results are shown in Table 14 and Figure 26, which present the measured EOID capacities, the estimated EOID capacities obtained from the measured SLT capacities, and the error for each pile. It should be noted that for the concrete piles data set, the average time period from EOID to SLT is 11.4 days.

Table 14: Error-values for reverse pile setup estimation for the concrete piles data set.

Pile	Pile Type	EOID measured (Ton-f)	EOID estimated (Ton-f)	**Error**
205	Concrete	157	110	**0.704**
501	Concrete	55	80	**1.455**
503	Concrete	68	56	**0.815**
202	Concrete	144	129	**0.894**
204	Concrete	201	112	**0.555**
207	Concrete	112	79	**0.706**
502	Concrete	49	42	**0.855**

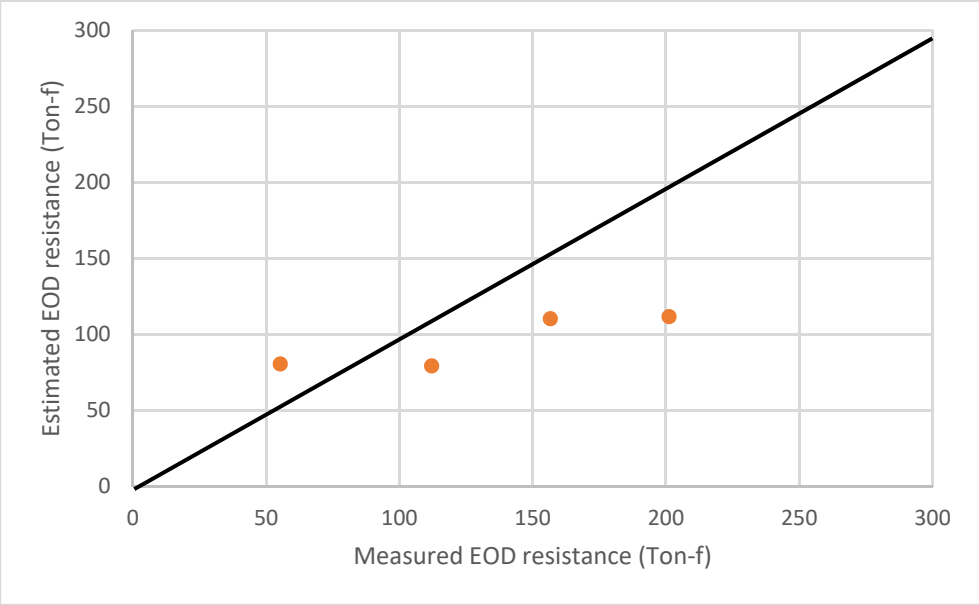

Figure 26: Comparison of estimated EOD and measured EOD for concrete piles data set.

When comparing the estimated EOID capacity with the measured EOID capacity for the concrete piles pile set, the average error is 0.855, which represents that Skov and Denver model under-estimates the EOID capacity for 14.5%.

5.3 Summary of the Evaluation of the Skov and Denver Model for Alabama Soils

The evaluation of the Skov and Denver model to estimate the SLT resistance based on measured EOID resistance shows that the Skov and Denver model over-estimates the SLT capacity by 7.6% for a group composed by steel H-piles and concrete piles. For exclusively steel H-piles, the Skov and Denver model under-estimates the SLT capacity by 4.4%. For exclusively concrete piles, the Skov and Denver model over-estimates the SLT capacity by 26.3%.

The evaluation of the Skov and Denver model to estimate the EOID resistance based on measured SLT resistance shows that the Skov and Denver model over-estimates

the EOID capacity by 3.4% for a group composed by steel H-piles and concrete piles. For exclusively steel H-piles, the Skov and Denver model over-estimates the EOID capacity by 14.8%. For exclusively concrete piles, the Skov and Denver model under-estimates the EOID capacity by 14.5%.

CHAPTER VI - CALIBRATION METHODOLOGY

This chapter describes the concepts and probabilistic-based methodologies applied to a LRFD calibration. These methodologies are based on random variables and the statistical characterization of their bias. This chapter also explains how to conduct an actual calibration and apply it to the development of LRFD design specifications.

As mentioned by Allen et al [9], there are three levels of probabilistic design. (1) Level I, (2) Level II, (3) and Level III. Firstly, the Level I is the simplest but least accurate. For Level I design methods, the uncertainties and safety are measured by a factor of safety. In other words, ASD design methodology can be considered to be Level I. Second, for the Level II, the uncertainties and safety are represented in terms of the reliability index (β). This reliability index measures the probability of failure of any design. In this way, LRFD design methodology can be considered to be Level II. Generally, Level II methods involve iterative techniques best performed by computer algorithms. Finally, Level III involves complex statistical data beyond what is usually available within geotechnical and structural engineering. Consequently, Levels I and II are the most viable methodologies used for geotechnical and structural design. Allen et al. [9] adds *that the goal of Level I or II analysis is to develop factors that increase the nominal load or decrease the nominal resistance to give a design with an acceptable and consistent probability of failure*.

This chapter begins by introducing the concept of random variables and bias values. Then, the statistical characterization of the load and resistance variables as well as specific pre-calibration considerations are described. Next, the First Order Second Moment (FOSM) calibration, the First Order Reliability method (FORM) calibration, and the Monte Carlo Simulation (MCS) calibration concept and procedure. Finally, the Reliability Based Efficiency factor is described.

6.1 Random variables and Bias.

This section defines the concept of random variables and bias, which both compose the basis to perform the LRFD calibration. First of all, Allen et al [9] define a random variable as a variable that does not have an exact value and *it pertains to a set of values, or a range, and the probability of occurrence*. Nowak and Collins [35] add that a random variable is a function that maps events onto intervals on the axis of real numbers. A probability function is defined on events and this definition can be extended by random variables. Figure 27 shows a schematic representation of a random variable as a function. For LRFD methodology in driven piles, the random variables consist of loads (dead and live loads) and resistances (capacity).

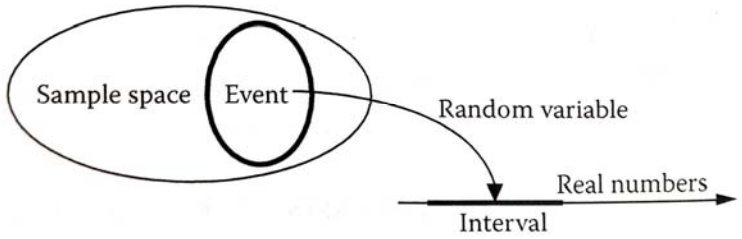

Figure 27: Schematic representation of a random variable as a function (Nowak and Collins, 2013).

Second, the definition of bias is the ratio of the true parameter value and the expected value. Within structural reliability field, the bias is the ratio of the measured (actual) to the nominal (predicted) value. The bias allows the soil characteristics, materials, and construction uncertainties to be included into a design method. Thus, a calibration must be performed for each prediction method independently. In this study, the bias for loads (λ_Q) and resistance (λ_R) are calculate as follows:

$$\lambda_Q = \frac{Q_m}{Q_p} \text{ and} \tag{19}$$

$$\lambda_R = \frac{R_m}{R_p}, \tag{20}$$

where Q_m is the measured load, Q_p is the predicted load, R_m is the measured resistance, and R_p is the predicted resistance. It is important to mention that a bias must be calculated for every pair (measured and predicted) of data, and then, they shall be grouped to obtain some of their basic descriptive statistical features, which are explained in the next section.

6.2 Statistical Characterization and Calibration considerations

This section describes the statistical characterization of the load and resistance random variables as well as specific pre-calibration considerations, for which both are required prior to performing the LRFD calibration. Once the bias values have been calculated for each pile, the mean, standard deviation, and the coefficient of variation shall be calculated for each data case. In this study, the data cases consist of deciding whether to include statistical outliers obtained through different criteria. Since the LRFD calibration methods are probabilistic-based procedures, the probability density function and cumulative density functions must be computed for each data set as well as the type of probability distribution. The most common type of distributions for piles are normal and lognormal [6]. Besides the statistical characterization of the data, the target reliability index and load factor shall be established before performing the actual calibration. The target reliability index measures the safety and is related to the probability of occurrence of a failure event. The load factors are not actually calibrated in this study and are obtained from NCHRP 507 [6].

6.2.1 Mean, Standard deviation, and Coefficient of Variation of random variables.

As mentioned by Allen et al [9], the mean, standard deviation, and coefficient of variation from the random variables considered in the limit state equation are necessary to perform the resistance factor calibration. In this study, the mean, standard deviation, and coefficient of variation values correspond to the bias random resistance values and bias random load variables since they are present in the limit state equation. Paikowsky et al. [6] states that load and resistance random variables can be taken as normal or lognormal distributed variables and both type of distributions are defined in the following sections. For a normal distribution, the mean ($\widehat{\mu_x}$) is the sum of the individual values from a sample divided by the total number of values *n*.

$$\widehat{\mu_x} = \frac{X_i + X_3 + \cdots + X_i}{n}. \tag{21}$$

The second parameter is the standard deviation (σ_x or $\widehat{\sigma_x}$), which *measures of the dispersion about the mean of the data representing the random variable* [9]. For a population, it can be calculated as follows:

$$\sigma_x = \sqrt{\frac{\sum_{i=1}^{n}(X_i - \mu)^2}{N}}. \tag{22}$$

For a sample (from a larger population), the standard deviation can be calculated as follows:

$$\widehat{\sigma_x} = \sqrt{\frac{\sum_{i=1}^{n}(X_i - \mu)^2}{n-1}}. \tag{23}$$

Lastly, the coefficient of variation (*COV* or V_x) is the third statistical value required for the LRFD calibration. Nonetheless, the COV is not actually considered a third statistical parameter because it is just the standard deviation normalized by the mean. Therefore, other calibration documents just state the mean and COV or the mean and the standard deviation as initial calibration values. The COV is unitless and can be calculated as follows:

$$COV_x = V_x = \frac{\widehat{\sigma_x}}{\widehat{\mu_x}}. \tag{24}$$

Sometimes the term *variance* is used, however, both terms are different. The actual variance is a unit dependent value equals to the square of the standard deviation and it is not specifically used in this study for calibration purposes.

6.2.2 Data Cases: Filtering data.

In order to assess the quality of the provided data, it can be important to statistically analyze the data in order to filter the extreme points or outliers if possible. An outlier is a data point that lies outside of the overall pattern in a distribution. On one hand, it is known that these outliers can significantly increase the COV values. Therefore, filtering the data from outliers would produce higher calibrated resistance factors. On the other hand, from the purely statistical perspective, the consideration of a value as an "outlier" just implicates a deeper analysis and research about the reasons why the value is further from the mean. Consequently, the judgment of the researcher shall define whether to include the outliers, according to the reasons found in the investigation.

As mentioned by Allen et al [9], typical reasons to exclude an outlier include:

- The data obtained near the structure boundary are not specifically accounted for in the design model being used (for example, data obtained near the top or bottom of a wall)
- A different criterion is used to establish the value of a given point or set of points (e.g. a different failure criterion considered.)
- A different measurement technique is used.
- Data from a source may be suspect.
- Data that are affected by regional factors (for instance, regional geology effects on soil or rock properties) may alter the values.
- Other issues that would cause the data within a given data set not to be completely random in nature.

The data provided by ALDOT does not present actual proof to be subjected to outlier removal according to guide provided by Allen et al. [9]. Nevertheless, this study

still considers the data cases in order to evaluate their effect on the calibrated resistance factors. The most popular methods to assess the data and identify outliers for driven piles are based on two criteria. The first criterion consists of using boxplots, which consider the boundaries at one and a half Interquartile (IQR) range from the first and third quartile for the bottom and upper portion, respectively. The boxplot method is used in this study because it has extended data applicability since It does not make distributional assumptions and does not depend on the mean or standard deviation. The boxplot can be adequately applied to symmetric or non-symmetric and mount-shaped or non-mount shaped data distribution [36]. Therefore, it can be adequately used for normal or lognormal data. The second criterion consist of establishing the boundaries at two standard deviations distance from the mean for the bottom and upper portion equally. As mentioned by the Songwon [36], the two standard deviations method to identify outliers may not be adequate for skewed data such as lognormal data because it uses non-robust measures, such as the mean and standard deviation, which are highly affected by extreme values. Nonetheless, the two standard deviations method is still used in this study besides the boxplot method for two reasons. First, AASHTO specifications [37], which represents the most important federal specifications for driven piles, is mainly based on the NCHRP 507 [6] , which considers the two standard deviation method even with skewed data (lognormal distributed). Second, the boxplot method might not be adequate for small sample size [36] and this study considers relatively small data sizes once the entire data sample is categorized. Therefore, this study considers three data cases. (1) Data case A, which does not exclude any outlier; (2) data case B, which excludes the outliers identified according to boxplot criterion; and (3) data case C, which excludes the outliers identified according to two standard deviations criterion.

6.2.2.1 Data Case A.

Data case A follows the statistical principle that the entire data is evaluated regardless of the presence of outliers. This case is usually followed when no significant reasons exist to exclude outliers. On one hand, this criterion can have an over-conservatism nature. On the other hand, this criterion is consistent with data that have natural extreme values. The natural phenomenon can be represented by these extreme

values and no mistakes or different collection data methods has been made when collecting these extreme values.

6.2.2.2 Data Case B.

Data Case B uses boxplots as statistical tool to analyze the data to identify any outliers, and then decide to exclude them. The boxplots identify outliers using the IQR value, which is based on the location of quartiles on the data distribution. The lower portion of outliers is composed of values at a distance larger than 1.5IQR from the first quartile. The upper portion of outliers is composed by values at a distance larger than 1.5IQR from the third quartile. Under this criterion, the outliers can be also graphically seen through boxplots. Figure 28 shows an example of boxplot and the IQR criterion.

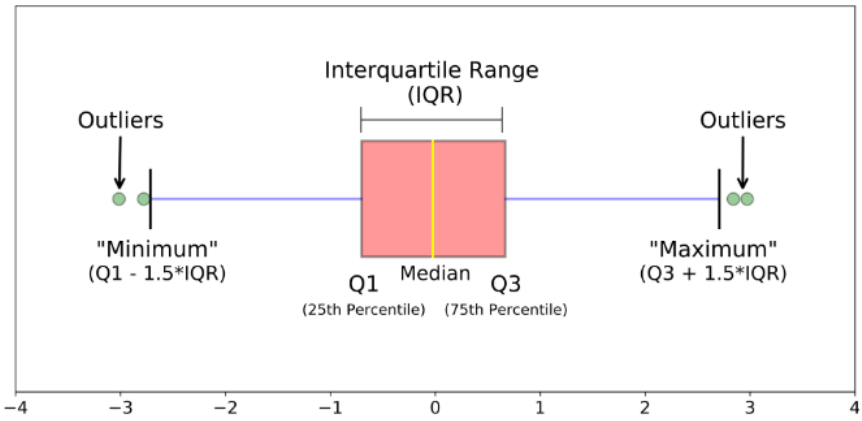

Figure 28: Different parts of a boxplot and the IQR criterion (Galarnyk, 2018).

In case no graphical tools are used, the following equations can be used once the quartiles are established:

$$IQR = Q3 - Q1, \tag{25}$$

$$Lower\ limit = Q1 - (1.5 * IQR), \text{and} \tag{26}$$

$$Upper\ limit = Q3 + (1.5 * IQR), \tag{27}$$

where *IQR* is the Interquartile Range, *Q1* is the first quartile, and *Q3* is the third quartile. The values that are not within the lower limit and the upper limit are considered outliers and shall be investigated.

6.2.2.3 Data Case C

Data Case C follows the statistical principle to analyze the data to identify any outliers using the two standard deviations criteria, and then deciding to exclude them. The two-standard deviations criterion is used in the NCHRP 507 [6]. It is based on considering the points from the data set located at a larger distance than two standard deviations from the mean in a normal distribution as outliers. In other words, the following equations can be used:

$$Lower\ limit = Mean - (2 * \hat{\sigma}) \text{ and} \tag{28}$$

$$Upper\ limit = Mean + (2 * \hat{\sigma}), \tag{29}$$

where $\hat{\sigma}$ is the standard deviation of the evaluated data sample. The values that are not within the lower limit and the upper limit are considered outliers and shall be investigated.

6.2.3 Type of distribution for random variables.

As stated before, random variables are the basis of the LRFD calibration. Any random variable is defined by its probability density function (pdf) and cumulative density function (cdf) [36]. A probability density function is essentially the representation of a continuous random variable. While several continuous variables exist, the main difference between them is the probability distribution [7]. Therefore, identifying the type of distribution for the random variable is vital for calibration purposes. Nowak and Collins [36] states that the most important type of random variable distributions used in structural reliability are the following: uniform, normal, lognormal, gamma, extreme type I, extreme type II, extreme type III, and Poisson. Nevertheless, Paikowsky et al [6] says that the resistance random variable can be taken as a normal or lognormal variable. AASHTO LRFD specifications [38] states that the load and resistance pdfs shall follow a

lognormal distribution. Moreover, Scott and Salgado [39] contend that loads and resistance variables found in geotechnical engineering must be represented by a lognormal distribution even if the variables do not follow a lognormal distribution. Scott and Salgado [38] justify this idea based on the two facts. The first one relies on the fact that load and resistance variables are always positive, which produces a lower limit but not an upper limit. This upper limit is usually unknown and is true usually for transient loads (live loads, wind loads, and earthquake loads). These transient loads are better represented by extreme type I or II distributions; however, these distributions require more information than the first and second moment (mean and variance), which is not typically available in the geotechnical field. Thus, these distributions generally do not represent the least biased distribution for loads. The second one relies on the fact that lognormal distribution represent transient loads better since it is completely defined by the first and second moment. Normal and lognormal distributions as well as the pdf and cdf concept are explained in the next section.

6.2.3.1 Probability density functions (pdf) and cumulative distribution function (cdf)

Allen et al [9] contends that probability density functions (pdfs) and cumulative distribution functions (cdfs) are necessary throughout the calibration procedure to statistically characterize the random variables used. Basically, the pdf represents the probability of occurrence for certain ranges. *Taking the integral of a pdf between two values yields the probability of the random variable being within those limits. Consequently, integrating a pdf from negative infinity to positive is always 1* [7]. For continuous random variables, the *probability function is defined as the first derivative of the cdf* [36].

The cumulative distribution function (cdf) *represents the integration of a probability density function (pdf) from negative infinity up until the function point. The cdf symbolizes the probability that a random number is less than x. It will approach a value of 1 as x goes to positive infinity* [7].

This study uses Excel to compute the pdf and cdf of the random variables. Some useful functions related to pdf and cdf when working with random variables are shared by Styler [7] and found in Table 15.

Table 15: Microsoft Excel Random Variables (Styler, 2006)

Excel Function	Description
=NORMDIST(x, m_x, σ_x, True/False)	This function is for a normal random variable. If the parameter is True, it uses the cdf function. If False, it uses the pdf function.
=NORMINV(probability, m_x, σ_x)	This is the inverse of the cdf function. It returns the location on the pdf at which an integration from negative infinity would yield the given probability.
=NORMSDIST(x)	This is the cdf for a normally distributed variable with a mean of 0 and a standard deviation of 1.
=NORMSINV(x)	This is the inverse of the cdf with a mean of 0 and standard deviation of 1.
=LOGNORMALDIST(x, ξ_x, ζ_x)	This is the cdf for a lognormal distribution with the given lognormal mean and standard deviation.
=LOGINV(probability, ξ_x, ζ_x)	This is the inverse of the lognormal cdf.

6.2.3.2 Normal probability distribution

The normal or Gaussian probability distribution for random variables is the most common in the structural reliability field [36]. The pdf for a normal random variable X is:

$$f_x(x) = \frac{1}{\sigma_x\sqrt{2\pi}} \exp\left[-\frac{1}{2}\left(\frac{x-\mu_x}{\sigma_x}\right)^2\right], \tag{30}$$

$$f_x(x) = \frac{1}{\sigma_x\sqrt{2\pi}} \exp\left[-\frac{1}{2}\left(\frac{x-\mu_x}{\sigma_x}\right)^2\right], \tag{31}$$

where $f_x(x)$ is the pdf of the normal variable X. The cdf of the same normal random variable X is:

$$F_x(x) = F_x\left(\frac{x-\mu_x}{\sigma_x}\right) = F_z(z), \tag{32}$$

where $F_x(x)$ is the cdf of the normal variable X, and $F_z(z)$ is the cdf of the standard normal variable Z. Figure 29 and 30 show the general shape of both the pdf and cdf of a normal random variable.

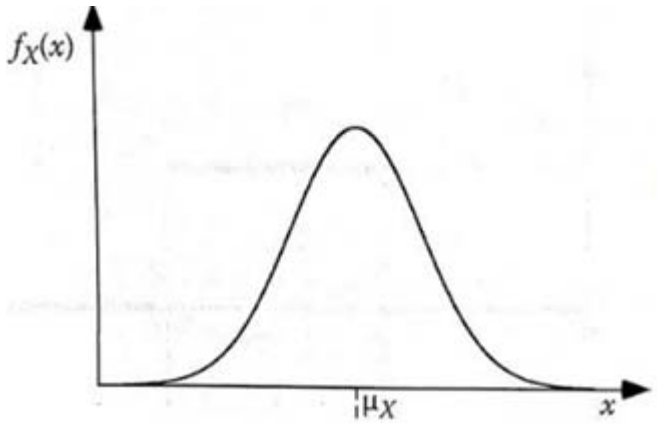

Figure 29: Example of pdf of a normal random variable (Nowak and Collins, 2013).

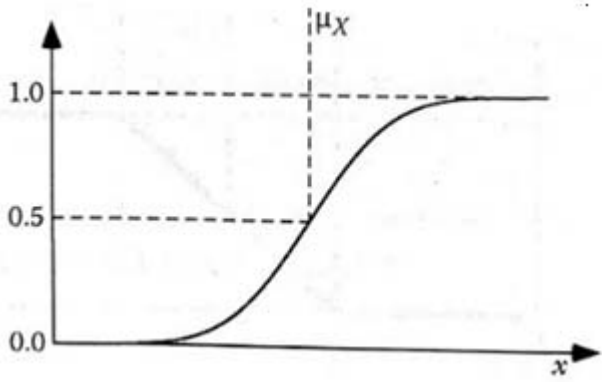

Figure 30: Example of cdf of a normal random variable (Nowak and Collins, 2013).

In case of standard normal variables, the pdf can be computed as follows:

$$\phi(z) = \frac{1}{\sqrt{2\pi}} \exp\left[-\frac{1}{2}(z)^2\right] = f_z(z), \quad (33)$$

and the cdf of standard normal variable is denoted by Φ(z).

Furthermore, Nowak and Collins [36] state that the normal random variable distribution has the following properties:

1. The pdf $f_x(x)$ is symmetrical about the mean.

$$f_x(\mu_x + x) = f_x(\mu_x - x) \quad (34)$$

2. The sum of $F_x(\mu_x + x)$ and $F_x(\mu_x - x)$ is equal to 1.

$$F_x(\mu_x + x) + F_x(\mu_x - x) = 1 \quad (35)$$

3. Due to it symmetry property, the cdf of the standard normal variable satisfies the following equation:

$$\Phi(z) = 1 - \Phi(z) \quad (36)$$

6.2.3.3 Lognormal probability distribution

The lognormal probability distribution for random variables is also one of the most important within the structural field. Also, the lognormal probability distribution for random variables is one of the distributions considered in NCHRP 507 [6] for calibrating LRFD resistance factor for piles. Nowak and Collins [36] say that the random normal variable X has a lognormal distribution if $Y = \ln(x)$ is normally distributed. A lognormal random variable is usually characterized for being composed of only positive values. (x > 0). The lognormal basic parameter such us the mean and standard deviation can be calculated as follows [36]:

$$\sigma_{ln-x}^2 = \ln(COV_x^2 + 1) \text{ and} \quad (37)$$

$$\mu_{;n-x} = \ln(\mu_x) - \frac{1}{2}\sigma_{ln-x}^2. \quad (38)$$

The pdf and cdf can be calculated using distributions ϕ(z) and Φ(z), respectively, for the standard normal variable Z as follows:

$$F_x(x) = P(X \leq x) = P(ln\, X \leq ln\, x) = P(Y \leq y) = F_y(y). \quad (39)$$

The pdf can be calculated as follows:

$$f_x(x) = \frac{1}{x\sigma_{ln-x}} \phi\left(\frac{\ln(x) - \mu_{ln-x}}{\sigma_{ln-x}}\right), \quad (40)$$

where y = ln(x), $\mu_y = \mu_{ln\text{-}x}$= mean value of ln(x), and $\sigma_y = \sigma_{ln\text{-}x}$ = standard deviation of ln(x). Figure 31 shows an example of pdf for a lognormal random variable. Since *y* is normally distributed, the cdf can be calculated as follows:

$$F_x(x) = F_y(y) = \Phi\left(\frac{y - \mu_y}{\sigma_y}\right). \quad (41)$$

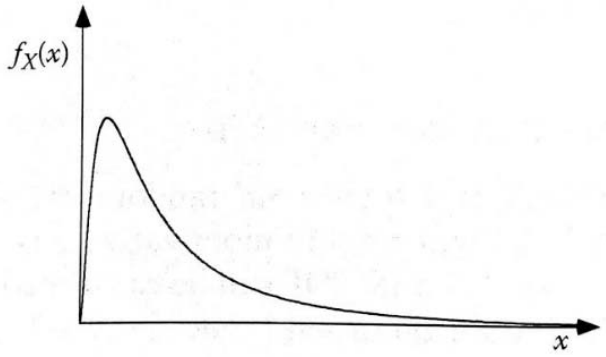

Figure 31: Example of pdf of a lognormal random variable (Nowak and Collins, 2013).

6.2.4 Target Reliability Index.

AbdelSalam et al. [22] declares that, for LRFD specifications, the target reliability index (β_T) is defined as *the measure of safety associated with a probability of failure (P_f).* In other words, the reliability index determines the magnitude of the load and resistance

factors because it measures the probability of failure (P_f). In this way, *the probability of failure represents the probability for the condition at which the resistance multiplied by the resistance factors will be less than the load multiplied by the load factors* [6]. Rosenbleuth et al. [40] suggests an equation that relates the probability of failure (P_f) and the reliability index (β) with reasonable proximity, seen as,

$$P_f = 460e^{-4.3\beta}. \quad (42)$$

6.2.5 Load factors.

An estimate of the load factor should be set before starting the resistance factor calibration. Since loads are generally better known than resistances, the load effect usually has a smaller variability than the resistance. Many load combinations can be developed according to the reliability index β or probability of failure desired P_f. In LRFD specifications, the load factors should be larger than 1.0 and the resistance factors should be less than 1.0. Nevertheless, in some cases, this might not be possible due to the grade of conservatism of the prediction methods considered for load and resistance [9].

It is possible to estimate the load factor using the following equation,

$$\gamma_Q = \lambda_Q(1 + n_\sigma COV_Q), \quad (43)$$

where γ_Q is the load factor, λ_Q is the bias factor for the load, COV_Q is the coefficient of variation of the ratio of measured to predict load, and n_σ is a constant representing the number of standard deviations from the mean needed to obtain the desired probability if exceedance. The Ontario Highway Bridge Design Code and AASHTO LRFD Bridge Design specifications [38] suggest using $n_\sigma = 2$.

Moreover, the dead-to-live ratio considered for load combinations on bridges depends on the deck lengths and it has a small influence on the calculated resistance factors. Paikowsky et al. [6] suggest using a value between 2 and 2.5.

6.3 FOSM calibration concept and procedure

The First Order Second Moment (FOSM) is a closed form solution and a probabilistic reliability method [41]. It is called FOSM because it is *a first-order expansion about the mean value and a linear approximation of the second corrected moment (variance)* [42]. This method was developed largely by Cornell [43] and Lind [44]. FOSM belongs to the level II of probabilistic-based analysis. FOSM is one of the two methods used by AASHTO specifications [38] for calibrating LRFD resistance factors. This method involves the consideration of statistical characteristics such as the mean, standard deviation, and coefficient of variation (COV) to describe the probability functions of the load and resistance variables. FOSM assumes that the load and resistance random variables are modeled following a lognormal distribution [7]. The procedure is listed below:

Step 1: Obtain the bias mean, standard deviation, and COV of the load and resistance values independently using equations 21 to 24. Moreover, the load factors for the dead load and live loads shall be known.

Step 2: Establish the target reliability index based on the probability of failure desired. Both concepts are explained in section 4.2.4.

Step 3: According to Cornell [42] and Lind [43], the following equation can be used to compute the resistance factor:

$$\phi_R = \frac{\lambda_R\left(\frac{\gamma_{QD} Q_D}{Q_L} + \gamma_{QL}\right)\sqrt{\left[\frac{1 + COV_{QD}^2 + COV_{QL}^2}{1 + COV_R^2}\right]}}{\left(\frac{\lambda_{QD} Q_D}{Q_L} + \lambda_{QL}\right)\exp\{\beta_T\sqrt{\ln[(1 + COV_R^2)(1 + COV_{QD}^2 + COV_{QL}^2)]}\}}, \quad (44)$$

where ϕ_R is the calibrated resistance factor, λ_R is the mean resistance bias factor, λ_{QD} is the dead load bias factor, λ_{QL} is the live load bias factor, β_T is the target reliability index, COV_{QD} is the coefficient of variation for dead load, COV_{QL} is the coefficient of variation for live load, and COV_R is the coefficient of variation for resistance.

6.4 FORM calibration concept and procedure

FORM means First Order Reliability Method (FORM) because it is based in the first-order terms in the Taylor series expansion, where only means and variances are required [36]. NCHRP 507 [6] states that the structural design codes used FORM calibration, hence Geotechnical resistance factors shall follow the same methodology in order to be consistent when using the load factors. In addition, the same report [6] mentions that FORM resistance factors are about 10% higher than FOSM resistance factors. The procedure listed in this report follows the actual FORM procedure (not Hasofer-Lind method), which is based on Styler thesis [7]; and Phoon, Kulhawy, and Grigoriu's paper [45].

Step 1: Define the failure equation

The failure equation is adapted from the limit state equation and consists on the relation used to represent a specific limit state of a system of variables. Failure takes place when the failure equation is less than or equal to zero. The failure equation is usually the difference between the resistance and the load random variables:

$$G = R - Q, \tag{45}$$

where R is the resistance random variable and Q is the load random variable. Thus, When G is less than or equal to zero, failure of the system occurs. It should be noted that no loading factors are used in this equation. These R and Q random variables are function of the bias factor variables:

$$R = r_n * \lambda_R \text{ and} \tag{46}$$

$$Q = \left(q_D * \lambda_{QD}\right) + (q_L \lambda_{QL}), \tag{47}$$

where r_n is the nominal (predicted) resistance, q_D is the dead load value, and q_L is the live load value.

Step 2: Choose random variable distributions

The distributions of the random variables will typically be considered as normal or lognormal. The case of calibration of driven piles, Paikowsky et al [6] suggests taking bias factors as lognormal random variables. However, Styler [7] suggest performing a chi-squared test to justify a chosen random variable.

Step 3: Choose LRFD factors to analyze

The probability of failure is based on the load factors, the specific reliability index, and the dead to live load ratio. Usually, load factors are specified by organization. The case of driven pile reliability indices and dead to live ratios, the values are discussed and stated by Paikowsky et al [6]. When using the FORM calibration, a resistance factor is computed for its corresponding reliability index. Therefore, multiple resistance factors will be required to be computed to match the target reliability index.

Styler [7] contends that the design space is separated from the failure space due to the load and resistance factors. A design point is based on the LRFD limit equation; however, the randomness of the bias factors results in unknown exact resistance and load values. FORM method determines the probability that the actual resistance and load occurs within the failure space for a specific design that takes place on the boundary of the acceptable design space. The slope of the design space can be computed from the dead to live load ratio and the load and resistance factors as follows:

$$\phi_R * r_n = (\gamma_{QD} * q_D) + (\gamma_{QL} * q_L)\,, \tag{48}$$

$$q_D/q_L = \eta\,, \tag{49}$$

$$\phi_R * r_n = (\gamma_{QD} * \eta * q_L) + (\gamma_{QL} * q_L), \tag{50}$$

$$\phi_R * r_n = q_L(\eta * \gamma_{QD} * \gamma_{QL}), \tag{51}$$

$$q_L = \frac{\phi_R * r_n}{\eta * \gamma_{QD} + \gamma_{QD}}\,, \tag{52}$$

$$q_D = \eta * q_L = \frac{\eta * \phi_R * r_n}{\eta * \gamma_{QD} + \gamma_{QD}}\,, \text{and} \tag{53}$$

$$Slope = \frac{q}{r} = \frac{q_D + q_L}{r_n} = \frac{\frac{\eta * \phi_R * r_n}{\eta * \gamma_{QD} * \gamma_{QL}} + \frac{\phi_R * r_n}{\eta * \gamma_{QD} + \gamma_{QL}}}{r_n} = \frac{\phi_R}{\eta * \gamma_{QD} + \gamma_{QL}}(\eta + 1), \quad (54)$$

where γ_{QD} is the dead load factor, γ_{QL} is the live load factor, η is the dead-to-live load ratio.

Step 4: Calculate the initial design point

The FORM calibration starts at this step. Using the given nominal resistance and dead to live load ratio, the dead and live loads can be computed as follows:

$$\phi_R * r_n = (\gamma_{QD} * q_D) + (\gamma_{QL} * q_L), \quad (55)$$

$$\frac{q_D}{q_L} = \eta, \quad (56)$$

$$q_D = \eta * q_L, \quad (57)$$

$$\phi_R * r_n = q_L(\gamma_{QD}\eta + \gamma_{QL}), \text{ and} \quad (58)$$

$$q_L = \frac{\phi_R * r_n}{\gamma_{QD} * \eta + \gamma_{QL}}, \quad (59)$$

As mentioned before, the resistance and load random variables are function of the lognormal bias random variables.

$$R = r_n * \lambda_R \text{ and} \quad (60)$$

$$Q = q_D * \lambda_{QD} + q_L * \lambda_{QL}. \quad (61)$$

Likewise, the expected values for the *R* and *Q* random variables are calculated using the following equations:

$$E[R] = r_n * \lambda_R \text{ and} \quad (62)$$

$$E[Q] = (q_D * \lambda_{QD}) + (q_L * \lambda_{QL}) \quad (63)$$

where $E[R]$ is the expected value of the resistance random variable, and $E[Q]$ is the expected value of the load random variable. Then, the normal standard deviation for the resistance and load can be computed as follows:

$$\sigma_R = r_n \sigma_{\lambda R} \text{ and} \quad (64)$$

$$\sigma_Q = \sqrt{q_D^2 \sigma_{\lambda D}^2 + q_L^2 \sigma_{\lambda L}^2} \quad (65)$$

where σ_R is the standard deviation of the resistance R, σ_Q is the standard deviation of the load Q, $\sigma_{\lambda R}$ is the standard deviation of the resistance dataset, $\sigma_{\lambda D}$ the standard deviation of the dead load dataset, and $\sigma_{\lambda Q}$ the standard deviation of the live load dataset.

Step 5: Transform into an equivalent normal distribution

In this step, it is necessary to transform an equivalent normal distribution using the design point (*r, q*). For the first iteration, the design point is equal to the expected resistance and load random values (*E[R], E[Q]*). The mean and standard deviation can be computed with the following equations:

$$\sigma_{RN} = \frac{\phi(\Phi^{-1}(F_R(r)))}{f_R(r)}, \tag{66}$$

$$[R_N] = r - \Phi^{-1}(F_R(r))\sigma_{RN}\,, \tag{67}$$

$$\sigma_{QN} = \frac{\phi\left((\Phi^{-1}\left(F_Q(q)\right)\right)}{f_q(q)}\,, \text{and} \tag{68}$$

$$[Q_N] = q - \Phi^{-1}(F_Q(q))\sigma_{QN}\,, \tag{69}$$

Where $E[R_N]$ is the expected equivalent normal random variable for the resistance, and $E[Q_N]$ is the expected equivalent normal random variable for the load. The function Φ^{-1} represents the inverse of the standard cumulative distribution function. $F_R(r)$ represents the cumulative function for random variable R. It should be noted that the pdf depends of the chosen distribution.

Styler [7] says that when FORM is performed, the lognormal random variable is positively biased, and the mean of the resulting normal random is lower.

Step 6: Transform original random variables to standard normal random variables

To perform this transformation, the following equations are required:

$$R_{SN} = \frac{R - E[R_N]}{\sigma_{RN}} \text{ and} \tag{70}$$

$$Q_{SN} = \frac{Q - E[Q_N]}{\sigma_{QN}}, \tag{71}$$

where R and Q are the original lognormal random variables, and R_{SN} and Q_{SN} are the standard normal random variables for resistance and load, respectively. In the same way, the design point shall be transformed from real space to standard normal random variable space. It should be noted that in the first iteration, the design point in real space is the most probable values of the resistance and load lognormal random variables. In other words, the design point is the mode of the lognormal distribution. Thus, the standard normal space design point shall be calculated from the real space design point using the following equations:

$$r = \frac{E[R] - E[R_N]}{\sigma_{RN}} \text{ and} \tag{72}$$

$$q = \frac{E[Q] - E[Q_N]}{\sigma_{QN}}. \tag{73}$$

Step 7: Rewrite the failure in terms of the standard normal random variables

It is important to transform the failure equation to standard normal random variables using the following equations:

$$G = R - Q \text{ and} \tag{74}$$

$$G' = (R_{SN}\sigma_{RN} + E[R_N]) - (Q_{SN}\sigma_{QN} + E[Q_N]). \tag{75}$$

Step 8: Compute a new trial design point

Styler [7] states that a new trial design point (r^*, q^*) shall be computed using the following equations:

$$r^* = \frac{(-E[R_N] + E[Q_N])\sigma_{RN}}{(\sigma_{RN})^2 + (\sigma_{QN})^2} \text{ and} \tag{76}$$

$$q^* = \frac{(-E[R_N] + E[Q_N])\sigma_{QN}}{(\sigma_{RN})^2 + (\sigma_{QN})^2}. \tag{77}$$

This new design point represents the closest distance from the origin to this failure line. It should be noted that the failure line barely varies after each iteration.

Step 9: Calculate the reliability index.

The reliability index is the closest distance from the origin to the failure line and can be calculated as follow:

$$\beta = \sqrt{(r^*)^2 + (q^*)^2}. \tag{78}$$

Step 10: Repetitive iteration (FORM iteration)

The new design point shall be transformed back to the real space using the following equations:

$$r = r^* \sigma_{RN} + E[R_N] \text{ , and} \tag{79}$$

$$q = q^* \sigma_{QN} + E[Q_N] \tag{80}$$

Then, recalculate the equivalent normal distribution using this new design point (*r, q*). This procedure must be repeated until the reliability index β remains stable as shown in the Figure 32.

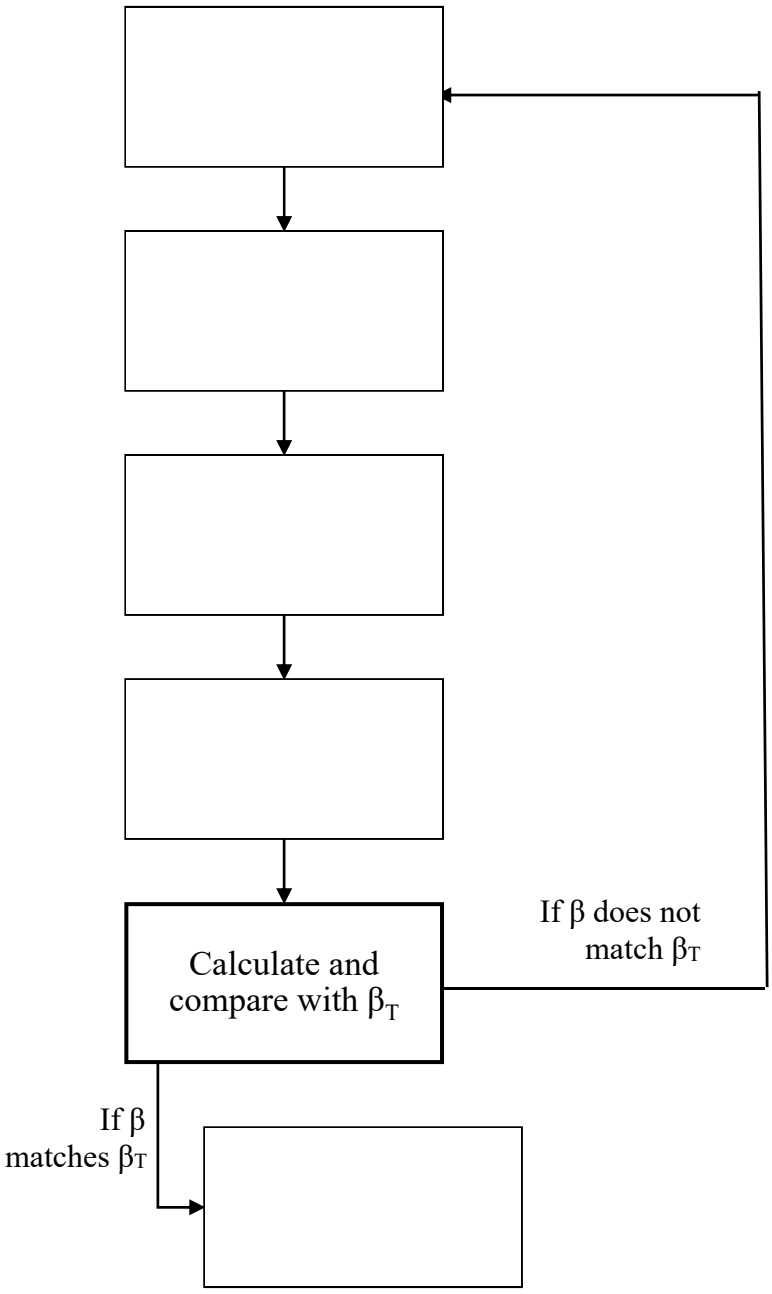

Figure 32: Iteration procedure flowchart from Step 9.

Finally, the resistance factor established in the step 3 shall be altered until the reliability index β matches the target reliability index β_T. The resistance factor that satisfies the target reliability index is the final FORM calibrated resistance factor.

6.5 Monte Carlo simulation concept and procedure

Nowak and Collins [36] mention that the basic idea of the Monte Carlo Simulation (MCS) is based on *numerically simulating some phenomenon and then observing the number of times some event of interest occurs*. Moreover, Allen et al [9] states that *Monte Carlo Simulation is simply a tool to curve fit and extrapolate available measured statistical data; in this case, load and resistance data, or more generally, for any random variable that affects the outcome of a limit state calculation*. According to Nowak and Collins [36], the Monte Carlo Simulation is generally applied to the following cases:

- It is used when closed-form solutions are not possible or extremely difficult.
- It is used when closed-form solutions require too many simplifying assumptions.
- It is used to revise the results provided from other solution techniques.

The Monte Carlo procedure stated in this report is extracted from Allen et al. [9] and Reddy and Stuedlein [45] in order to present a detailed and understandable procedure. MCS calibration is performed to revise the resistance and efficiency factors from FOSM and FORM in this study. The procedure is listed below.

Step 1: It is first important to establish a limit state function. According to AASHTO [47], for geotechnical and structural design, the basic limit state function is expressed as:

$$\phi_R R_n \geq \sum_{j=1}^{k} \gamma_Q Q_n \,. \tag{81}$$

This equation represents failure when the applied loads are equal to the available resistance. However, Reddy and Stuedlein [46] contend that for calibration purposes, the limit state equation shall be expressed in terms of distribution in the margin of safety (g_i), and the load and resistance biases as [48]:

$$g_i = \lambda_{R,i} \frac{\gamma_{avg}}{\varphi_R} - \lambda_{Q,i} \geq 0\,, \tag{82}$$

where γ_{avg} is a weighted load factor representing multiple load sources and λ_Q is the bias of the applied load. Stuedlein et al. [49] says that in case of multiple load sources (such as bridges and other superstructures), λ_Q can be computed as follows:

$$\lambda_{Q,i} = \lambda_Q = \frac{\lambda_{QD}\eta + \lambda_{QL}}{\eta + 1}, \tag{83}$$

where λ_{QD} is the bias for dead loads, λ_{QL} is the bias for live loads, and η is the ratio of the dead to live load. Stuedlein et al. [49] adds that in cases of having multiple loads, a weighted load factor may be used:

$$\Upsilon_{avg} = \frac{\lambda_{QD}\gamma_{QD}\eta + \lambda_{QL}\gamma_{QL}}{\lambda_{QD}\eta + \lambda_{QL}}, \tag{84}$$

where $\gamma_{Q,D}$ is the dead load factor, and $\gamma_{Q,L}$ is the live load factor.

Step 2: Establish the reliability-target value β_T, which is a function of the probability of failure p_f. Paikowsky et al. [6] indicates that redundant piles (groups of 5 piles or more) require a β_T of 2.33. On other hand, non-redundant piles require a β_T of 3.0.

Step 3: Establish the number of simulations (*N)* required prior to performing the simulation. This can be calculated according to the true probability of failure $P_{f\ true}$ established, which corresponds to the target reliability index, and the coefficient of variation of the estimate probability V_p as follows:

$$N = \frac{1 - P_{f\ true}}{\left(V_p^2\right) * P_{f\ true}}. \tag{85}$$

Step 4: The data is extrapolated (simulation) following the distributions of the two variables *Q* and *R*. This simulation is performed considering three statistical parameters that characterize the data: mean, standard deviation, and cumulative distribution function (cdf). It should be noted that the closed-form methods use just the mean and the standard deviation. In case of load and resistance values, they may be considered as normal or lognormal random variables.

In case Q has a normal distribution, randomly determined data shall be generated in accordance to the specified distribution characterized by a mean, a standard deviation, and a coefficient of variation using a random number generator as shown below [36]:

$$Q_i = \lambda_Q(1 + COV_Q z_{i-Q}) , \quad (86)$$

where Q_i is a randomly generated value of Q using a specified set of statistical parameters, z_i is the inverse normal function of u_{ia} and is equal to $\Phi^{-1}(u_{ia})$, u_{ia} is a random number between 0 and 1 representing a probability of occurrence.

In case Q has a lognormal distribution, randomly determined data shall be generated in accordance to the specified distribution characterized by lognormal mean, a lognormal standard deviation, and a coefficient of variation using a random number generator as shown below [36]:

$$Q_i = exp(\mu_{ln-Q} + \sigma_{ln-Q} z_{i-Q}) \text{ and} \quad (87)$$

where:

$$\mu_{ln-Q} = LN(\lambda_Q) - 0.5\sigma_{ln-Q}^2 , \text{and} \quad (88)$$

$$\sigma_{ln-Q} = \left\{LN\left[\left(COV_Q\right)^2 + 1\right]\right\}^{0.5} . \quad (89)$$

Similarly, the resistance values R have a lognormal distribution. Thus, randomly determined data shall be generated in accordance to the specified distribution characterized by a mean, a standard deviation, and a coefficient of variation using a random number generator as shown below:

$$R_i = \exp(\mu_{ln-R} + \sigma_{ln-R} z_{i-R}) , \quad (90)$$

where:

$$\mu_{ln-R} = LN(\lambda_R) - 0.5\sigma_{ln-R}^2 , \quad (91)$$

$$\sigma_{ln-R} = \{LN[(COV_R)^2 + 1]\}^{0.5}, \quad (92)$$

and where R_i is a randomly generated value of R using a specified set of statistical parameters, z_i is the inverse normal function of u_{ib} and is equal to $\Phi^{-1}(u_{ib})$, u_{ib} is a random number between 0 and 1 representing a probability of occurrence.

It is important to mention that the random numbers u_{ia} and u_{ib} shall be generated independently assuming that Q and R are independent variables [9].

Step 5: Once the simulated data for each distribution has been generated, set a trial resistance factor and the limit state function g is computed for each couple of Q and R values.

Step 6: Determine the probability of failure of the simulation performed using the following equation:

$$P_f = \frac{n}{N}, \tag{93}$$

where n is the number of times that a particular criterion is achieved. In this case n is the number of times when g is lower than zero (which indicates failure). N is the number of simulations performed.

Step 7: Calculate the reliability index using the probability of failure computed in the previous step. It can be calculated in Microsoft Excel using the function NORMSINV as shown:

$$\beta = NORMSINV(P_f). \tag{94}$$

Step 8: Set different values for the resistance factor until β and β_T converge. The final resistance factor has been calculated.

6.6 Reliability Based Efficiency factor.

The values of the calibrated resistance factor alone do not represent an objective measurement of the design method efficiency. Such efficiency can be better measured if the efficiency factor is considered [31], which can be calculated as follows:

$$Efficiency\ factor = \frac{\phi_R}{\lambda_R}, \tag{95}$$

where ϕ_R is the calibrated resistance factor by each method, and λ_R is the mean bias resistance. According to NCHRP 507 [6] and Figure 33, the *efficiency factor is systematically higher for methods which predict more accurately regardless of the bias*. In this way, a design or prediction method can be more efficient only if its variability

(COV) is reduced. The ideal method would have a bias factor of 1, a COV of 0, hence a resistance factor of 0.80. It is suggested to choose the design methods according to their COV [6].

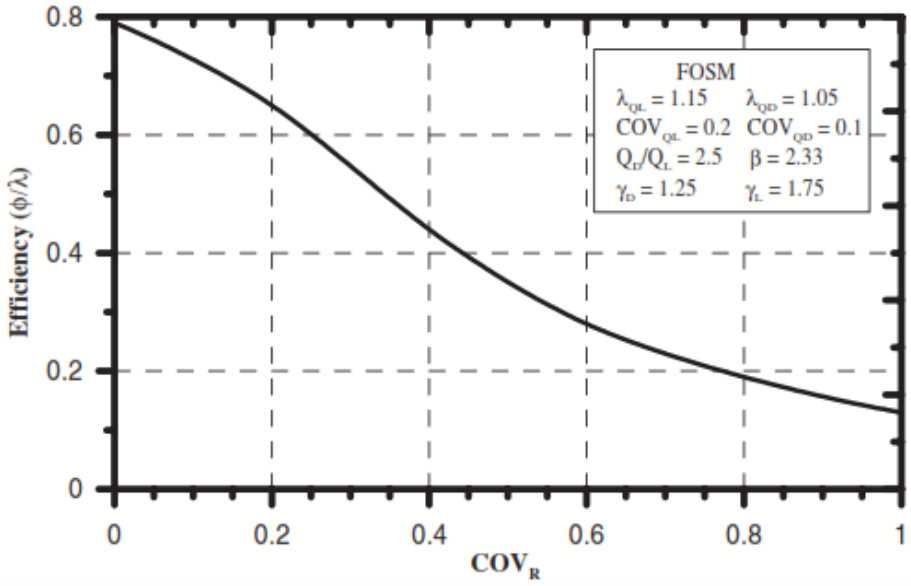

Figure 33: Illustration of the efficiency factor as a measure of the effectiveness of a design method when using resistance factors (Paikowsly et al, 2004)

Jabo [50] adds that computing a higher resistance factor does not necessarily imply an efficient pile design method. While reducing the standard deviation (σ) value would always improve the precision of the prediction method, increasing the λ_R could make prediction overestimate the pile capacity. Therefore, the economy factor of the structure would be affected. In addition, Jabo [49] states that the design equation for an axial pile can be rewritten as follows:

$$P_{design} = \phi_R R_n, \quad (96)$$

where P_{design} is the design pile capacity, ϕ_R is the calibrated resistance factor, and R_n is the nominal resistance of the pile. If the resistance bias factor λ_R is defined as the ratio of

measured resistance (R_m) to predicted nominal resistance (R_n), the equation 95 can be modified as follows:

$$P_{design} = \left(\frac{\phi_R}{\lambda_R}\right) R_m. \quad (97)$$

Using this relationship, Jabo [49] demonstrates that *only a portion of the measured capacity is allowed for design to meet the required reliability level*. Consequently, the efficiency factor can efficiently quantify the performance of the pile design method. To put it briefly, a higher efficiency factor implies a better pile design method [51].

6.7 Summary of Calibration methodology.

This chapter illustrates the conceptual background behind the probabilistic methods applied to a LRFD calibration. The three probabilistic-based methods used in this study, which are FOSM, FORM, and MCS; involve the application of the information described in this chapter. In other word, random variables, bias values, target reliability indices, and pre-calibration considerations are defined prior to performing the LRFD calibration. The next chapter shows in actual example of the application of these concepts into a LRFD calibration.

CHAPTER VII - LRFD RESISTANCE FACTORS CALIBRATION

This chapters illustrates the way to conduct an actual calibration of LRFD resistance factors using FOSM, FORM, and MCS methodology. As explained in the next chapter, the random variables are defined as loads and resistance for this study. The bias values are calculated for each pile. Then, the mean, standard deviation, and coefficient of variation are calculated for each data set considering the data cases. While the loads have their statistical previously established according to NCHRP 507, the resistance statistical characteristics are calculated in this study. Moreover, the load factors are also pre-established according to NCHRP 507 as well as the target reliability index. These are the statistical characterization and pre-calibration considerations required to perform the LRFD calibration. Then, the actual LRFD calibration is performed using FOSM, FORM, and MCS methodology.

7.1 Pre-calibration considerations.

The LRFD calibration of resistance factors can performed once specific reliability levels and load characteristics have been established. Therefore, this section describes the target reliability index used in this study as well as the statistical parameter that represent the load variables.

7.1.1 Target Reliability Index.

The target reliability index represents the probability of failure desired. Therefore, it determines magnitude of the load and resistance factors for a LRFD calibration. In this project, the reliability index and probability of failure are obtained from the Federal Highway Administration [21], Paikowsky et al. [6], and Luna [3] as shown in Table 16.

Table 16: Reliability index values based on pile groups

Pile Group type	β	P*f*
Redundant (5 or more piles per pile cap)	2.33	1.00%
Intermediate point between redundant and non-redundant piles	2.50	0.99%
Non-redundant (4 or fewer piles per pile cap)	3.00	0.10 %

7.1.2 Dead and Live loads characterization.

Prior to performing the calibration of resistance factors, the statistical characteristics of the dead and lives loads shall be known as well as the load factors. In this report, the values used by AASHTO [38] and suggested by Paikowsky [6] are used. These values are shown in the Table 17.

Table 17: Load statistical values used.

Dead Load		Live Load	
Parameter	Recommended value	Parameter	Recommended value
λ_{QD}	1.050	λ_{QL}	1.150
COV_{QD}	0.100	COV_{QL}	0.200
$\sigma_{\lambda D}$	0.105	$\sigma_{\lambda L}$	1.230
γ_{QD}	1.250	γ_{QL}	1.750

In addition, Paikowsky et al. [6] indicates that a dead-to-live ratio of 2 or 2.5 is reasonable due to the small influence of this factor on the calibrated resistance factors. Therefore, in this report, the value for Q_D/Q_L is taken as 2 and can be also represented by the symbol η.

7.2 Statistical data characterization for WBUZPILE and DRIVEN.

This section shows the statistical characterization for the resistance random variable since it is required for LRFD calibration of resistance factors. The resistance data set is composed by the resistance bias values, which are basically the ratio of the measured resistance and the predicted resistance. In this section, the prediction methods consist of the design programs WBUZPILE and DRIVEN. The statistical characterization includes the type of probability distribution as well as the mean, standard deviation, and coefficient of variation for each data case.

7.2.1 Resistance random variable and bias.

As mentioned before, the random variables in this study are defined as loads and resistance. While the loads were statistically defined in the section 7.1.2, the resistance statistical characteristics shall be calculated using the data provided by ALDOT. Within the structural reliability field, the value used is the bias, which is the ratio of the measured resistance and the predicted resistance. In this way, the bias shall be calculated for each pile and each prediction method (WBUZPILE and DRIVEN) independently, as shown in Table 18.

Table 18: Resistance bias values for WBUZPILE and DRIVEN.

Pile	Type	λ_R DRIVEN	λ_R WBUZPILE
210	HP	2.294	0.965
3002	HP	0.833	1.110
3003	HP	1.862	0.991
4301	HP	0.817	0.369
4601	HP	1.231	0.753
6503	HP	0.316	0.518
Celeste Rd Bent 2	HP	0.346	0.379
Moores Mill Rd	HP	5.123	1.239
5702	HP	0.514	0.341
6502	HP	1.057	1.527
Celeste RD A1	HP	0.579	0.611
SR 41	HP	0.209	0.220
212	HP	0.599	0.521
1901	HP	2.157	1.486
5502	HP	2.187	1.304
6504	HP	0.602	0.641
213	HP	1.132	2.692
214	HP	1.900	2.038
301	HP	0.795	1.575
1101 (pre-splice)	HP	1.314	2.631
5501	HP	0.600	0.791
5703	HP	0.573	0.667
5704	HP	1.089	1.115
5705	HP	0.788	0.859
5801	HP	1.493	1.851
6303	HP	0.597	1.172
6501	HP	1.033	1.343
6506	HP	1.292	1.540
CBD Bridge A1	HP	2.383	1.593
CBD 7A Bent 2	HP	1.107	2.278
3001	HP	0.645	0.659
4001	HP	0.993	0.931
4801	HP	1.674	2.634
6301	HP	1.191	0.802
6302	HP	1.383	1.125
6304	HP	1.581	1.028

Table 18, cont.

Pile	Type	λ_R DRIVEN	λ_R WBUZPILE
201	Concrete	0.687	0.627
202	Concrete	1.050	0.850
206	Concrete	0.109	0.438
207	Concrete	0.849	0.598
211	Concrete	0.372	0.244
501	Concrete	0.481	0.710
502	Concrete	0.452	0.631
503	Concrete	0.762	0.710
504	Concrete	0.311	0.232
505	Concrete	0.545	0.423
5103	Concrete	0.678	0.667
204	Concrete	1.549	0.815
205	Concrete	0.485	0.302
506	Concrete	0.541	0.491
203	Concrete	0.464	0.220
208	Concrete	1.189	1.277
209	Concrete	0.762	0.354

Table 18 shows that the bias values for WBUZPILE range from 0.232 to 2.692 while the bias values for DRIVEN range from 0.316 to 5.123. Some of these bias values might be excluded due to the evaluation of data cases performed in the next section.

7.2.2 Data cases: Filtering data.

Filtering data from outliers in order to assess the quality of the provided data can be important for a LRFD calibration project. When an outlier is found, it must be investigated prior to its removal. Removing outliers without investigation is considered as data fixing, hence it is unethical and frowned upon. After reviewing the data and documents provided by ALDOT, it was noticed that no pile data point from WBUZPILE or DRIVEN satisfies the requirements to be excluded as an outlier according to Allen et al. [9]. In other words, the definitive resistance factors shall be calibrated with the entire

dataset. Nevertheless, this section still evaluates the magnitude of the effect of the data cases on the calibrated resistance factors. The data cases consist basically of filtering data from outliers in order to assess the quality of the provided data. An outlier is a data point that lies outside of the overall pattern in a distribution. Once the outlier is identified, it is excluded from the data set for this particular study. As stated in the previous chapter, the data cases evaluated are three. (A) All data set, (B) dataset without outliers based on boxplots, and (C) dataset without outliers based on $\bar{X} \pm 2SD$ criterion.

7.2.2.1 Data cases for all piles set.

This section shows the quality assessment the data for corresponding for the entire set of piles. The all piles data set includes 100% of the resistance bias values. In other words, the data set includes the 36 steel H-Piles and the 17 concrete piles data as one single group.

The data case B uses boxplots as graphical tool to identify outliers. Figure 34 box plot for WBUZPILE (all piles) and Figure 35 shows the boxplot for DRIVEN (all piles). These graphs mark outliers with an asterisk (*).

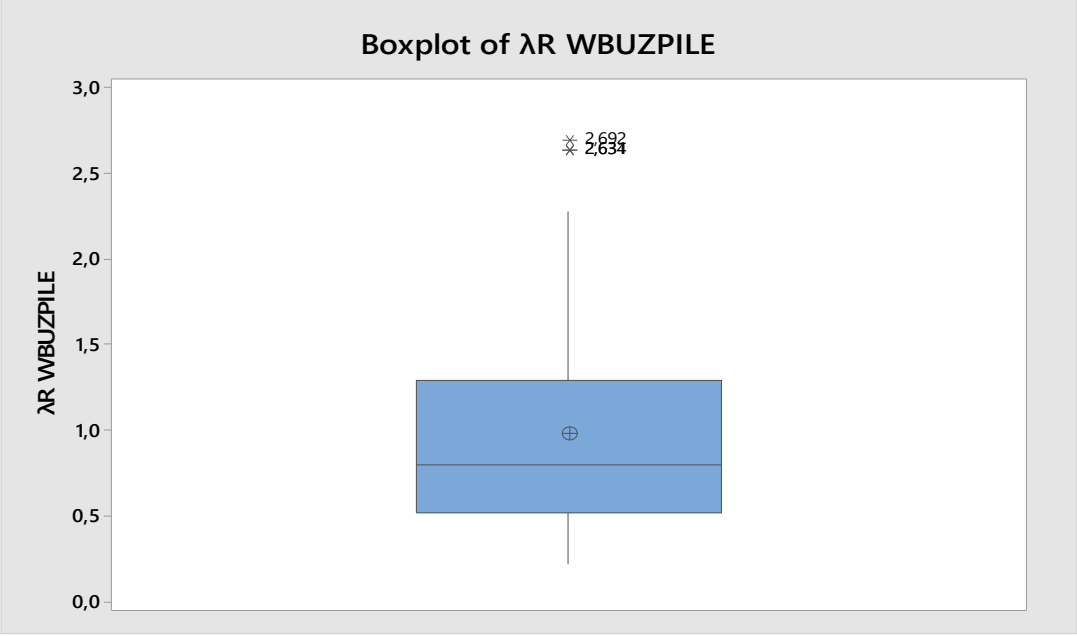

Figure 34: Boxplot of resistance bias values for WBUZPILE (All piles)

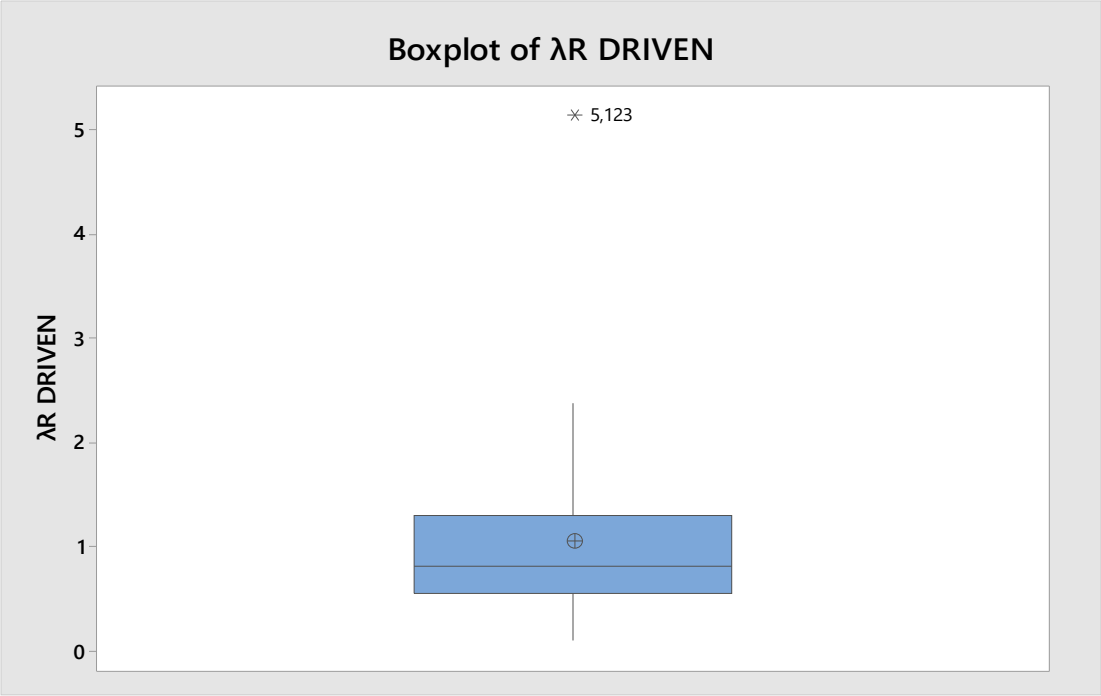

Figure 35: Boxplot of resistance bias values for DRIVEN (All piles)

As shown in Figures 34 and 35, the WBUZPILE data shows 3 outliers and the DRIVEN data shows 1 outlier for data case B.

The data case C uses the two standard deviations criterion to identify outliers. The outliers and excluded data points are 4 values for WBUZPILE data (all piles) and 1 value for DRIVEN data (all piles).

7.2.2.2 Data cases for steel H-piles set.

As stated before, filtering the data from outliers can be important to assess the quality of the provided data. This section illustrates the evaluation and exclusion of outliers for the steel H-Piles data set. The steel H-Piles dataset is composed by 36 driven steel H-Piles as a single group.

The data case B uses boxplots as graphical tool to identify outliers. Figure 36 box plot for WBUZPILE (steel H-piles) and Figure 37 shows the boxplot for DRIVEN (steel H-Piles). These graphs mark outliers with an asterisk (*).

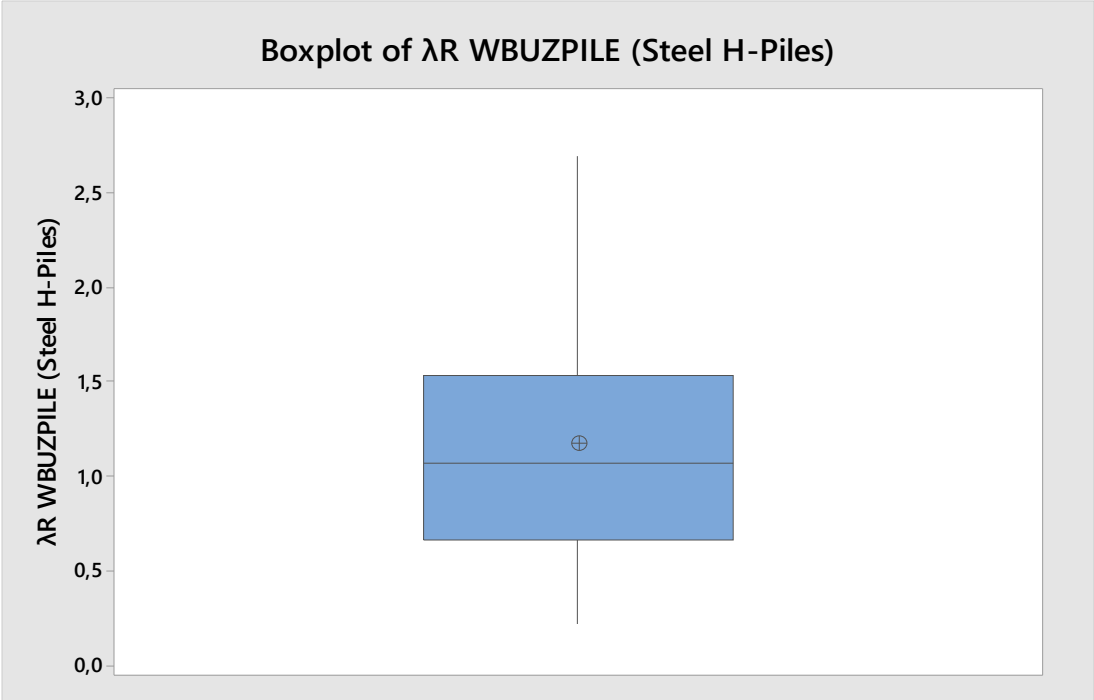

Figure 36: Boxplot of resistance bias values for WBUZPILE (Steel H-Piles)

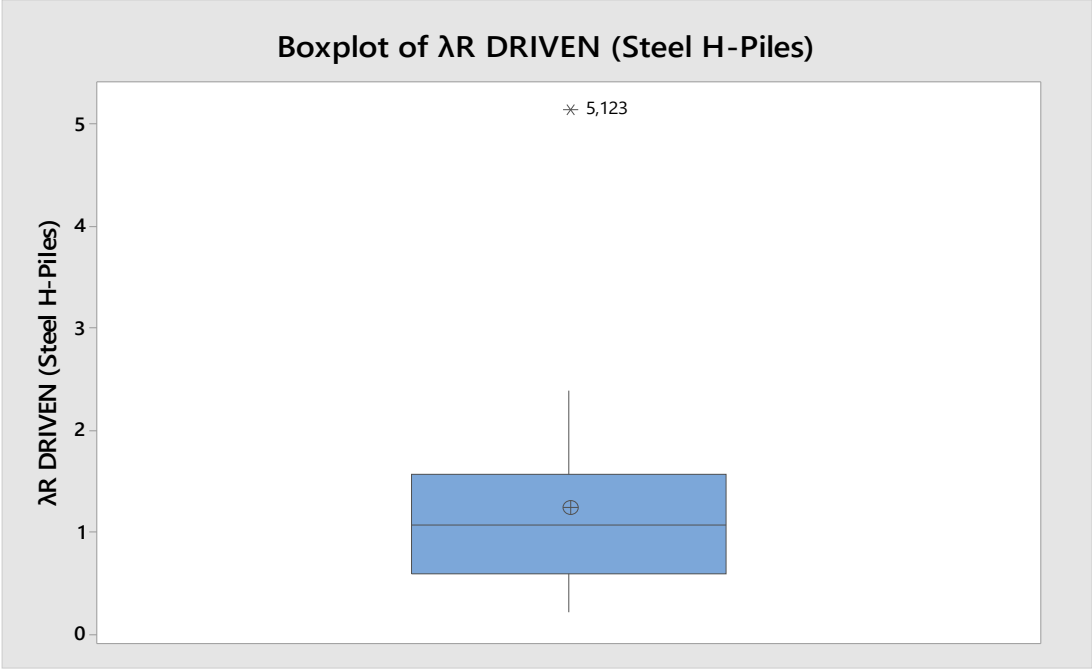

Figure 37: Boxplot of resistance bias values for DRIVEN (Steel H-Piles).

As shown in Figures 36 and 37, the WBUZPILE data (steel H-piles) shows no outliers and the DRIVEN data (steel H-Piles) shows 1 outlier for data case B.

The data case C uses the two standard deviations criterion to identify outliers. The outliers and excluded data points are 3 values for WBUZPILE data (steel H-piles) and 1 value for DRIVEN data (steel H-piles).

7.2.2.3 Data cases for concrete piles set.

As stated before, filtering the data from outliers can be important to assess the quality of the provided data. This section illustrates the evaluation and exclusion of outliers for the concrete piles data set. The concrete dataset is composed by 17 driven concrete piles as a single group.

The data case B uses boxplots as graphical tool to identify outliers. Figure 38 box plot for WBUZPILE (concrete piles) and Figure 39 shows the boxplot for DRIVEN (concrete piles). These graphs mark outliers with an asterisk (*).

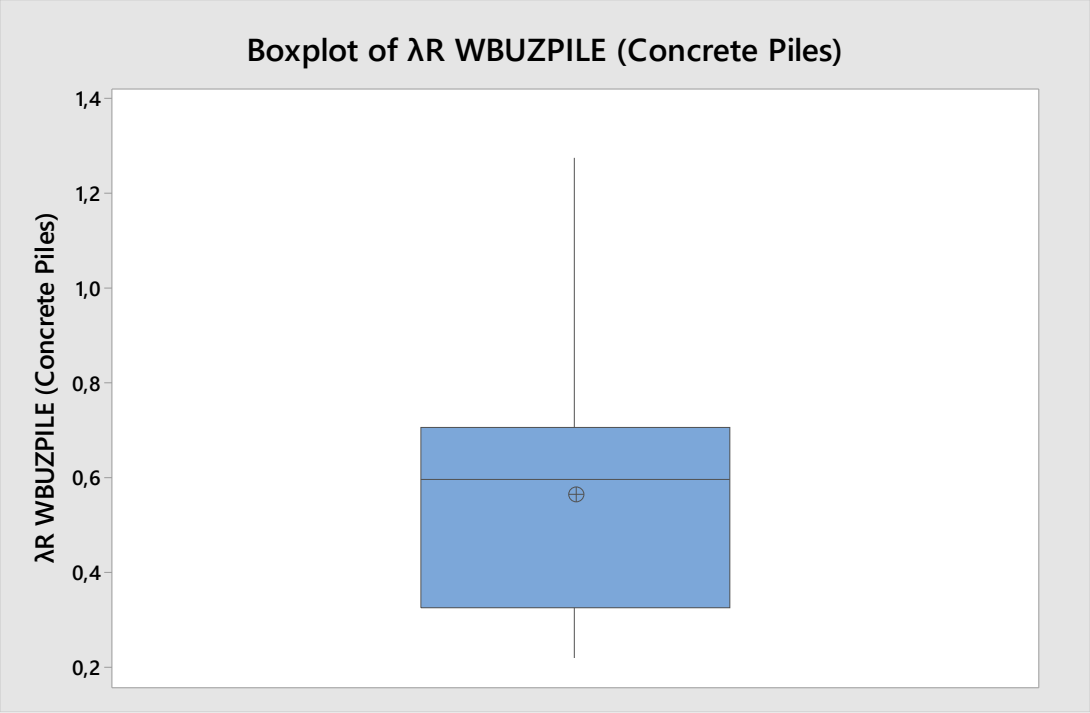

Figure 38: Boxplot of resistance bias values for WBUZPILE (Concrete Piles)

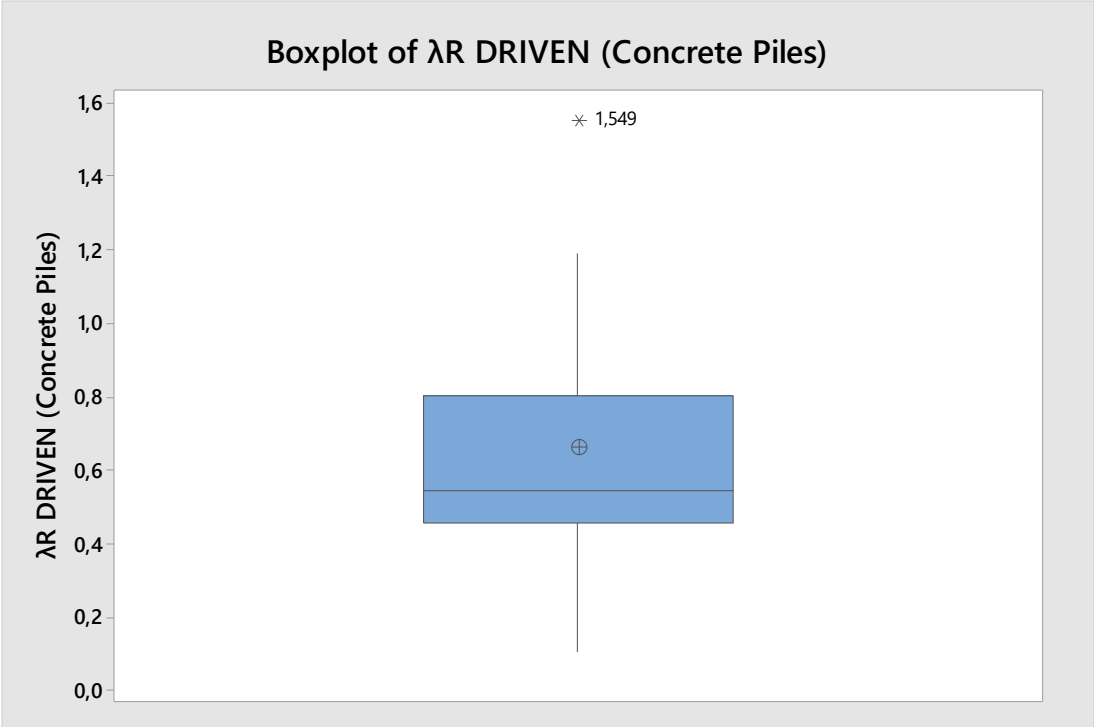

Figure 39: Boxplot of resistance bias values for DRIVEN (Concrete Piles).

As shown in Figures 38 and 39, the WBUZPILE data (concrete piles) shows no outliers and the DRIVEN data (concrete piles) shows 1 outlier for data case B.

The data case C uses the two standard deviations criterion to identify outliers. The outliers and excluded data points are 1 value for WBUZPILE data (concrete piles) and 1 value for DRIVEN data (concrete piles).

7.2.3 Type of probability distribution.

As previously stated, random variables are the basis of the LRFD calibration. Any random variable is defined by its probability density function (pdf) and cumulative density function (cdf) [35]. Moreover, the three reliability calibration methods utilized in this study require establishing the most accurate type of probability distribution.

While the most common type of distributions are uniform, normal, lognormal, gamma, extreme type I, extreme type II, extreme type III, and Poisson ; AASHTO LRFD specifications [38] and Scott and Salgado [39] suggest considering a lognormal distribution even if they are not lognormally distributed. Therefore, this study examines the data to determine if the data can be assumed as lognormal probability distributed with 95% as confidence interval.

This study considers the Anderson-Darling test and 95% Confidence Intervals (95% CI) performed the three data sets and three data cases to check the normality of each data group. The alternative hypothesis states that the data does not follow the specified distribution while the null hypothesis states that the data follows the specified distribution. The p-value represents how likely the studied data actually follows the corresponding distribution. Thus, if the p-value is very small, the alternative hypothesis is accepted, and the null is rejected. Table 19 shows the results of the normality tests.

Table 19: Anderson-Darling test results for WBUZPILE and DRIVEN

Design method	Data set	Data Case	Data size	Lognormal	
				AD	**p-value**
WBUZPILE	All piles	Data Case A	53	0.197	**0.884**
		Data Case B	50	0.319	**0.525**
		Data Case C	49	0.391	**0.367**
	Steel H-Piles	Data Case A	36	0.213	**0.841**
		Data Case B	36	0.213	**0.841**
		Data Case C	33	0.358	**0.433**
	Concrete Piles	Data Case A	17	0.358	**0.410**
		Data Case B	17	0.358	**0.410**
		Data Case C	16	0.544	**0.136**
DRIVEN	All piles	Data Case A	53	0.238	**0.771**
		Data Case B	52	0.275	**0.648**
		Data Case C	52	0.275	**0.648**
	Steel H-Piles	Data Case A	36	0.255	**0.708**
		Data Case B	35	0.343	**0.471**
		Data Case C	35	0.343	**0.471**
	Concrete Piles	Data Case A	17	0.431	**0.271**
		Data Case B	16	0.552	**0.129**
		Data Case C	16	0.552	**0.129**

As previously stated, the main variable to assess is the p-value since it represents how likely the studied data actually follows the corresponding distribution. In this way, the results illustrated in table 9 reveal that the probability of 95% CI (p-value) is greater than 0.05 for all data subsets. Consequently, the lognormal distribution is accepted for all data cases.

7.2.4 Mean, standard deviation, and coefficient of variation.

As stated before, filtering or not the data can produce a significant modification of the basic descriptive characteristics of the data. The mean, standard deviation, and COV are shown in Table 20 for all data cases.

Table 20: Resistance statistical characteristics for WBUZPILE and DRIVEN.

Statistical data summary for resistance R					
Design method	Data set	Statistical Parameter	Data case A	Data case B	Data case C
WBUZPILE	All data	Mean (λ_R)	0.979	0.879	0.850
		$\widehat{\sigma_{\lambda R}}$	0.633	0.493	0.455
		COV_R	0.646	0.561	0.535
	Steel H-Piles	Mean (λ_R)	1.175	1.175	1.041
		$\widehat{\sigma_{\lambda R}}$	0.662	0.662	0.505
		COV_R	0.563	0.563	0.486
	Concrete Piles	Mean (λ_R)	0.564	0.564	0.520
		$\widehat{\sigma_{\lambda R}}$	0.274	0.274	0.210
		COV_R	0.486	0.486	0.404
DRIVEN	All data	Mean (λ_R)	1.049	0.970	0.970
		$\widehat{\sigma_{\lambda R}}$	0.799	0.559	0.564
		COV_R	0.762	0.582	0.582
	Steel H-Piles	Mean (λ_R)	1.230	1.119	1.119
		$\widehat{\sigma_{\lambda R}}$	0.887	0.592	0.592
		COV_R	0.721	0.529	0.529
	Concrete Piles	Mean (λ_R)	0.664	0.609	0.609
		$\widehat{\sigma_{\lambda R}}$	0.350	0.274	0.274
		COV_R	0.527	0.450	0.450

As shown in Table 20, the effect of data cases is seen in different mean, standard deviation, and coefficient of variation values. The data case A shows the largest bias values as well as the standard deviation and coefficient of variation values. These results were expected since the excluded values are typically located in the upper limit within the structural reliability field. On the other hand, the data case C shows the lowest bias values as well as the standard deviation and coefficient of variation values. As mentioned before, the data shown in Table 20 represents the initial point to perform the actual LRFD calibration of resistance factors.

7.3 Statistical data characterization for DLT.

This section shows the statistical characterization for the resistance random variable since it is required for LRFD calibration of resistance factors. The resistance data set is composed by the resistance bias values, which are basically the ratio of the measured resistance and the predicted resistance. In this section, the prediction methods consist of the dynamic load testing (DLT) performed by PDA with iCAP as signal matching. The statistical characterization includes the type of probability distribution as well as the mean, standard deviation, and coefficient of variation for each data case.

7.3.1 Resistance random variable and bias.

As mentioned before, the bias is the primary factor considered in the structural reliability field. The case of LRFD calibration for DLT considers the resistance bias factor as ratio of the measured resistance (Davisson or SLT) and the control field test (DLT or EOID). In this way, the bias factor must be computed for each pile from the database as displayed in Table 21.

Table 21: Calculation of resistance bias values for DLT.

N°	Pile	Pile Type	λ_R DLT
1	**205**	Concrete	1.149
2	**501**	Concrete	2.278
3	**503**	Concrete	1.277
4	**6501**	H-Pile	1.219
5	**Celeste Rd Bent 2**	H-Pile	1.446
6	**Celeste RD A1**	H-Pile	2.006
7	**Moores Mill RD**	H-Pile	1.732
8	**CBD 7A Bent 2**	H-Pile	3.114
9	**SR 41**	H-Pile	1.008
10	**202**	Concrete	1.387
11	**204**	Concrete	0.875
12	**207**	Concrete	1.186
13	**502**	Concrete	1.372
14	**213**	H-Pile	1.778
15	**1101**	H-Pile	2.316
16	**1901**	H-Pile	1.880
17	**6502**	H-Pile	1.622
18	**CBD Bridge A1**	H-Pile	1.152

Table 21 shows that the bias values for DLT range from 0.875 to 3.114. Some of these bias values might be excluded due to the evaluation of data cases performed in the next section

7.3.2 Data cases: Filtering data.

In the same way as done WBUZPILE and DRIVEN, the DLT data shall be filtered from outliers in order to assess its quality. After reviewing the data and documents provided by ALDOT, it was noticed that no pile data point from DLT satisfies the requirements to be excluded as an outlier according to Allen et al. [9]. In other words, the definitive resistance factors shall be calibrated with the entire dataset. Nevertheless, this section still evaluates the magnitude of the effect of the data cases on the calibrated resistance factors for DLT. The evaluation of DLT is performed as a single group since

the data is composed by just 18 points and the considered data cases are similar to the evaluation of WBUZPILE and DRIVEN.

The data case B uses boxplots as graphical tool to identify outliers. Figure 40 shows the boxplot for DLT data. These graphs mark outliers with an asterisk (*).

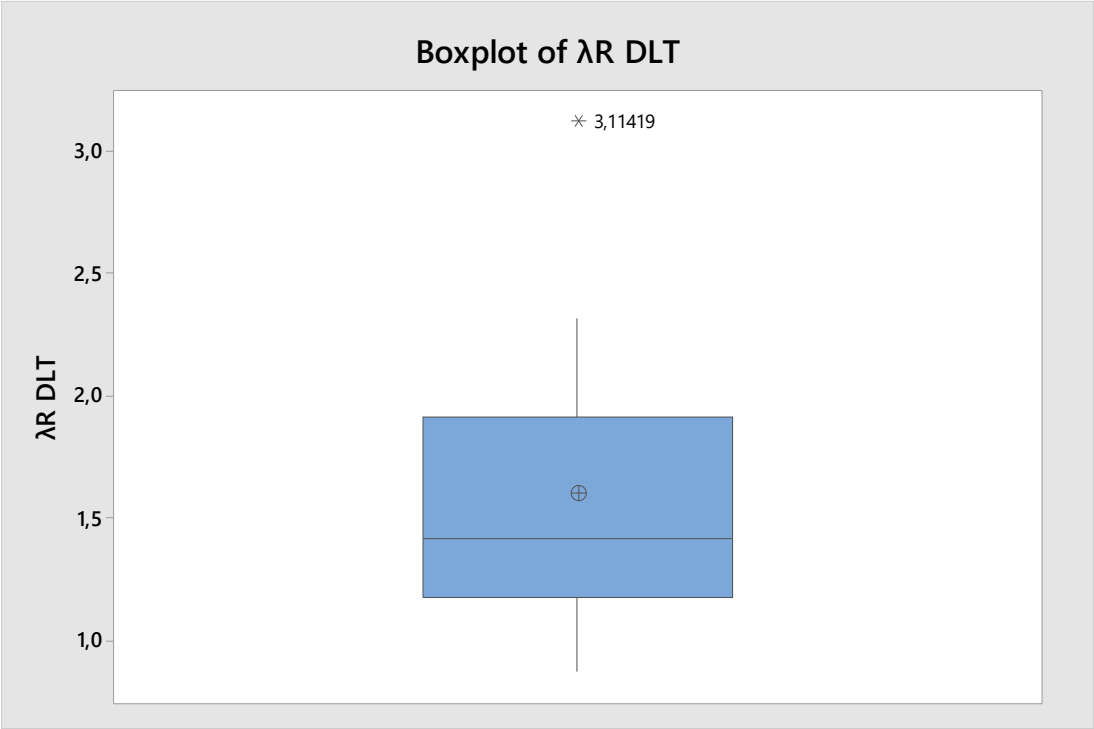

Figure 40: Boxplot of resistance bias values for DLT.

As shown in Figure 40, the DLT data shows 1 outlier (3.114) for data case B.

The data case C uses the two standard deviations criterion to identify outliers. The outlier and excluded data point is just 1 value (3.114) for DLT dataset, which is the same for database B as well. Therefore, the evaluation of data case B and C are equal for DLT.

7.3.3 Type of probability distribution.

This section illustrates the examination of the distribution for the DLT data. The data is subjected to the Anderson-Darling test in order to determine can be assumed as lognormal probability distributed with 95% as confidence interval. Table 22 shows the results of the Anderson-Darling test applied to the three data cases of DLT.

Table 22: Goodness Fit Test results for DLT.

Design method	Data set	Case	Lognormal	
			AD	**p-value**
DLT	All piles	Data Case A	0.211	**0.831**
		Data Case B	0.208	**0.840**
		Data Case C	0.208	**0.840**

The p-values shown in Table 22 are larger than 0.05, which indicate that the lognormal distribution is accepted.

7.3.4 Mean, standard deviation, and coefficient of variation.

As stated before, filtering or not the data can produce a significant modification of the basic descriptive characteristics of the data. The mean, standard deviation, and COV for DLT data cases are shown in Table 23.

Table 23: Resistance statistical characteristics for DLT.

Statistical data summary for λR					
Design method	Data set	Case	Data case A	Data case B	Data case C
DLT (PDA/iCAP)	All data	Mean (λ_R)	1.600	1.511	1.511
		$\widehat{\sigma_{\lambda R}}$	0.563	0.430	0.430
		COV_R	0.352	0.284	0.284

As shown in Table 23, the effect of data cases is seen in different mean, standard deviation, and coefficient of variation values. The data case A shows the largest bias values as well as the standard deviation and coefficient of variation values. These results were expected since the excluded values are typically located in the upper limit within the structural reliability field. On the other hand, the data case B and C produce the same statistical parameters, which values are lower than the data case A. As mentioned before, the data shown in Table 23 represents the initial point to perform the actual LRFD calibration of resistance factors.

7.4 Actual LRFD Resistance factor calibration.

Once the statistical characterization and the pre-calibration considerations have been successfully completed, the actual calibration based on probabilistic methods can be performed. This section shows the detailed procedure of the FOSM, FORM, and MCS calibration only for the design program WBUZPILE, redundant piles, all piles data set, and data case A. The procedure for the rest of calibrations are not shown but they follow the same methodology.

7.4.1 Actual FOSM calibration.

As mentioned before FOSM is a closed-form solution based in reliability. The actual FOSM calibration procedure is shown as follows:

Step 1: The statistical parameters for resistance and load variables used are the values from Table 24.

Table 24: Statistical parameters for resistance and load variables for example of calibration.

Parameter	Resistance	Dead load	Live load
λ	0.979	1.050	1.150
COV	0.633	0.100	0.200
σ	0.646	0.105	1.230
γ	----	1.25	1.75

Step 2: The target reliability index, which measures the probability of failure desired, is found in section 7.1.1 of this study, and for redundant piles. is the following:

$\beta_{T1} = 2.33$

Step 3: Considering the Eq. 43, the resistance factor is computed for every β_T:

For $\beta_{T1} = 2.33$:

$$\phi_R = \frac{\lambda_R\left(\frac{\gamma_{QD}Q_D}{Q_L} + \gamma_{QL}\right)\sqrt{\left[\frac{1 + COV_{QD}^2 + COV_{QL}^2}{1 + COV_R^2}\right]}}{\left(\frac{\lambda_{QD}Q_D}{Q_L} + \lambda_{QL}\right)\exp\{\beta_T\sqrt{\ln[(1 + COV_R^2)(1 + COV_{QD}^2 + COV_{QL}^2)]}\}}$$

$$= \frac{0.979 * (1.25 * 2 + 1.75)\sqrt{\left[\frac{1 + 0.1^2 + 0.2^2}{1 + 0.633^2}\right]}}{(1.05 * 2 + 1.15)\exp\{2.33\sqrt{\ln[(1 + 0.633^2)(1 + 0.1^2 + 0.2^2)]}\}}$$

$$= \mathbf{0.25}$$

Step 4: Once the resistance factor has been calculated, the efficiency bias factor is obtained through the following equation:

$$\frac{\phi_R}{\lambda_R} = \frac{0.25}{0.979} = \mathbf{0.26}$$

The calibration shown in this section belongs to the all data set, data case A, and β_T=2.33. Nevertheless, the FOSM calibration is also performed for all data sets (all piles, steel H-piles, and concrete piles), all data cases (A, B and C), and all target reliability index (2.33, 2.50, and 3.00).

7.4.2 Actual FORM calibration.

The actual FORM calibration procedure for WBUZPILE (All data set of piles) with data case A for $\beta_T = 2.33$ is shown in the next procedure:

Step 1: Define the failure equation

As stated before, the failure equation is usually the difference between the resistance and the load random variable. Thus, the failure equation considered for the case of driven piles is the following:

$G = R - Q,$

where:

$R = r_n * \lambda_R$, and

$Q = (q_D * \lambda_{QD}) + (q_L \lambda_{QL})$

Step 2: Choose random variable distributions

As mentioned before, Paikowsky et al. [6] suggests taking bias factors as lognormal random variables. In addition, histograms and probability plots for resistance and load bias values developed in the FOSM calibration suggest the following random variable distribution:

- Resistance random variable distribution: Lognormal (as recommended by AASHTO [38] and Scott and Salgado [39])
- Load random variable distribution: Lognormal (as suggested by NCHRP 507 [6])

Step 3: Choose LRFD factors to analyze

Following LRFD methodology and Styler's procedure [7], the calculations are performed as shown below:

$q_D/q_L = \eta = 2$

$$q_L = \frac{\phi_R * r_n}{\eta * \gamma_{QD} + \gamma_{QD}} = \frac{0.27 * 630\ kips}{(2 * 1.25) + 1.75} = 40.02\ kips$$

$q_D = \eta * q_L = 2 * 40.02\ kips = 80.05\ kips$

$$Slope = \frac{\phi_R}{\eta * \gamma_{QD} + \gamma_{QL}}(\eta + 1) = \frac{0.27 * (2 + 1)}{(2 * 1.25) + 1.75} = 0.19$$

Step 4: Calculate the initial design point

Assuming a nominal resistance of 630 kips, in accordance to Styler [7] who said that the first nominal resistance assumed will not affect the calibration, the maximum acceptable load is 151.2 kips. Considering the dead-to-live ratio of 2, the dead load is 100.8 kips and the live load is 50.4 kips. Consequently, the limit state equation shows acceptable values:

$$\phi_R r_n \geq \sum \gamma Q$$

$$0.27 * 630 \geq (1.25 * 80.05) + (1.75 + 40.02)$$

$$170.1\ kips \geq 170.1\ kips$$

Therefore, the initial design point is taken as (630 kips, 120.07 kips). Then, the expected resistance is calculated as follows:

$R = r_n * \lambda_R = 630\ kips * 0.979 = 616.80\ kips,$

The expected load is calculated as follows:

$Q = q_D * \lambda_{QD} + q_L * \lambda_{QL} = (80.05\ kips * 1.05) + (40.02\ kips * 1.15)$

$= 130.08\ kips,$

Thus, the most probable resistance and load combinations is (616.8 kips, 130.8 kips). In the first iteration in table 15, these values are used to calculate the equivalent normal variable parameters.

Moreover, the expected values for the R and Q random variables are calculated as shown below:

$E[R] = r_n * \lambda_R = 630\ kips * 0.979 = 616.80\ kips$

$E[Q] = q_D * \lambda_{QD} + q_L * \lambda_{QL} = (80.05\ kips * 1.05) + (40.02\ kips * 1.15)$

$= 130.08\ kips$

Then, the normal standard deviation for the resistance and load is also computed as follows:

$\sigma_R = r_n \sigma_{\lambda R} = 630\ kips * 0.633 = 398.72\ kips$

$$\sigma_Q = \sqrt{q_D^2\sigma_{\lambda D}^2 + q_L^2\sigma_{\lambda L}^2} = \sqrt{(80.05^2 * 0.105^2) + (40.02^2 * 0.23^2)}$$
$$= 12.465\ kips$$

Step 5: Transform into an equivalent normal distribution

In this step, it is necessary to transform an equivalent normal distribution using the design point (r, q). For the first iteration, the design point is equal to the expected resistance and load random values (E[R], E[Q]). The mean and standard deviation can be computed with the following equations:

$$\sigma_{RN} = \frac{pdf(\Phi^{-1}(F_R(r)))}{f_R(r)} = \frac{pdf(\Phi^{-1}(F_R(616.80)))}{f_R(616.80)} = \frac{0.3819}{0.0010} = 364.4681$$

$$E[R_N] = r - \Phi^{-1}(F_R(r))\sigma_{RN} = 616.80 - \Phi^{-1}(F_R(616.80))364.4681$$
$$= 616.80 - (0.2931 * 364.4681) = 509.1113$$

$$\sigma_{QN} = \frac{pdf(\Phi^{-1}\left(F_Q(q)\right))}{f_q(q)} = \frac{pdf(\Phi^{-1}\left(F_Q(130.08)\right))}{f_q(130.08)} = \frac{0.3985}{0.0320} = 12.4368$$

$$E[Q_N] = q - \Phi^{-1}\left(F_Q(q)\right)\sigma_{QN} = 130.08 - \Phi^{-1}\left(F_Q(130.08)\right)12.4368$$
$$= 130.08 - (0.0478 * 12.4368) = 129.4819$$

Step 6: Transform original random variables to standard normal random variables

The standard normal space design point is calculated from the real space design point as follows:

$$r = \frac{E[R] - E[R_N]}{\sigma_{RN}} = \frac{616.80 - 509.1113}{364.4681} = 0.29545$$

$$q = \frac{E[Q] - E[Q_N]}{\sigma_{QN}} = \frac{130.08 - 129.4819}{12.4368} = 0.04781$$

Step 7: Rewrite the failure in terms of the standard normal random variables

It is important to transform the failure equation to standard normal random variables using the following equations:

$$G = R - Q$$

$$G' = (R_{SN}\sigma_{RN} + E[R_N]) - (Q_{SN}\sigma_{QN} + E[Q_N])$$

Step 8: Compute a new trial design point

The new trial design point (r^*, q^*) is computed using as shown below:

$$r^* = \frac{\left[r\frac{\partial G'}{\partial R_{SN}} + q\frac{\partial G'}{\partial Q_{SN}} - G'(r,q)\right]\frac{\partial G'}{R_{SN}}}{\left(\frac{\partial G'}{\partial R_{SN}}\right)^2 + \left(\frac{\partial G'}{\partial Q_{SN}}\right)^2} = \frac{(-E[R_N] + E[Q_N])\sigma_{RN}}{(\sigma_{RN})^2 + (\sigma_{QN})^2}$$

$$= \frac{(-509.1113 + 129.4816) * 364.4681}{(364.4681)^2 + (12.4368)^2} = -1.04039$$

$$q^* = \frac{\left[r\frac{\partial G'}{\partial R_{SN}} + q\frac{\partial G'}{\partial Q_{SN}} - G'(r,q)\right]\frac{\partial G'}{Q_{SN}}}{\left(\frac{\partial G'}{\partial R_{SN}}\right)^2 + \left(\frac{\partial G'}{\partial Q_{SN}}\right)^2} = \frac{(-E[R_N] + E[Q_N])\sigma_{QN}}{(\sigma_{RN})^2 + (\sigma_{QN})^2}$$

$$= \frac{(-509.1113 + 129.4819) * 12.4368}{(364.4681)^2 + (12.4368)^2} = 0.03550$$

As mentioned by Styler [7], this new design point represents the closest distance from the origin to this failure line. The failure line barely varies after each iteration.

Step 9: Calculate the reliability index.

The reliability index, which is the closest distance from the origin to the failure line, is calculated as follows:

$$\beta = \sqrt{(r^*)^2 + (q^*)^2} = \sqrt{(-1.05323)^2 + (0.03622)^2} = 1.04099$$

Step 10: Repetitive iteration (FORM iteration)

The new design point is transformed back to the real space using the following equations:

$$r = r^*\sigma_{RN} + E[R_N] = (-1.04039 * 364.4681) + 509.1113 = 129.9234$$

$$q = q^*\sigma_{QN} + E[Q_N] = (0.03550 * 12.4368) + 129.4819 = 129.9234$$

Then, the equivalent normal distribution using this new design point (r, q) is recalculated. This procedure is repeated until the reliability index β remains stable. It should be noted that if the stable value of β is not the desired value, the resistance factor is not the right one. Therefore, the initial value of φ shall be

modified until getting a stable β similar to β_T. The iteration process is shown in Tables 25 and 26:

Table 25: FORM iterations for Real Space to Equivalent Normal Variable Parameters

	Real space		Normal Random variables parameters			
Iteration	*r*	*q*	*E [Rn]*	*σRn*	*E [Qn]*	*σQn*
	630.0000	120.0705				
1	616.7945	130.0764	509.1113	364.4681	129.4819	12.4368
2	129.9234	129.9234	309.6083	76.7726	129.4825	12.4221
3	134.0780	134.0780	315.2883	79.2276	129.4027	12.8194

Table 26: FORM Iterations in Normal Space

	Normal space					
Iteration	*r*	*q*	*r**	*q**	β	β
1	0.29545	0.04781	-1.04039	0.03550	1.04099	**1.04**
2	-2.34048	0.03549	-2.28636	0.36994	2.31610	**2.32**
3	-2.28721	0.36471	-2.28636	0.36994	2.31610	**2.32**

As seen in Tables 25 and 26, the value of the reliability index remains stable in the third iteration hence it is possible to stop the iteration process in this step for this specific case. However, the spreadsheet developed for this research paper contemplates 6 iterations since other cases need a greater number of iterations. If more iterations than needed are performed, the value for β will not be affected. In this case, the closest two decimal resistance factor value that matches the reliability index ($\beta_T = 2.33$) is 0.27 with a β of 2.32. Consequently, it is possible to conclude that for this specific case, the FORM calibrated resistance value is **0.27**.

Step 10: Once the resistance factor has been calculated, the efficiency bias factor is obtained through the following equation:

$$\frac{\phi_R}{\lambda_R} = \frac{0.27}{0.979} = \mathbf{0.28}$$

The calibration shown in this section belongs to the all data set, data case A, and β_T=2.33. Nevertheless, the FORM calibration is also performed for all data sets (all piles, steel H-piles, and concrete piles), all data cases (A, B and C), and all target reliability index (2.33, 2.50, and 3.00).

7.4.3 Actual Monte Carlo Simulation Calibration.

The actual Monte Carlo calibration procedure for WBUZPILE (All data set of piles) with data case A for β_T = 2.33 is described as follows:

Step 1: The limit state equation used for this calibration is the one stated in Equation 44.

Step 2: In this example, the target reliability index is 2.33 considered for non-redundant piles.

Step 3: The number of simulations is computed as follows

$$N = \frac{1 - P_{f\ true}}{\left(V_p^2\right) * P_{f\ true}} = \frac{1 - 0.01}{0.1^2 * 0.01} = 9900\ simulations$$

Step 4: As mentioned before, Q and R have lognormal distributions. Prior to the simulation, the values for μ_{ln} and σ_{ln} must be computed. The live load and dead load shall be separated for the load random variable. In case of the dead load, μ_{ln} and σ_{ln} are calculated as follows:

$$\sigma_{ln-QD} = \{LN[\left(COV_{QD}\right)^2 + 1]\}^{0.5} = \{LN[(0.10)^2 + 1]\}^{0.5} = 0.0998,$$

Then, the value of $\overline{QL}$ is taken λ_{QD}. Thus,

$$\mu_{ln-QD} = LN\left(\lambda_{QD}\right) - 0.5\sigma_{ln}^2 = LN(1.05) - 0.5 * (0.0998)^2 = 0.0438,$$

In case of the live load, μ_{ln} and σ_{ln} are calculated as follows:

$$\sigma_{ln-QL} = \{LN[\left(COV_{QD}\right)^2 + 1]\}^{0.5} = \{LN[(0.20)^2 + 1]\}^{0.5} = 0.198,$$

Then, the value of $\overline{QL}$ is taken λ_{QD}. Thus,

$$\mu_{ln-QL} = LN(\lambda_{QL}) - 0.5\sigma_{ln}^2 = LN(1.15) - 0.5 * (0.198)^2 = 0.120,$$

For the resistance, calculate μ_{ln} and σ_{ln} as follows:

$$\sigma_{ln-R} = \{LN[(COV_R)^2 + 1]\}^{0.5} = \{LN[(0.646)^2 + 1]\}^{0.5} = 0.591,$$

Then, the value of $\bar{R}$ is taken λ_R. Thus,

$$\mu_{ln-R} = LN(\lambda_R) - 0.5\widehat{\sigma_{ln}^2} = LN(0.979) - 0.5 * (0.591)^2 = -0.196,$$

Next, the simulations are generated. For the dead load, it is shown the way 1 simulated value is generated:

$$QD_i = \exp(\mu_{ln-QD} + \sigma_{ln-QD} z_{i-QD}) = exp(0.0438 + (0.0998 * -0.176))$$
$$= 1.027$$

In the same way, for the live load, it is shown the way 1 simulated value is generated:

$$QL_i = \exp(\mu_{ln-QL} + \sigma_{ln-QL} z_{i-QL}) = exp(0.120 + (0.198 * -0.822)) = 0.958$$

For the resistance, it is shown the way 1 simulated value is generated:

$$R_i = \exp(\mu_{ln-R} + \sigma_{ln-R} z_{i-R}) = exp(-0.196 + (0.591 * -1.428)) = 0.354$$

Step 5: Before, calculating the limit state function g, γ_{avg} is calculated as follows.

$$\Upsilon_{avg} = \frac{\lambda_{QD}\gamma_{QD}\eta + \lambda_{QL}\gamma_{QL}}{\lambda_{QD}\eta + \lambda_{QL}} = \frac{1.05 * 1.25 * 2 + 1.15 * 1.75}{1.05 * 2 + 1.15} = 1.427$$

Then, the resistance trial factor set $\boldsymbol{\varphi_R}$ is 0.28. Next, calculate g as follows:

$$g_i = \lambda_{R,i}\frac{\gamma_{avg}}{\varphi_R} - \frac{\lambda_{QD,i}\eta + \lambda_{QL,i}}{\eta + 1} = R_i\frac{\gamma_{avg}}{\varphi_R} - \frac{QD_i\eta + QL_i}{\eta + 1}$$

$$= 0.354\frac{1.427}{0.28} - \frac{1.027(2) + 0.958}{2 + 1} = 0.798 > 0\ (No\ failure)$$

It should be noted that this example shows the calculation of just 1 simulation. The rest of the simulations shall be computed in the same way.

Step 6: Once, the 9900 simulations were performed. Some of them are shown in Table 27.

Table 27: First 10 simulations out of 9900 for the case exposed in the MC example

N°	$Z_{i\text{-}R}$	R_i	$Z_{i\text{-}QL}$	QL_i	$Z_{i\text{-}QD}$	QD_i	g_i
1	-1.427883	0.353626	-0.821766	0.958302	-0.175508	1.026657	0.798261
2	1.079001	1.555535	0.241724	1.182964	-1.249959	0.922313	6.918050
3	0.898706	1.398335	-1.398701	0.854832	-0.759289	0.968579	6.195465
4	0.891439	1.392343	-0.415830	1.038523	0.125609	1.057962	6.044113
5	0.567311	1.149651	0.516243	1.249058	0.468670	1.094793	4.712586
6	0.136265	0.891144	-0.285137	1.065754	-1.009415	0.944712	3.556349
7	0.347604	1.009679	1.956198	1.661235	-0.255430	1.018505	3.912732
8	1.133966	1.606887	0.893180	1.345868	1.866520	1.258604	6.901253
9	-0.220153	0.721907	0.939831	1.358359	0.183949	1.064137	2.516737
10	-1.427883	0.353626	-0.821766	0.958302	-0.175508	1.026657	0.798261

As shown in Table 27, the simulations for each random variable are generated individually. Then, they interact with each other once the limit state equation is applied. The limit state function is denoted by g_i and determines if failure exists or not. If g_i is lower than zero, failure occurs. Table 27 shows the first 10 iterations where no failure exists since every g_i are equal or larger than zero. Nonetheless, when the 9900 simulations are evaluated, the number of failures n (when $g_i < 0$) is 102. Therefore, the probability of failure is calculated:

$$P_f = \frac{n}{N} = \frac{102}{9900} = 0.0103$$

Step 7: The reliability index is calculated as follows:

$$\beta = NORMSINV(P_f) = NORMSINV(0.0103) = 2.32$$

Step 8: It is supposed to alter the resistance factor until β and β_T (2.33) converge. However, in this case, the difference between β and β_T is already within or lower than the coefficient of variation established before (0.10). Consequently, it is

concluded that the resistance factor calibrated through Monte Carlo simulation for this case is **0.28**.

Step 9: Once the resistance factor has been calculated, the efficiency bias factor is obtained through the following equation:

$$\frac{\phi_R}{\lambda_R} = \frac{0.28}{0.979} = \mathbf{0.29}$$

The calibration shown in this section belongs to the all data set, data case A, and β_T=2.33. Nevertheless, the MCS calibration is also performed for all data sets (all piles, steel H-piles, and concrete piles), all data cases (A, B and C), and all target reliability index (2.33, 2.50, and 3.00).

CHAPTER VIII - PRELIMINARY RESISTANCE FACTORS

This chapter presents the preliminary results of the LRFD calibration of resistance factors for WBUZPILE, DRIVEN, and DLT. The results for each prediction or construction control method, each calibration method, each data sets, data cases, and target reliability index, are organized in tables and graphs for a better understanding.

8.1 Preliminary resistance factors for WBUZPILE and DRIVEN.

Tables 28 to 30 present the preliminary resistance factors obtained through FOSM, FORM, and Monte Carlo Simulation, for WBUZPILE and DRIVEN, as well as an average between the three methods, for all data sets, data cases, and target reliability index. The tables include the summary of the statistics of the mean resistance bias, along with the individual resistance factors ϕ_R and efficiency factors for every calibration method.

Table 28: Preliminary resistance factors for Data Case A.

Design Method	Dataset	# of Piles	Mean (λ_R)	COV_R	β	FOSM		FORM		MC		Average	
						ϕ_R	ϕ_R/λ	ϕ_R	ϕ_R/λ	ϕ_R	ϕ_R/λ	ϕ_R	ϕ_R/λ
WBUZPILE	All Piles	53	0.979	0.64	3.00	**0.17**	0.17	**0.18**	0.18	**0.19**	0.19	**0.18**	0.18
					2.50	**0.23**	0.23	**0.24**	0.25	**0.25**	0.26	**0.24**	0.25
					2.33	**0.25**	0.26	**0.27**	0.28	**0.28**	0.29	**0.27**	0.27
	Steel H-Piles	36	1.175	0.563	3.00	**0.25**	0.21	**0.27**	0.23	**0.26**	0.22	**0.26**	0.22
					2.50	**0.33**	0.28	**0.35**	0.30	**0.37**	0.31	**0.35**	0.30
					2.33	**0.36**	0.31	**0.38**	0.32	**0.39**	0.33	**0.38**	0.32
	Concrete Piles	17	0.564	0.486	3.00	**0.15**	0.27	**0.16**	0.28	**0.17**	0.30	**0.16**	0.28
					2.50	**0.19**	0.34	**0.20**	0.35	**0.21**	0.37	**0.20**	0.35
					2.33	**0.21**	0.37	**0.22**	0.39	**0.23**	0.41	**0.22**	0.39
DRIVEN	All Piles	53	0.979	0.640	3.00	**0.13**	0.12	**0.14**	0.13	**0.14**	0.13	**0.14**	0.13
					2.50	**0.19**	0.18	**0.20**	0.19	**0.20**	0.19	**0.20**	0.19
					2.33	**0.21**	0.20	**0.22**	0.21	**0.22**	0.21	**0.22**	0.21
	Steel H-Piles	36	1.230	0.721	3.00	**0.17**	0.14	**0.18**	0.15	**0.20**	0.16	**0.18**	0.15
					2.50	**0.24**	0.20	**0.25**	0.20	**0.26**	0.21	**0.25**	0.20
					2.33	**0.27**	0.22	**0.28**	0.23	**0.28**	0.23	**0.28**	0.22
	Concrete Piles	17	0.664	0.527	3.00	**0.15**	0.23	**0.17**	0.26	**0.17**	0.26	**0.16**	0.25
					2.50	**0.20**	0.30	**0.21**	0.32	**0.23**	0.35	**0.21**	0.32
					2.33	**0.22**	0.33	**0.23**	0.35	**0.25**	0.38	**0.23**	0.35

Table 29: Preliminary resistance factors for Data Case B.

Design Method	Data set	# of Piles	Mean (λ_R)	COV_R	β	FOSM		FORM		MC		Average	
						ϕ_R	ϕ_R/λ	ϕ_R	ϕ_R/λ	ϕ_R	ϕ_R/λ	ϕ_R	ϕ_R/λ
WBUZPILE	All Piles	50	0.879	0.561	3.00	**0.19**	0.22	**0.20**	0.23	**0.21**	0.24	**0.20**	0.23
					2.50	**0.25**	0.28	**0.27**	0.31	**0.27**	0.31	**0.26**	0.30
					2.33	**0.27**	0.31	**0.29**	0.33	**0.30**	0.34	**0.29**	0.33
	Steel H-Piles	33	1.175	0.563	3.00	**0.25**	0.21	**0.27**	0.23	**0.26**	0.22	**0.26**	0.22
					2.50	**0.33**	0.28	**0.35**	0.30	**0.37**	0.31	**0.35**	0.30
					2.33	**0.36**	0.31	**0.38**	0.32	**0.39**	0.33	**0.38**	0.32
	Concrete Piles	17	0.564	0.486	3.00	**0.15**	0.27	**0.16**	0.28	**0.16**	0.28	**0.16**	0.28
					2.50	**0.19**	0.34	**0.20**	0.35	**0.20**	0.35	**0.20**	0.35
					2.33	**0.21**	0.37	**0.22**	0.39	**0.22**	0.39	**0.22**	0.38
DRIVEN	All Piles	52	0.970	0.582	3.00	**0.20**	0.21	**0.21**	0.22	**0.22**	0.23	**0.21**	0.22
					2.50	**0.26**	0.27	**0.28**	0.29	**0.29**	0.30	**0.28**	0.29
					2.33	**0.29**	0.30	**0.31**	0.32	**0.31**	0.32	**0.30**	0.31
	Steel H-Piles	35	1.119	0.529	3.00	**0.26**	0.23	**0.28**	0.25	**0.29**	0.26	**0.28**	0.25
					2.50	**0.34**	0.30	**0.36**	0.32	**0.38**	0.34	**0.36**	0.32
					2.33	**0.37**	0.33	**0.40**	0.36	**0.41**	0.37	**0.39**	0.35
	Concrete Piles	17	0.609	0.450	3.00	**0.17**	0.28	**0.19**	0.31	**0.20**	0.33	**0.19**	0.31
					2.50	**0.22**	0.36	**0.24**	0.39	**0.24**	0.39	**0.23**	0.38
					2.33	**0.24**	0.39	**0.26**	0.43	**0.26**	0.43	**0.25**	0.42

Table 30: Preliminary resistance factors for Data Case C.

Design Method	Dataset	# of Piles	Mean (λ_R)	COV_R	β	FOSM		FORM		MC		Average	
						ϕ_R	ϕ_R/λ	ϕ_R	ϕ_R/λ	ϕ_R	ϕ_R/λ	ϕ_R	ϕ_R/λ
WBUZPILE	All Piles	49	0.850	0.535	3.00	**0.19**	0.22	**0.21**	0.25	**0.22**	0.26	**0.21**	0.24
					2.50	**0.26**	0.31	**0.27**	0.32	**0.28**	0.33	**0.27**	0.32
					2.33	**0.28**	0.33	**0.30**	0.35	**0.30**	0.35	**0.29**	0.35
	Steel H-Piles	33	1.041	0.486	3.00	**0.27**	0.26	**0.30**	0.29	**0.31**	0.30	**0.29**	0.28
					2.50	**0.35**	0.34	**0.38**	0.37	**0.38**	0.37	**0.37**	0.36
					2.33	**0.38**	0.37	**0.41**	0.39	**0.41**	0.39	**0.40**	0.38
	Concrete Piles	16	0.520	0.404	3.00	**0.17**	0.33	**0.19**	0.37	**0.19**	0.37	**0.18**	0.35
					2.50	**0.21**	0.40	**0.23**	0.44	**0.24**	0.46	**0.23**	0.44
					2.33	**0.23**	0.44	**0.24**	0.46	**0.25**	0.48	**0.24**	0.46
DRIVEN	All Piles	52	0.970	0.582	3.00	**0.20**	0.21	**0.21**	0.22	**0.22**	0.23	**0.21**	0.22
					2.50	**0.26**	0.27	**0.28**	0.29	**0.28**	0.29	**0.27**	0.28
					2.33	**0.29**	0.30	**0.31**	0.32	**0.31**	0.32	**0.30**	0.31
	Steel H-Piles	35	1.119	0.529	3.00	**0.26**	0.23	**0.28**	0.25	**0.30**	0.27	**0.28**	0.25
					2.50	**0.34**	0.30	**0.36**	0.32	**0.38**	0.34	**0.36**	0.32
					2.33	**0.37**	0.33	**0.40**	0.36	**0.40**	0.36	**0.39**	0.35
	Concrete Piles	16	0.609	0.450	3.00	**0.17**	0.28	**0.19**	0.31	**0.20**	0.33	**0.19**	0.31
					2.50	**0.22**	0.36	**0.24**	0.39	**0.24**	0.39	**0.23**	0.38
					2.33	**0.24**	0.39	**0.26**	0.43	**0.26**	0.43	**0.25**	0.42

Tables 28 to 30 reveal that the data case A presents the most conservative method with an average resistance factor of 0.23 and average efficiency factor 0.25. The data case B shows an average resistance factor of 0.27 and an average efficiency factor of 0.31, which represents a 17% and 24% of increase from data case A results, respectively. The data case C shows an average resistance factor of 0.28 and an average efficiency factor of 0.33, which represents a 22% and a 32% of increase from data case A results, respectively. Data cases B and C shows very similar resistance and efficiency factors.

Data case A is used to compare the results from calibrations method FOSM, FORM, and MCS. Data cases B and C results are not compared since they are not able to be taken as definitive factors for the conclusions of this study. Figure 41 shows a comparison of the resistance factor between FOSM and FORM, Figure 42 shows a comparison of the resistance factor between FOSM and MCS, and Figure 43 shows a comparison of the resistance factor between FORM and MCS.

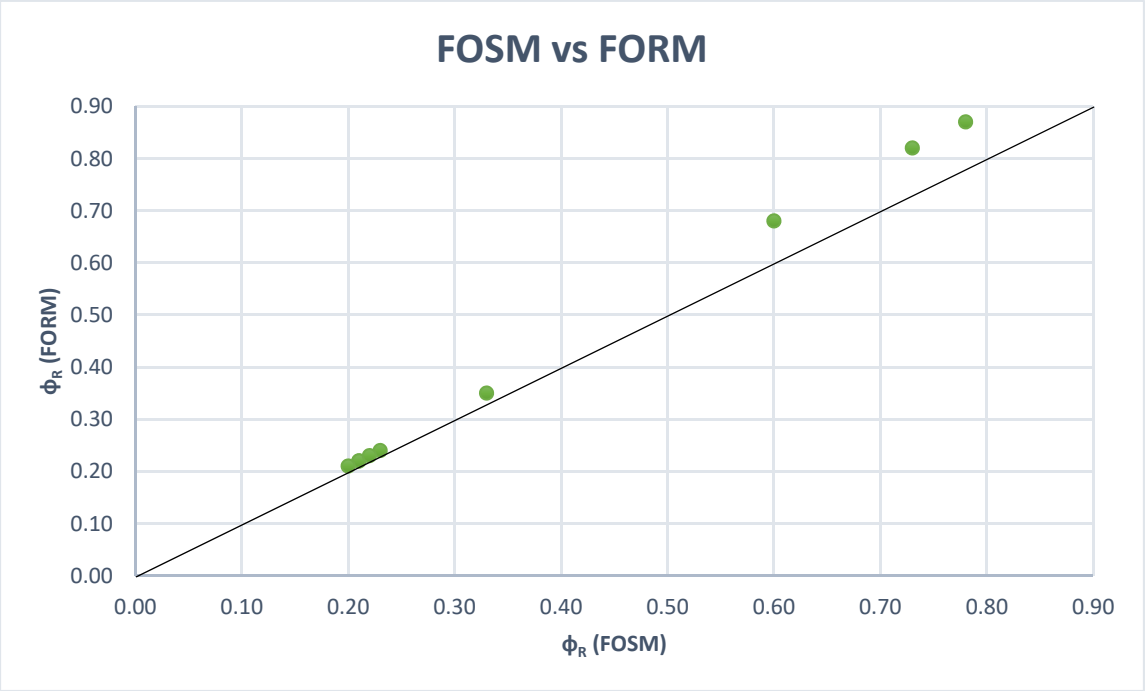

Figure 41: FOSM vs FORM results.

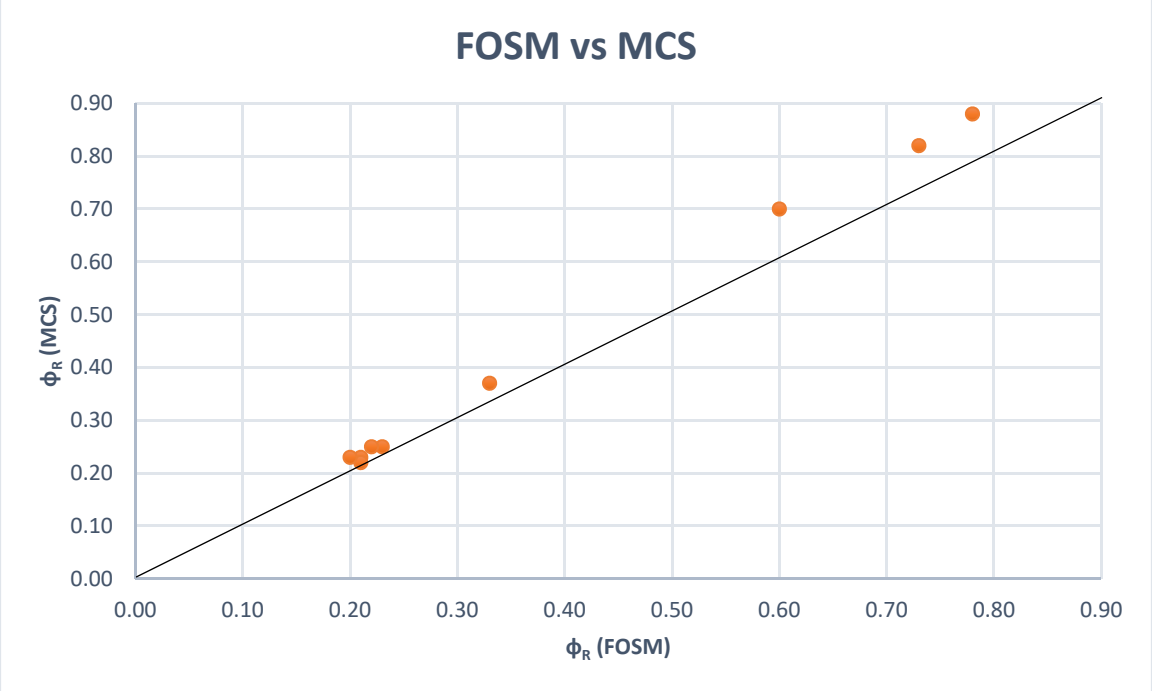

Figure 42: FOSM vs MCS results

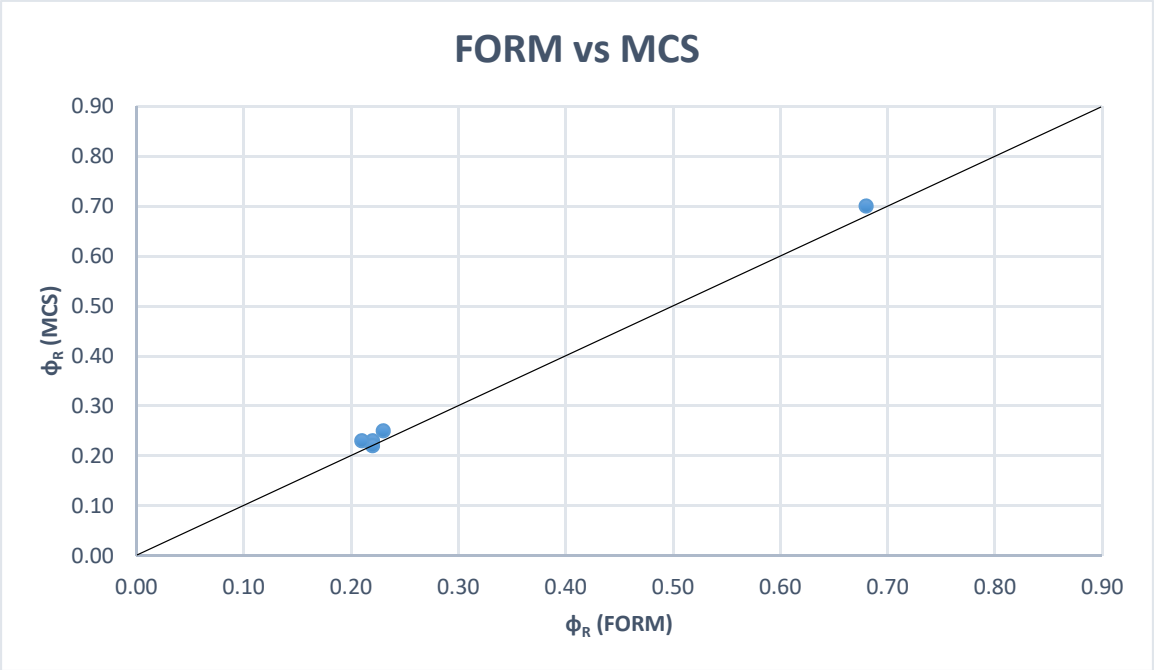

Figure 43: FORM vs MCS results.

When comparing FOSM, FORM, and MCS results from data case A, Table 28 and Figures 41 to 43 show that FORM produces 8.1% higher resistance factors than FOSM in average, MCS produces 11.1% than FOSM in average, and MCS produces 2.8% higher resistance factors than FORM in average. Therefore, it can be concluded that FOSM is the most conservative calibration method while MCS is the least most conservative calibration method.

8.2 Preliminary resistance factors for control field tests.

Tables 31 to 32 present the preliminary resistance factors obtained through FOSM, FORM, and Monte Carlo Simulation, for DLT, as well as an average between the three methods, for all data sets, data cases, and target reliability index. The tables include

the summary of the statistics of the mean resistance bias, along with the individual resistance factors ϕ_R and efficiency factors for every calibration method.

Table 31: DLT Resistance factors for Data Case A.

Design Method	Data set	# of Piles	Mean (λ_R)	COV_R	β	FOSM		FORM		MC		Average	
						ϕ_R	ϕ_R/λ	ϕ_R	ϕ_R/λ	ϕ_R	ϕ_R/λ	ϕ_R	ϕ_R/λ
DLT	All Piles	18	1.600	0.352	3.00	**0.60**	0.38	**0.68**	0.43	**0.70**	0.44	**0.66**	0.41
					2.50	**0.73**	0.46	**0.82**	0.51	**0.82**	0.51	**0.79**	0.49
					2.33	**0.78**	0.49	**0.87**	0.54	**0.88**	0.55	**0.84**	0.53

Table 32: DLT Resistance factors for Data Case B and C.

Design Method	Data set	# of Piles	Mean (λ_R)	COV_R	β	FOSM		FORM		MC		Average	
						ϕ_R	ϕ_R/λ	ϕ_R	ϕ_R/λ	ϕ_R	ϕ_R/λ	ϕ_R	ϕ_R/λ
DLT	All Piles	17	1.511	0.284	3.00	**0.67**	0.44	**0.79**	0.52	**0.80**	0.53	**0.75**	0.50
					2.50	**0.80**	0.53	**0.91**	0.60	**0.92**	0.61	**0.88**	0.58
					2.33	**0.85**	0.56	**0.96**	0.64	**0.97**	0.64	**0.93**	0.61

Tables 31 to 32 reveal that the data case A presents the most conservative method with an average resistance factor of 0.76 and average efficiency factor 0.48. Data cases B and C shows equal resistance and efficiency factors since both cases use the dame data. The data case B and C show an average resistance factor of 0.85 and an average efficiency factor of 0.53, which represents a 12% and 17% of increase from data case A results, respectively.

When comparing FOSM, FORM, and MCS results from data case A, Tables 31 and 32 show that FOSM is the most conservative calibration method. For the data case A, FOSM results show an average resistance factor of 0.70 and an average efficiency factor of 0.44. FORM results show an average resistance factor of 0.79 and an average efficiency factor of 0.49, which represents a 13% and 11% of increase from FOSM results, respectively. MCS results show an average resistance factor of 0.80 and an

average efficiency factor of 0.50, which represents a 14% and 14% of increase from FOSM results, respectively. MCS shows an average resistance factor 1% higher and an efficiency factor 2% higher than FORM.

8.3 Summary of preliminary resistance factors.

This chapter showed the preliminary LRFD resistance and efficiency factor results for WBUZPILE, DRIVEN, and DLT. Each calibration was performed for each prediction method, each calibration method, each data set, each data case, and each target reliability index. The results confirmed what was expected since the data case A is the most conservative case with the lowest resistance factors and efficiency factors. The evaluation of WBUZPILE and DRIVEN shows that the effect of data case B produces 17% higher resistance factors and 19% higher efficiency factors than data case A. Data case C generates 22% higher resistance factors and 30% higher efficiency factors compared to data case A. The evaluation of DLT shows that the effect of data case B and C produce 12% higher resistance factors and 10% higher efficiency factors than data case A. Unfortunately, the data provided by ALDOT does not show proof enough to consider data case B or C as definitive results for the final conclusion. However, it was still useful to evaluated how significant is their effect on the calibrated resistance factors.

In addition, it was observed that the calibration method MCS is the least conservative method in average with the highest resistance and efficiency factors. However, FORM results are slightly lower in average than MCS. The FOSM is the most conservative calibration method in every case.

CHAPTER IX - SETUP INCORPORATION IN THE CALIBRATION OF RESISTANCE FACTORS

According to Haque and Steward [29], the incorporation of pile setup in the design stage would produce meaningful construction cost savings. As stated in chapter 2, pile setup represents an increase on the pile capacity over time after the EOID. Larger pile capacity can be translated to smaller piles size, depth and number. These three factors represent less construction costs to the government and taxpayers. Therefore, this chapter attempts to evaluate the incorporation of pile setup in the calibration of resistance factors. Besides the static load testing data, dynamic load testing data is necessary to provide the increased pile capacity data at periods of time after EOID.

In regard of LRFD design, Yang and Liang [33] propose to incorporate setup resistance factors separated from the EOID resistance factors (following equation 18) as the ideal procedure. However, to perform that type of calibration, an acceptable data size with SLT or restrikes (BOR) at specific and close time intervals is necessary. The data considered in this paper has just 18 EOID data points with their corresponding 18 SLTs that have a large variation with data from 2 to 28 days after EOID, which would produce resistance factors with limited reliability. In case of restrikes, ALDOT data has just 9

BOR data points with an average time interval of 0.30 days after EOID. Other studies such us Haque and Abu Farsakh [8] consider time interval of 30, 45, 60, and 90 days after EOID. This few BOR tests would also produce resistance factors with limited reliability. Nonetheless, it is still possible to calibrate resistance factors for pile setup if the limit state equation considers EOID and setup in one term (following equation 17) using and the Skov and Denver [1] model.

The Skov and Denver [1] equation is used to calculate the pile setup resistance increase and add to the EOID or SLT resistance as a measured value. It should be noted that the Skov and Denver model [1] suggests using a setup factor A = 0.2 for sand and A = 0.6 for clay. Nevertheless, Haque and Steward [29] established A = 0.2 for soils in Alabama, hence this value is used. The time intervals considered are 30, 45, 60, and 90 days as considered by Haque and Abu-Farsah [8]. This paper evaluates two cases: The first case considers WBUZPILE and DRIVEN as predicted resistance and the SLT plus setup as a measured resistance. The second case considers DLT as predicted resistance and the SLT plus setup as measured resistance. The LRFD calibrations are performed using MCS with all data included (data case A), since it shows the least over-conservatism and reasonable rigorousness method with consistent results.

9.1 Setup Incorporation for WBUZPILE and DRIVEN.

The pile setup incorporation on the static analysis methods can also produce cost savings. Thus, this section shows the incorporation of setup on the calibration of resistance factors for the prediction methods WBUZPILE and DRIVEN (which work as static analysis methods). In order to incorporate the pile setup, the Skov and Denver [1] model is used considering the initial time as the actual time at SLT. In this way, setup resistance values for 30, 45, 60, and 90 days after EOID are calculated and added to the SLT. The resistance factors with setup incorporation for the entire pile data set evaluation are shown in Table 33. Also, the variation of the resistance and efficiency factor for the WBUZPILE evaluation and the entire pile data set is shown in Figures 44 and 45,

respectively. The variation of the resistance and efficiency factor for the DRIVEN evaluation and the entire pile data set is shown in Figures 46 and 47, respectively.

Table 33: Comparison of resistance factors incorporating setup for all data set.

Design method		WBUZPILE					DRIVEN				
Time interval after EOID		**SLT time**	30 days	45 days	60 days	90 days	**SLT time**	30 days	45 days	60 days	90 days
λ_R		**0.979**	1.135	1.170	1.194	1.228	**1.049**	1.213	1.250	1.276	1.313
σ_R		**0.633**	0.733	0.755	0.771	0.793	**0.799**	0.919	0.947	0.967	0.995
COV_R		**0.646**	0.646	0.646	0.646	0.646	**0.762**	0.758	0.758	0.758	0.758
β = 3.00	ϕ_R	**0.19**	0.21	0.22	0.22	0.23	**0.14**	0.17	0.18	0.18	0.18
	Incr.	**0%**	11%	16%	16%	21%	**0%**	21%	29%	29%	29%
	ϕ_R/λ	**0.19**	0.19	0.19	0.18	0.19	**0.13**	0.14	0.14	0.14	0.14
β = 2.50	ϕ_R	**0.25**	0.28	0.29	0.30	0.31	**0.20**	0.23	0.24	0.24	0.25
	Incr.	**0%**	12%	16%	20%	24%	**0%**	15%	20%	20%	25%
	ϕ_R/λ	**0.26**	0.25	0.25	0.25	0.25	**0.19**	0.19	0.19	0.19	0.19
β = 2.33	ϕ_R	**0.28**	0.31	0.32	0.33	0.34	**0.22**	0.26	0.26	0.27	0.28
	Incr.	**0%**	11%	14%	18%	21%	**0%**	18%	18%	23%	27%
	ϕ_R/λ	**0.29**	0.27	0.27	0.28	0.28	**0.21**	0.21	0.21	0.21	0.21
Average increase		*0%*	*11%*	*15%*	*18%*	*22%*	*0%*	*18%*	*22%*	*24%*	*27%*

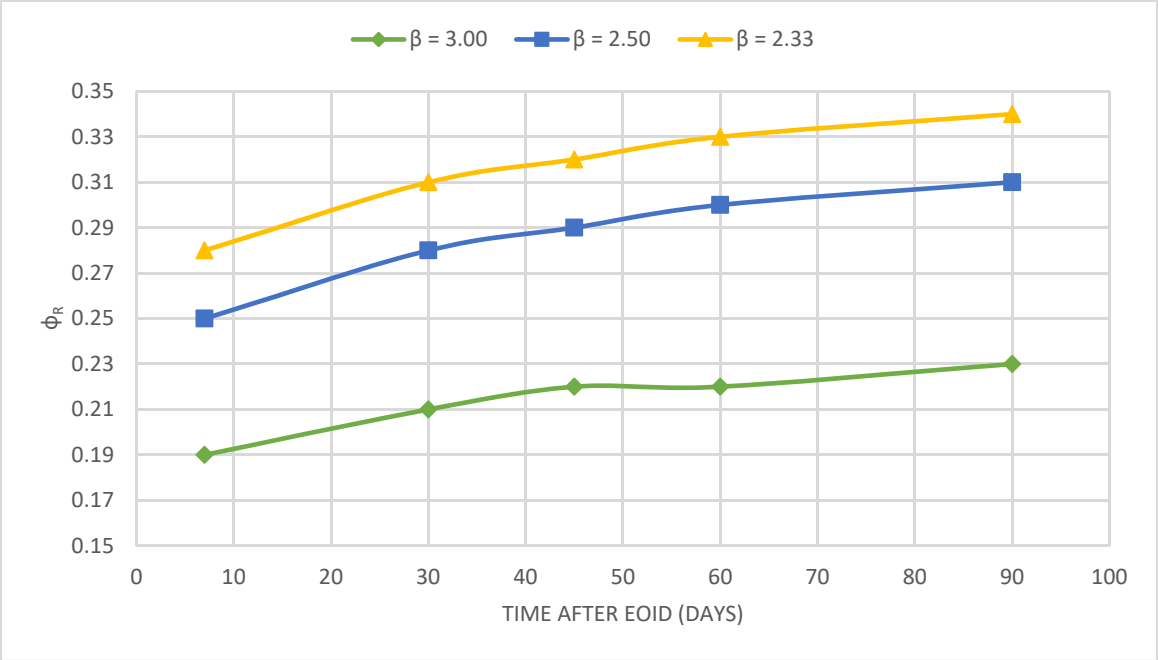

Figure 44: Variation of resistance factor with setup incorporation for WBUZPILE considering all data set.

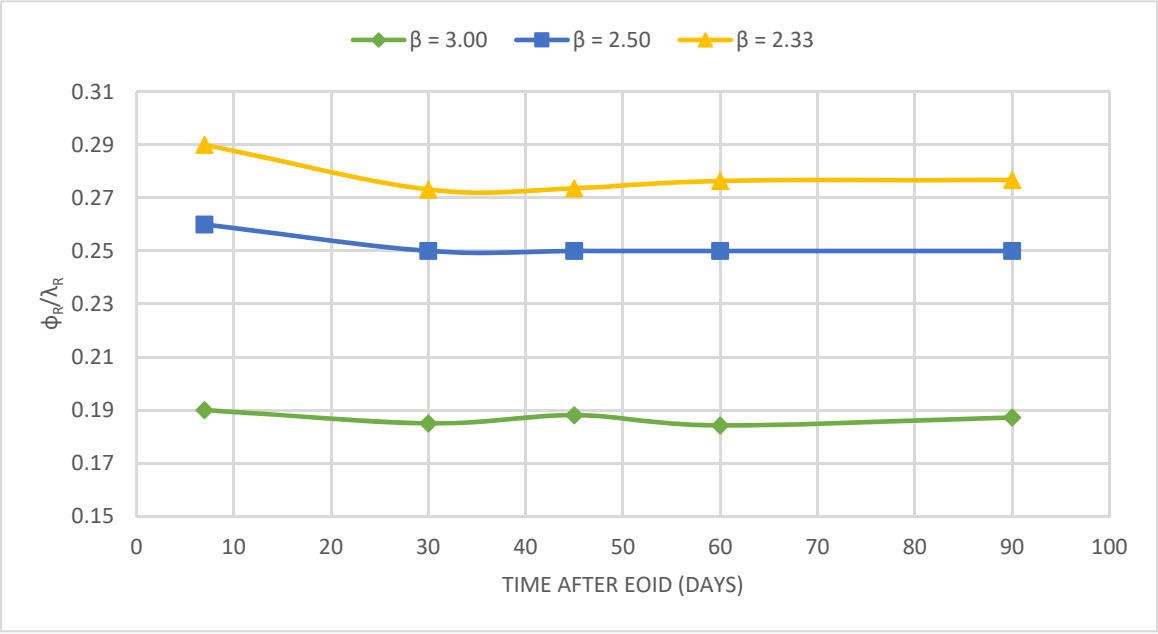

Figure 45: Variation of efficiency factor with setup incorporation for WBUZPILE, considering all data set.

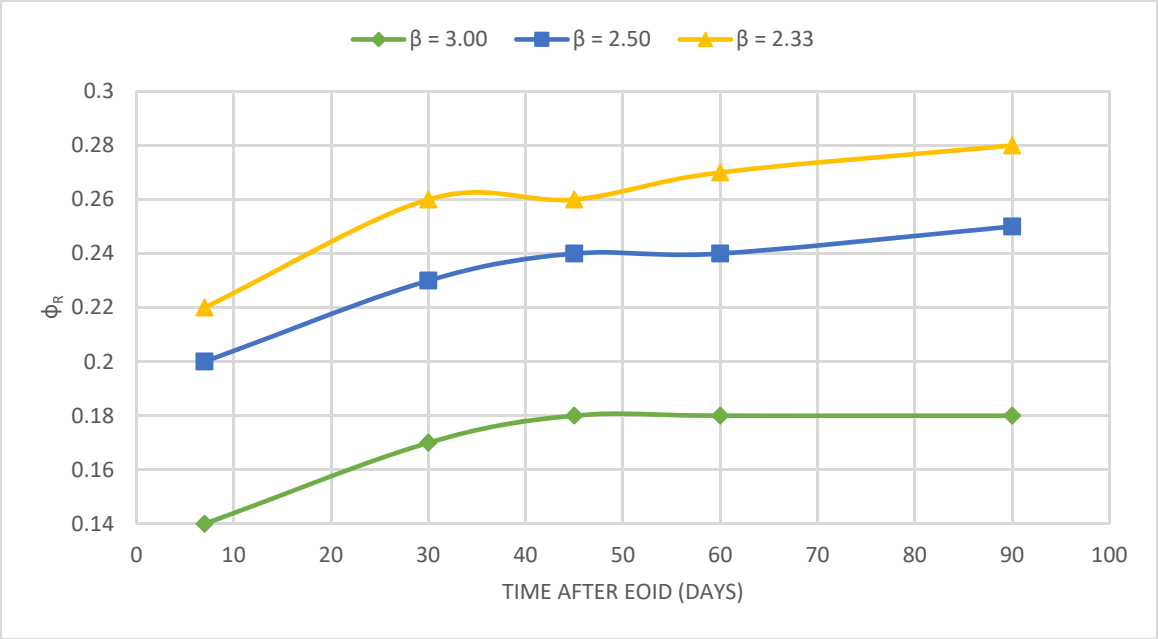

Figure 46: Variation of resistance factor with setup incorporation for DRIVEN, considering all data set.

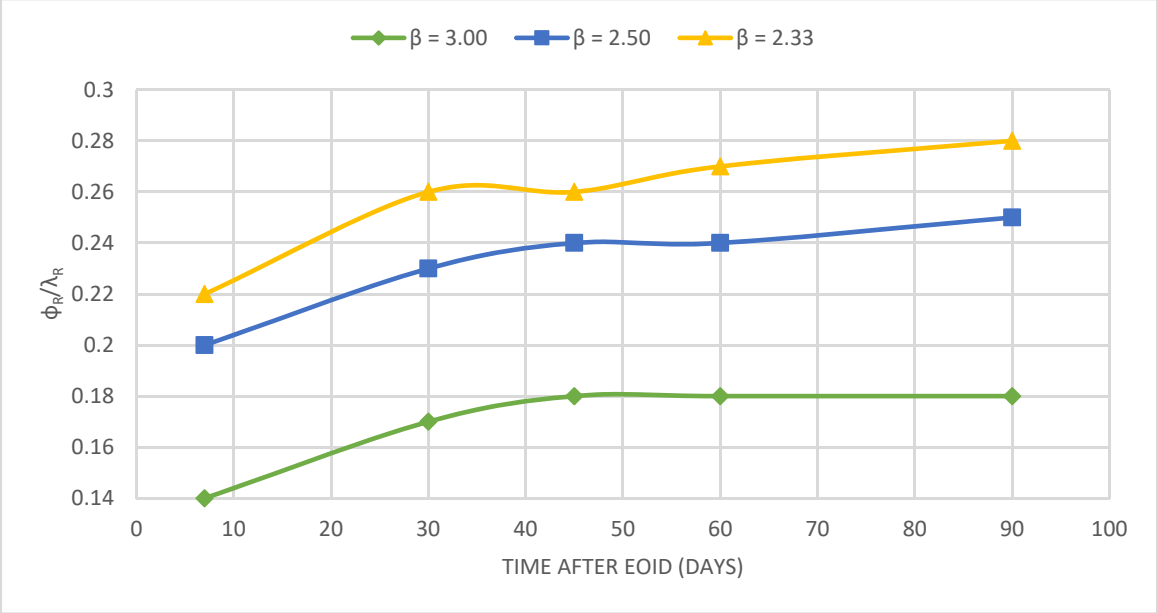

Figure 47: Variation of efficiency factor with setup incorporation for DRIVEN, considering all data set.

The resistance factors with setup incorporation for the steel H-piles data set evaluation is shown in Table 34. Also, the variation of the resistance and efficiency factor for the WBUZPILE evaluation and the steel H-piles data set is shown in Figures 48 and 49, respectively. The variation of the resistance and efficiency factor for the DRIVEN evaluation and the steel H-piles data set is shown in Figures 50 and 51, respectively.

Table 34: Comparison of resistance factors incorporating setup for Steel-H Piles.

Design method		WBUZPILE					DRIVEN				
Time Interval after EOID		**SLT time**	30 days	45 days	60 days	90 days	**SLT time**	30 days	45 days	60 days	90 days
λ_R		1.175	1.377	1.419	1.448	1.489	1.230	1.441	1.485	1.515	1.559
σ_R		0.662	0.752	0.775	0.792	0.815	0.887	1.009	1.040	1.062	1.093
COV_R		0.563	0.546	0.547	0.547	0.547	0.721	0.700	0.700	0.701	0.701
β = 3.00	ϕ_R	**0.26**	0.33	0.34	0.35	0.36	**0.20**	0.23	0.24	0.25	0.25
	Incr.	**0%**	35%	38%	38%	42%	**0%**	15%	20%	25%	30%
	ϕ_R/λ	**0.22**	0.24	0.24	0.24	0.24	**0.16**	0.16	0.16	0.16	0.16
β = 2.50	ϕ_R	**0.37**	0.44	0.44	0.45	0.47	**0.26**	0.32	0.34	0.35	0.35
	Incr.	**0%**	24%	24%	27%	30%	**0%**	23%	31%	35%	38%
	ϕ_R/λ	**0.31**	0.33	0.32	0.32	0.32	**0.21**	0.22	0.23	0.23	0.22
β = 2.33	ϕ_R	**0.39**	0.49	0.49	0.50	0.51	**0.28**	0.36	0.37	0.37	0.38
	Incr.	**0%**	28%	28%	31%	31%	**0%**	29%	32%	32%	43%
	ϕ_R/λ	**0.33**	0.36	0.35	0.35	0.34	**0.23**	0.25	0.25	0.24	0.24
Average increase		*0%*	*24%*	*25%*	*28%*	*32%*	*0%*	*22%*	*25%*	*31%*	*32%*

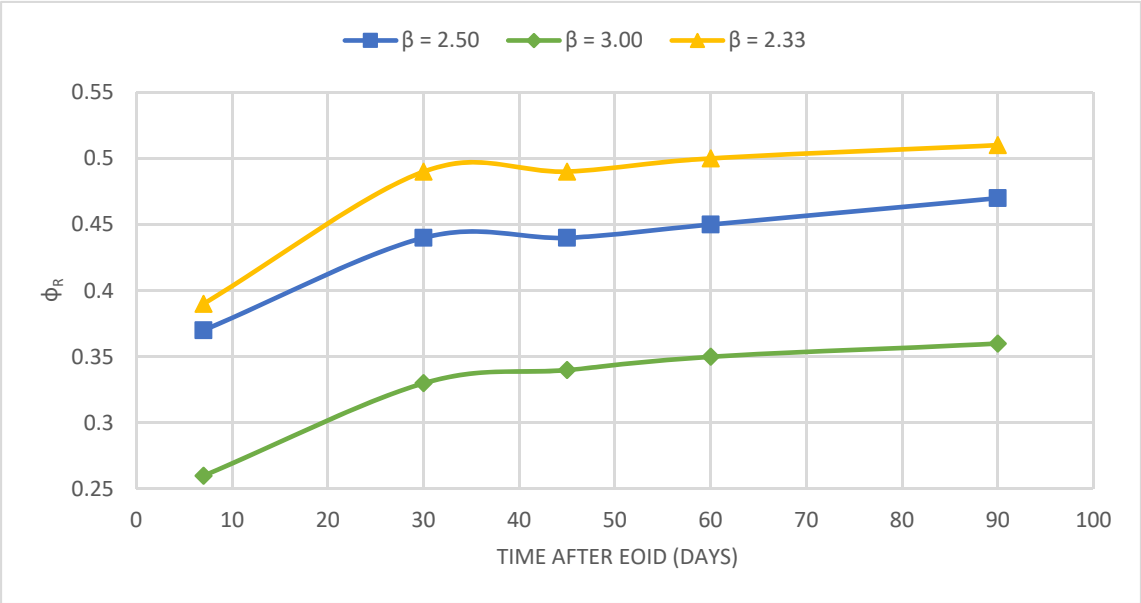

Figure 48: Variation of resistance factor with setup incorporation for WBUZPILE, considering Steel H-Piles data set.

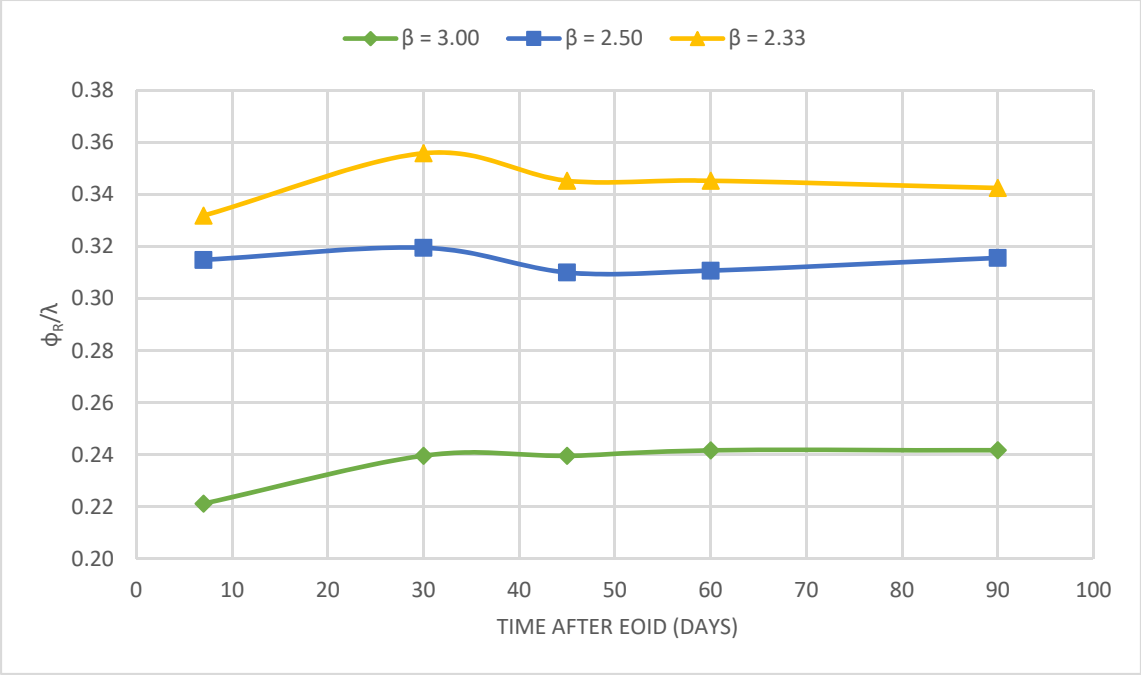

Figure 49: Variation of efficiency factor with setup incorporation for WBUZPILE, considering Steel H-Piles data set.

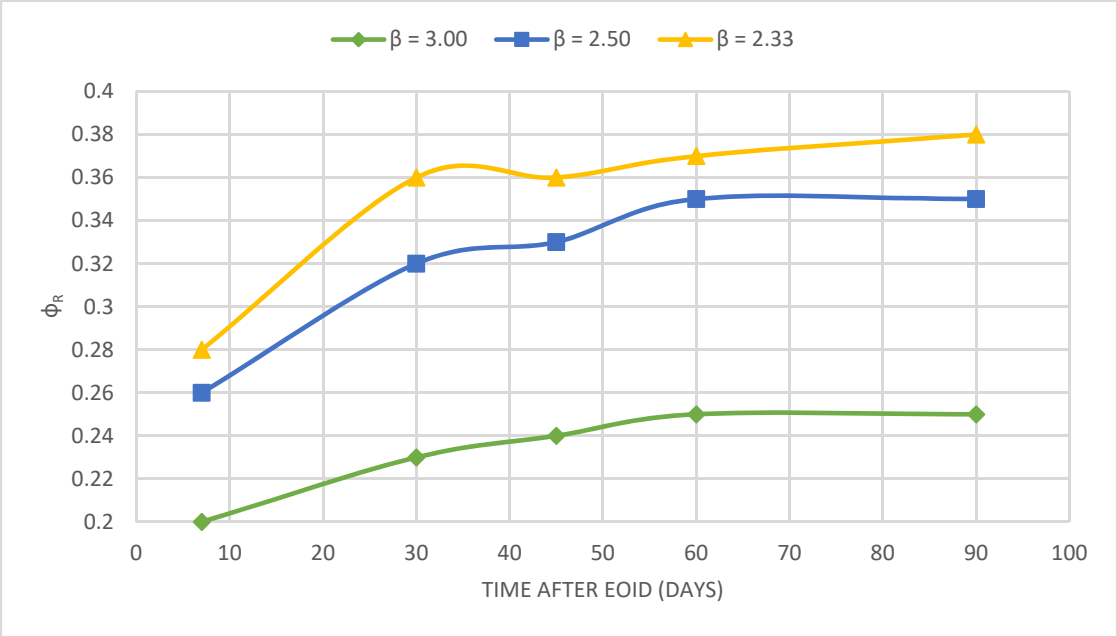

Figure 50: Variation of resistance factor with setup incorporation for DRIVEN, considering Steel H-Piles data set.

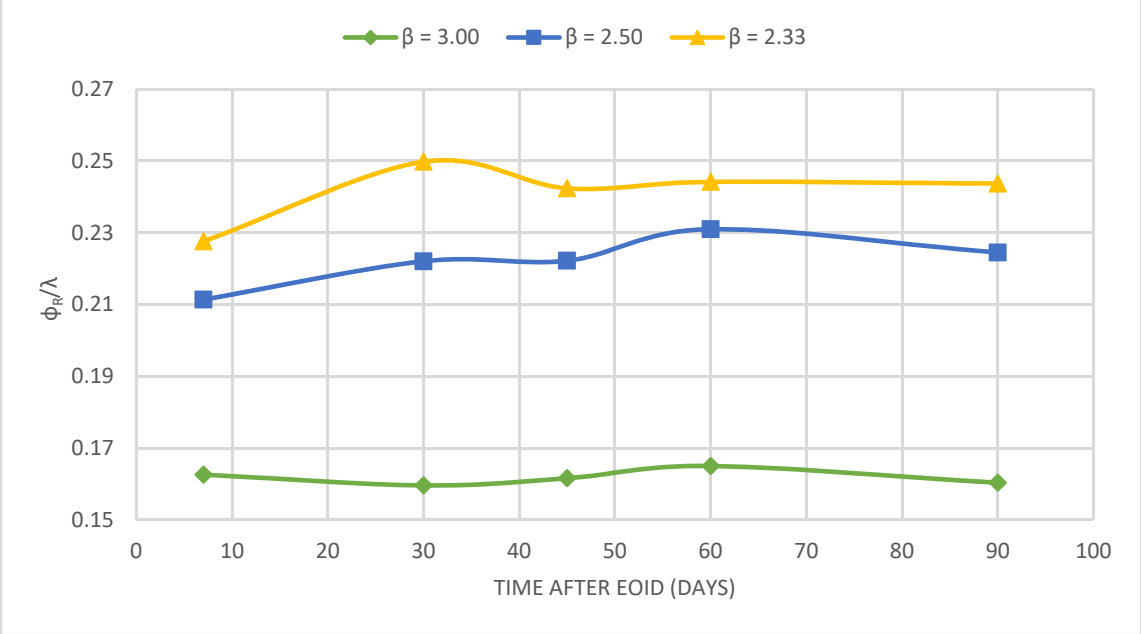

Figure 51: Variation of efficiency factor with setup incorporation for DRIVEN, considering Steel H-Piles data set.

The resistance factors with setup incorporation for the concrete piles data set evaluation is shown in Table 35. Also, the variation of the resistance and efficiency factor for the WBUZPILE evaluation and the concrete piles data set is shown in Figures 52 and 53, respectively. The variation of the resistance and efficiency factor for the DRIVEN evaluation and the concrete piles data set is shown in Figures 54 and 55, respectively.

Table 35: Comparison of resistance factors incorporating setup for Concrete Piles.

Design method		WBUZPILE					DRIVEN				
Time Interval after EOID		**SLT time**	30 days	45 days	60 days	90 days	**SLT time**	30 days	45 days	60 days	90 days
λ_R		**0.564**	0.622	0.642	0.656	0.676	**0.664**	0.728	0.752	0.768	0.792
σ_R		**0.274**	0.311	0.321	0.327	0.337	**0.350**	0.392	0.404	0.413	0.425
COV_R		**0.486**	0.500	0.500	0.499	0.499	**0.527**	0.538	0.538	0.537	0.537
β = 3.00	ϕ_R	**0.17**	0.17	0.18	0.19	0.19	**0.17**	0.18	0.18	0.19	0.21
	Incr.	**0%**	6%	12%	18%	18%	**0%**	18%	18%	24%	29%
	ϕ_R/λ	**0.30**	0.27	0.28	0.29	0.28	**0.26**	0.25	0.24	0.25	0.27
β = 2.50	ϕ_R	**0.21**	0.22	0.23	0.24	0.25	**0.23**	0.24	0.24	0.25	0.25
	Incr.	**0%**	10%	10%	14%	19%	**0%**	13%	13%	17%	22%
	ϕ_R/λ	**0.37**	0.35	0.36	0.37	0.37	**0.35**	0.33	0.32	0.33	0.32
β = 2.33	ϕ_R	**0.23**	0.24	0.25	0.25	0.26	**0.25**	0.26	0.26	0.27	0.28
	Incr.	**0%**	9%	13%	13%	17%	**0%**	12%	12%	16%	16%
	ϕ_R/λ	**0.41**	0.39	0.39	0.38	0.38	**0.38**	0.36	0.35	0.35	0.35
Average increase		*0%*	*3%*	*8%*	*12%*	*15%*	*0%*	*5%*	*5%*	*9%*	*15%*

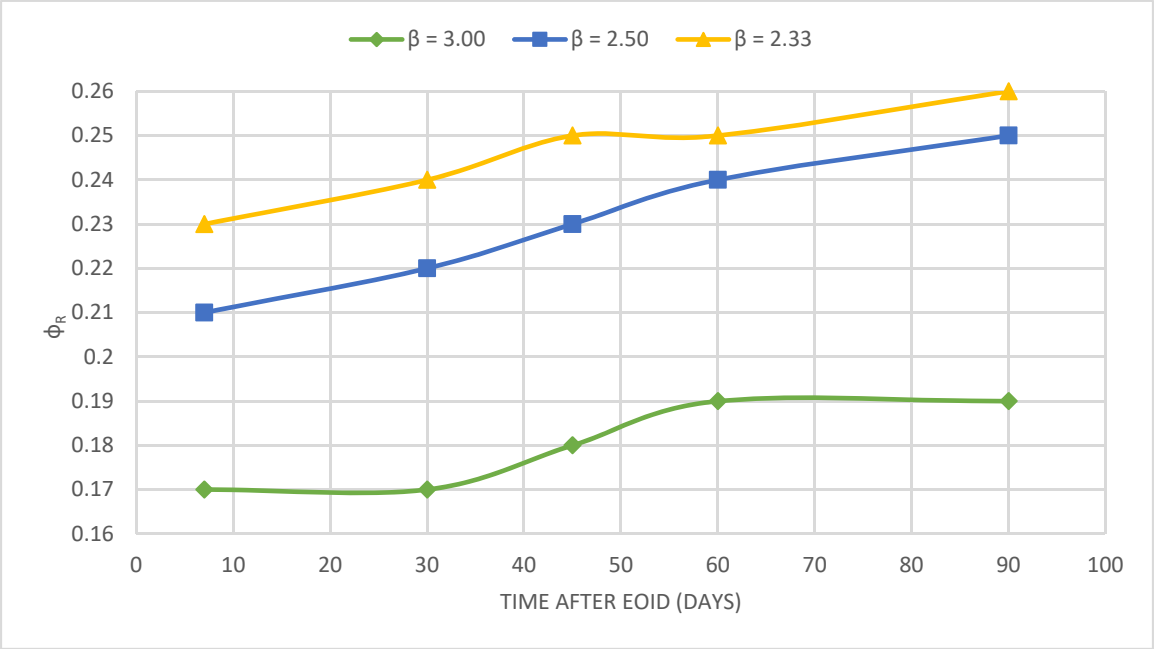

Figure 52: Variation of resistance factor with setup incorporation for WBUZPILE, considering Concrete Piles data set.

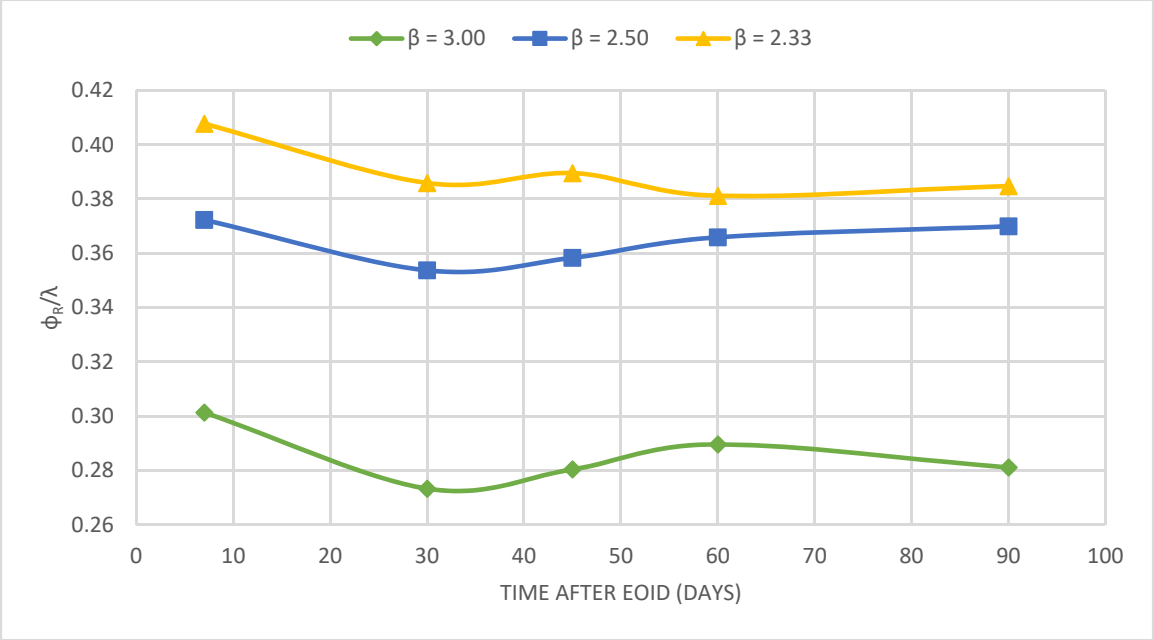

Figure 53: Variation of efficiency factor with setup incorporation for WBUZPILE, considering Concrete Piles data set.

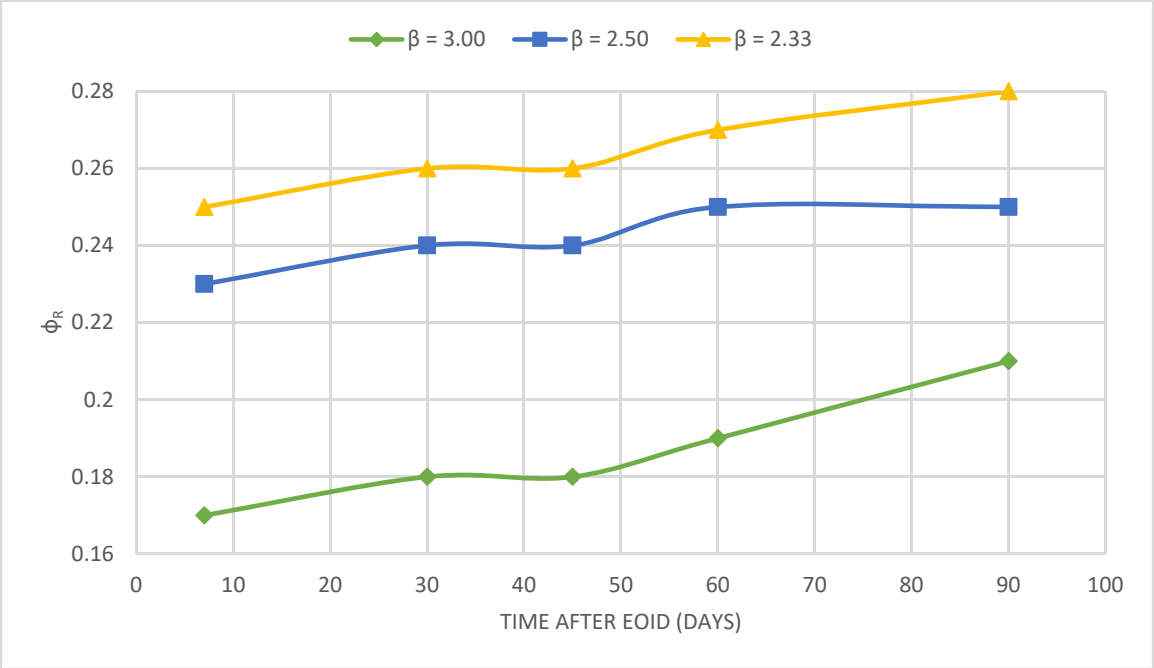

Figure 54: Variation of resistance factor with setup incorporation for DRIVEN, considering Concrete Piles data set.

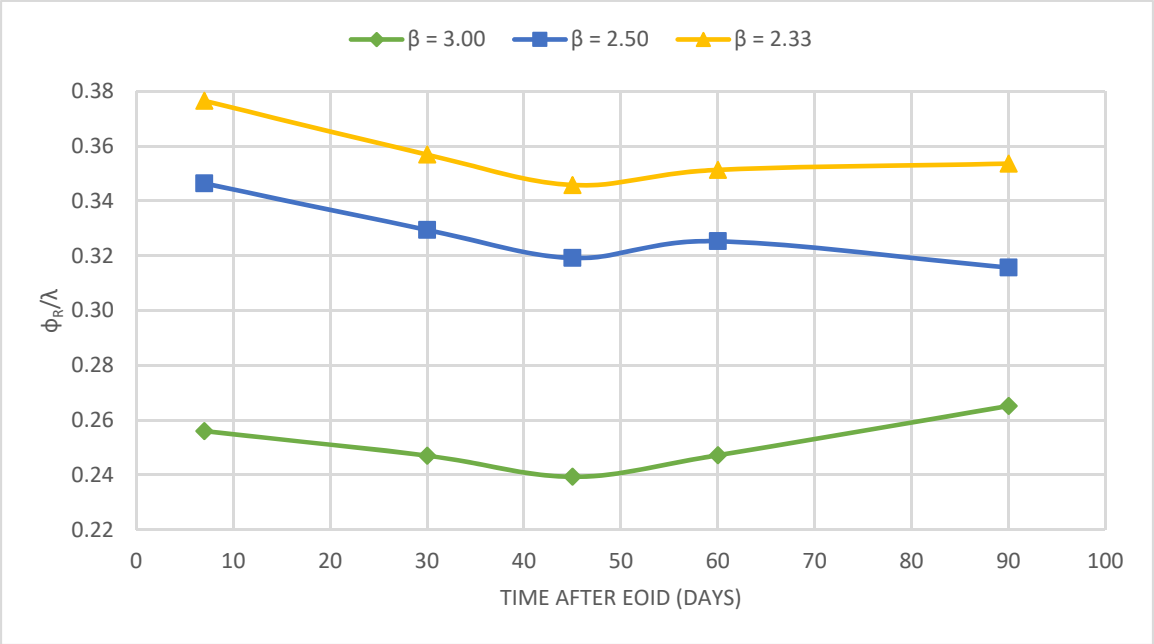

Figure 55: Variation of efficiency factor with setup incorporation for DRIVEN, considering Concrete Piles data set.

As shown in Tables 33 to 35 and Figures 44 to 55, the mean bias values increase for all the cases with respect of the ones with the actual SLTs as measured resistance, which decreases the COV, and generates an increase the resistance factors during the calibration stage. However, all the standard deviation values increase as well, which will increase the COV, and generates a decrease the resistance factors during the calibration. In other word, the standard deviation is inversely proportional to the mean ($\sigma \propto 1/\mu$) for the data distributions considered in this study. Consequently, it is better to evaluate the effect on the COV individually. The case of all data set shows that the COV remains stable for WBUZPILE and decreases for DRIVEN. The case of the steel H-Piles data set shows that the COV for WBUZPILE and DRIVEN slightly decrease. The case of concrete piles shows that the COV for WBUZPILE and DRIVEN slightly increase.

Since the resistance factor depends on the bias and the COV, each case shall be analyzed individually as well. For the case of all data set, the resistance factors increase from 11 % to 29 %. For the case of the steel H-piles, the resistance factors increase from 15% to 36%. For the case of the concrete piles, the resistance factors increase from 0% to 24%. It is demonstrated that even though the COV slightly increases (which tends to decrease the resistance factors), the substantially inflated bias value have a larger effect on the resistance factors. In addition, it is seen that the steel H-piles have the largest resistance factors increase. This phenomenon is a product of larger original bias values for the steel-H piles data set, compared to the other two data sets. In other words, larger original bias values produce higher bias values at 30, 45, 60, and 90 days. In addition, for the case of the steel-H piles, the COV is reduced at 30, 45, 60, and 90 days, which also contributes to generate higher resistance factors. Due to these reasons, it can be concluded that the setup incorporation has larger effects on steel-H Piles by showing the highest increase of resistance factors.

The bias efficiency values present an interesting behavior as well. The evaluation of the all data set reveals that the bias efficiency values slightly increase for some cases and decreases for other cases. Hence it is difficult to state a single conclusion about this case. However, the steel H-piles and concrete piles data set show a simpler behavior. On one hand, the evaluation of the Steel H-piles data set reveals that all the efficiency factors

increase. On the other hand, the evaluation of the concrete piles data set exhibits that the efficiency factors slightly decrease. The opposite efficiency behavior between the steel H-Piles data case and concrete data case is explained by the larger original bias values from the steel-H piles data set with respect of the original bias values from the concrete values. As stated before, larger original bias values produce higher bias values at 30, 45, 60, and 90 days. Consequently, the higher resistance factors and higher efficiency factors are generated when incorporating setup. These results confirm the fact that pile setup has a larger effect on steel H-Piles by showing the highest increase of efficiency factors.

To put it briefly, the Skov and Denver [1] model made possible the evaluation of pile setup incorporation effects on calibration of LRFD resistance factors at time intervals of 30, 45, 60, and 60 days. It is demonstrated that the resistance factors increase substantially with respect of the ones at SLT time due to the important increase in the bias value and the small modification of the COV. This also affects the efficiency bias factor by increasing it for the steel-H piles and decreasing it for the concrete piles. These reasons indicate that the setup incorporation is meaningful for the calibration of resistance factors and produce cost savings when using WBUZPILE and DRIVEN, especially, for steel-H Piles.

9.2 Setup Incorporation for Dynamic Load Testing.

The pile setup incorporation on the control field test such as Dynamic Load Tests (DLT) can also produce substantial cost savings. As stated in chapter 2, pile setup represents an increase on the pile capacity over time after the EOID. Larger pile capacity can be translated to smaller piles size, depth and number. These three factors represent less construction costs to the government and taxpayers. Thus, this section shows the incorporation of setup on the calibration of resistance factors for DLT as a prediction method. The DLT data consists of 18 resistance values obtained using PDA equipment and ICAP® signal matching. In the same way as the previous section, the pile setup is incorporated through the use of Skov and Denver [1] model considering the initial time

as the actual time at SLT. In this way, setup resistance values for 30, 45, 60, and 90 days after EOID are calculated and added to the SLT. The resistance values are shown in Table 26.

Table 36: Comparation of resistance factors incorporating setup for DLT.

All data set						
Design method		DLT				
Time		**SLT time**	30 days	45 days	60 days	90 days
λ_R		**1.600**	1.829	1.885	1.925	1.981
σ_R		**0.563**	0.680	0.699	0.713	0.733
COV_R		**0.352**	0.372	0.371	0.371	0.370
β = 3.00	ϕ_R	**0.70**	0.74	0.75	0.78	0.81
	Incr.	**0%**	6%	7%	11%	16%
	ϕ_R/λ	**0.44**	0.40	0.40	0.41	0.41
β = 2.50	ϕ_R	**0.82**	0.90	0.93	0.95	0.98
	Incr.	**0%**	10%	13%	16%	20%
	ϕ_R/λ	**0.51**	0.49	0.49	0.49	0.49
β = 2.33	ϕ_R	**0.88**	0.95	0.97	1.02	1.04
	Incr.	**0%**	8%	10%	16%	18%
	ϕ_R/λ	**0.55**	0.52	0.51	0.53	0.52
Average increase		*0%*	*8%*	*10%*	*14%*	*18%*

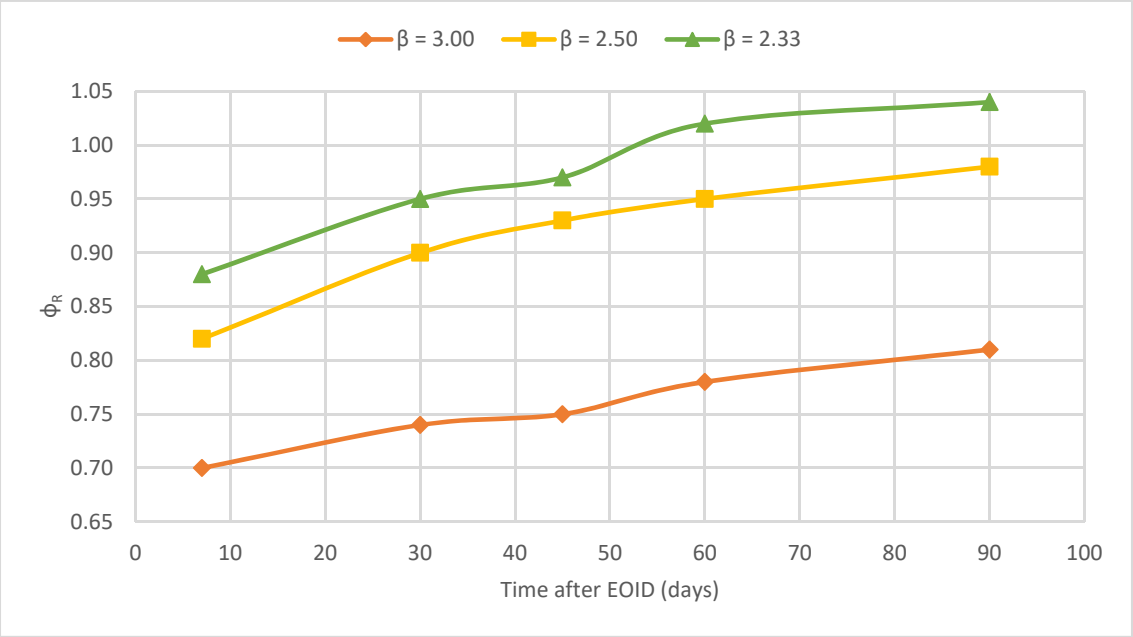

Figure 56: Variation of resistance factor with setup incorporation for DLT, considering entire data set.

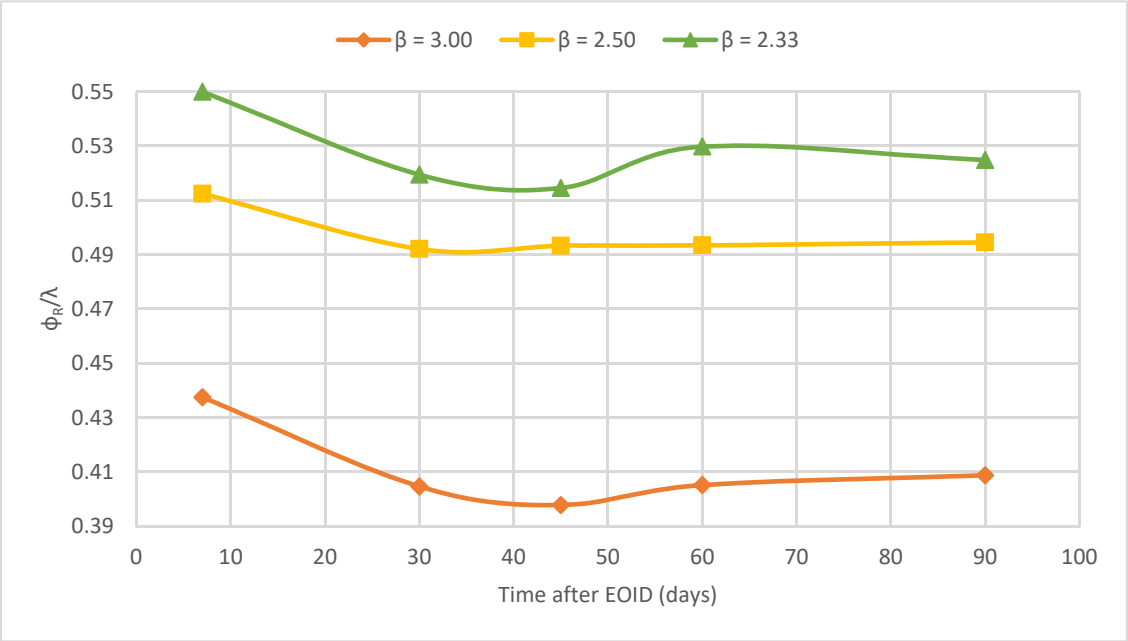

Figure 57: Variation of efficiency factor with setup incorporation for DLT, considering entire data set.

As shown in Table 26, the bias and standard deviation values increase for all the reliability index with respect of the ones with the actual SLTs as measured resistance. Consequently, it is better to evaluate the effect on the COV individually. The COV values for 30, 45, 60, and 90 days are very similar to each other and are slightly larger than the COV value at SLT time.

In regards of the resistance factor variation, Figure 56 shows that resistance factors have larger increase with a larger time interval after EOID. This means that the bias increase has a larger impact than the small COV increase on the calibrated resistance factors. Therefore, it is demonstrated that the setup resistance factors can produce cost savings in design and construction of driven piles.

In regards of the efficiency factor variation, Figure 57 shows that the efficiency factor slightly decreases once setup at 30 days in incorporated. Then, this efficiency factor remains almost stable for 45, 60, and 90 days. This means that the setup incorporation makes DLT slightly less efficient for control field purposes.

In summary, the Skov and Denver [1] model made possible the evaluation of pile setup incorporation effects on calibration of LRFD resistance factors at time intervals of 30, 45, 60, and 60 days. It is demonstrated that the resistance factors increase substantially with respect of the ones at SLT time due to the important increase in the bias value and the small increase of the COV. This also affects the efficiency bias factor by decreasing it once any time interval setup is incorporated. In other words, the setup incorporation makes DLT slightly less efficient. Nonetheless, since the main evaluated factor is the resistance factor, it is still fair to conclude that the setup incorporation is meaningful for the calibration of resistance factors and produces cost savings when using DLT as control field testing methods. Higher resistance factors involve larger usable pile capacities, which means smaller piles size, depth and number, hence cost savings.

9.3 Summary of Setup incorporation in the calibration of resistance factors.

The analysis presented in this chapter demonstrates that the setup incorporation in the calibration of LRFD resistance factors produces meaningful cost savings. As stated in chapter 2, pile setup represents an increase on the pile capacity over time after the EOID. Larger pile capacity can be translated to smaller piles size, depth and number. These three factors represent less construction costs to the government and taxpayers. The two cases evaluated are the static analysis method (WBUZPILE and DRIVEN) and dynamic load testing method (PDA with iCAP) as prediction methods. Both calibrations were performed considering SLT plus the setup increase modeled by Skov and Denver [1] Model at 30, 45, 60, and 90 days as measured resistance. Three data cases are evaluated (All piles data set, steel H-Piles data set, and concrete piles data set) for static analysis methods evaluation and just one general data case for the DLT analysis.

Regarding WBUZPILE and DRIVEN, the setup incorporation produces a significant increase in the resistance factors for the three data set. The efficiency presents an unstable behavior for the all piles set, increases for the steel H-Piles set, and decreases for the concrete piles set. Regarding dynamic load testing, the setup incorporation also produces a substantial increase of resistance factors. However, its efficiency decreases at 30 days and remains stable for 45, 60, and 90 days.

CHAPTER X COMPARISON OF RESISTANCE FACTORS WITH AASHTO, NCHRP, AND OTHER STATES

Pile design involves high uncertainty. While LRFD methodology proposes a more accurate design, the transition from ASD to LRFD is a slow process and expensive process due to the large amount of data required. According to a survey made by AbdelSalam et al [51] in 2009, 52% of state DOTs have fully implemented LRFD, 33% were in transition from ASD to LRFD, and 15% were still following ASD with FS of 2 and 2.5. In this chapter, the performance of Alabama prediction methods is evaluated by comparing it with bibliography from the federal government and other states according to the LFRD calibration performed. The compared bibliography consists of AASHTO and NCHRP 507 as federal type and other states such as Florida, Louisiana, Arkansas, Iowa, and Illinois. The prediction and construction control methods are evaluated in terms of reliability, efficiency, and consistency. In this study, the reliability is measured by the resistance factor. A higher resistance factor represents a more reliability method. The efficiency is measured by the efficiency factor if available. A higher efficiency factor represents a more efficient method. Finally, the consistency is measured by the COV value if available. A smaller COV value represents a more consistent method. It should be noted that, as seen in this chapter, specific comparisons are difficult due to the different cases study considered for each author. The different quality and quantity of

data are the main factors to decide which cases can be studied. For instance, while other documents consider the soil type factor, this document considers just the type pf pile due to the lack of data in specific soil types. Nevertheless, the comparison developed is useful to evaluate the performance of the prediction methods used by ALDOT.

10.1 Comparison of WBUZPILE and DRIVEN resistance factors.

As mentioned before, WBUZPILE and DRIVEN work as “static analysis methods” since can be used as the first methods to estimate the depth of piles. Therefore, both methods shall be compared just with other static analysis methods. This section compares the calibrated WBUZPILE and DRIVEN resistance factor with the resistance factors proposed by AASHTO, NCHRP 507, Florida, Louisiana, Iowa, and Illinois.

10.1.1 Comparison of WBUZPILE and DRIVEN resistance factors with AASHTO.

This section attempts to compare the resistance factors from WBUZPILE and DRIVEN with the resistance factors provided by AASHTO [38] specifications. AASHTO [37] presents resistance factors for static analysis methods and field determination methods. In regard of static analysis methods, AASHTO mainly considered the resistance factors calibrated by Paikowsky et al. [6]. However, since several resistance factors were calibrated, AASHTO [38] lists the average resistance factors for each method. It should be noted that AASHTO lists resistance factors for redundant piles. Nonetheless, its commentary suggests using an 80% of the redundant resistance factors for non-redundant piles.

A comparison between the resistance factors for WBUZPILE and DRIVEN method and the resistance factors for static analysis proposed by AASHTO [38] is shown in Table 37.

Table 37: Comparison of WBUZPILE and DRIVEN resistance factors with AASHTO specifications.

State	Alabama						AASHTO					
Year	2020						2014					
Pile Type	All Piles	All Piles	Steel-H Piles	Steel-H Piles	Concrete Piles	Concrete Piles	Side and End bearing resistance: Clay and Mixed Soils			Side and End bearing resistance: Sand		General
Design method	WBUZPILE	DRIVEN	WBUZPILE	DRIVEN	WBUZPILE	DRIVEN	α	β	λ	Nordlund/ Thurman	SPT	Schmertmann (CPT)
ϕ (β = 2.33)	**0.28**	**0.22**	**0.39**	**0.28**	**0.23**	**0.25**	**0.35**	**0.25**	**0.40**	**0.45**	**0.30**	**0.50**
ϕ (β = 3.00)	**0.19**	**0.14**	**0.26**	**0.20**	**0.17**	**0.17**	**0.28**	**0.20**	**0.32**	**0.36**	**0.24**	**0.40**

In terms of reliability, WBUZPILE and DRIVEN's resistance factors are almost similar with AASHTO's resistance factors for the α, β, λ and SPT method. Nevertheless, WBUZPILE and DRIVEN's resistance factors are significantly lower than AASHTO's resistance factors from the Nordlund/Thurman and the Schmertmann (CPT) method. These results indicate that, in average, WBUZPILE and DRIVEN are not as reliable as thee AASHTO static analysis methods.

In summary, according to the LRFD calibration performed, the WBUZPILE and DRIVEN are not, in average, as reliable as the static analysis methods provided by AASHTO. It is not possible to compare the efficiency and consistency since no efficiency and COV values from AASHTO specifications [37]. However, they can be considered implicit in the resistance factors.

10.1.2 Comparison of WBUZPILE and DRIVEN resistance factors with NCHRP 507.

This section attempts to compare the resistance factors from WBUZPILE and DRIVEN with the resistance factors provided by the report 507 from National Cooperative Highway Research Program (NCHRP) [6]. The NCHRP 507 [6] specifications is a document developed by Paikowsky et al. in order to address issues and to provide resistance factors for the load and resistance factor design of deep foundations. In case of driven piles, the database is composed by 338 static analysis case histories and 210 static and dynamic tested cases. The calibration methodology used is FOSM and FORM with 2.33 and 3.0 as reliability indices. All of the suggested resistance factors developed with for target reliability values can be found in the Tables 25 – 30 of NCHRP 507 [6] report.

Also, NCHRP 507 [6] states that static capacity design common methods tend to over-predict the capacity of observed pile capacities. On the other hand, dynamic capacity evaluation methods (CAPWAP) usually used for control tend to under-predict the observed pile capacities. However, it should be noted that parameters such as subsurface variability, site-specific technology, and previous experience, as well as amount and type of testing during construction, were bypassed for this study.

In addition, NCHRP 507 [6] found that the influence of the applied static load rate in the static pile tests has almost a null influence of the static pile capacity. Therefore, the Davisson's pile failure criterion can be used to determine the reference line for the capacity of driven piles, irrespective of the load-rate procedure. Furthermore, the research mentions that static or dynamic test (restrikes) should be performed no sooner than before the 75% of the pile capacity has been reached.

Several resistance factors were calibrated by Paikowsky et al. [6] in NCHRP 507. However, Table 38 and 39 shows the comparison of the resistance factors from Alabama with the resistance factors calibrated using FORM and dead-to-live load ratio of 2. Table 38 shows the comparison for the steel-H piles case and Table 39 shows the comparison for concrete piles case.

Table 38: Comparison of the resistance factors from WBUZPILE and DRIVEN with the resistance factors from NCHRP 507 (steel H-piles).

State		Alabama (2020)				NCHRP 507 (2004)	
Case w/o Pile Type		All Piles		Steel-H Piles		Steel-H Piles (Mixed Soils)	
Design method		WBUZPILE	DRIVEN	WBUZPILE	DRIVEN	α-API/ Norlund/ Thurmand	αTomlinson/ Norlund/ Thurman
Data set size		53	53	36	36	34	20
λ_R		0.979	1.049	1.175	1.230	0.790	0.590
COV_R		0.646	0.62	0.563	0.721	0.440	0.390
ϕ	β = 2.33	**0.28**	**0.22**	**0.39**	**0.28**	**0.35**	**0.30**
ϕ_R/λ_R		0.29	0.21	0.33	0.23	0.44	0.51
ϕ	β = 3.00	**0.19**	**0.14**	**0.26**	**0.20**	**0.25**	**0.25**
ϕ_R/λ_R		0.19	0.13	0.22	0.16*	0.32	0.42

Table 39: Comparison of the resistance factors from WBUZPILE and DRIVEN with the resistance factors from NCHRP 507 (concrete piles).

State		Alabama (2020)				NCHRP 507	
Case w/o Pile Type		All Piles		Concrete Piles		Concrete Pile (Mixed soils)	
Design method		WBUZPILE	DRIVEN	WBUZPILE	DRIVEN	β-method/ Thurman	αTomlinson/ Norlund/ Thurman
Data set size		53	53	17	17	80	33
λ_R		0.979	1.049	0.564	0.664	0.810	0.960
COV_R		0.646	0.762	0.486	0.527	0.380	0.490
ϕ_R	β = 2.33	**0.28**	**0.22**	**0.23**	**0.25**	**0.40**	**0.40**
ϕ_R/λ_R		0.29	0.21	0.41	0.44	0.49	0.42
ϕ_R	β = 3.00	**0.19**	**0.14**	**0.17**	**0.17**	**0.30**	**0.30**
ϕ_R/λ_R		0.19	0.13	0.30	0.26	0.37	0.31

In terms of reliability, WBUZPILE and DRIVEN show generally lower reliability than NCHRP's static analysis methods. Regarding concrete piles, WBUZPILE and DRIVEN show lower resistance factors than NCHRP. Regarding steel H-Piles, WBUZPILE shows slightly higher resistance factors than NCHRP, but DRIVEN shows slightly lower resistance factors than NCHRP. Regarding all piles case, WBUZPILE and DRIVEN show lower resistance factors. These results indicate that, in average, WBUZPILE and DRIVEN as not as reliable as NCHRP's static analysis methods, with the exception of WBUZPILE applied to steel H-piles.

In terms of efficiency, WBUZPILE and DRIVEN show lower efficiency than NCHRP's static analysis methods. WBUZPILE and DRIVEN show lower efficiency factors than NCHRP regarding all piles data set, steel H-Piles data set, and concrete piles data set. There results indicate that WBUZPILE and DRIVEN are not as efficient as NCHRP's static analysis methods.

In terms of consistency, WBUZPILE and DRIVEN show lower consistency than NCHRP static analysis methods. WBUZPILE and DRIVEN show larger COV values than NCHRP regarding all piles data set, steel H-Piles data set, and concrete piles data set. There results indicate that WBUZPILE and DRIVEN are not as consistent as NCHRP's static analysis methods.

In summary, according to the LRFD calibration performed, WBUZPILE is generally not as reliable, efficient, and consistent as NCHRP's static analysis methods, with the exception of the steel-H Piles case, where WBUZPILE reveals more reliability than NCHRP 507. DRIVEN is not as reliable, efficient, and consistent as NCHRP static analysis methods for the three data sets.

10.1.3 Comparison of WBUZPILE and DRIVEN resistance factors with the state of Florida.

This section attempts to compare the resistance factors from WBUZPILE and DRIVEN with the resistance factors used by the state of Florida. The state of Florida is

still on transition from ASD to LRFD. The section 1810 Deep Foundation of the sixth edition of Florida Building Code [53] just states that *Driven piles shall be designed and manufactured in accordance with accepted engineering practice to resist all stresses induced by handling, driving and service loads.* In other words, it still follows an ASD design methodology for driven piles. Nonetheless, researchers such as Styler [7] explored the incorporation of LRFD for piles driven in Florida Soils.

Styler [7] developed LRFD resistance factors using the Data Interchange for Geotechnical and Geoenvironmental Specialists (DIGGS) and following a FOSM and FORM calibration methodology. DIGGS consists of a new developed standard for digitally storing data tool. Prior to the calibration, the piles are also evaluated using the Bridge Software Institute's FB-Deep program. This software estimates the total pile capacity based on the full skin friction and one third of the end-bearing resistance. Both are calculated using blow counts and soil types provided by SPT boring logs. The calibration is performed by FORM and FOSM. A total number of 62 prestressed concrete piles from the state of Florida are considered for this study. The target reliability index β_T considered are 2, 2.25, 2.5, 2.75, 3, 3.5, 4, 4.5, and 5; and dead-to-live load ratios of 2, 2.5, and 3.

The results found by Styler [7] match the final statements made by Paikowsky et al [6]. The resistance factors calibrated by FORM are 8% to 23% greater than the ones calibrated by FOSM. Once the results are delivered, this project implements a modified FOSM method which agrees with the FORM results. Table 40 show the calibrated resistance factor from Alabama compared to the resistance factors from Florida by Styler [7].

Table 40: Comparison of the resistance factors from WBUZPILE and DRIVEN with the resistance factors from the state of Florida.

State		Alabama (2020)				Florida (2006)		
Case w/o Pile Type		All Piles		Concrete Piles		Concrete Piles		
Design method		WBUZPILE	DRIVEN	WBUZPILE	DRIVEN	FB-Deep (SPT)		
Number of Piles		53	53	17	17	63	63	63
λ_R		0.979	1.049	0.564	0.664	1.516	1.516	1.516
COV_R		0.646	0.762	0.486	0.527	0.472	0.472	0.472
ϕ_R	$\beta = 2.25$	----	----	----	----	**0.61**	**0.68**	**0.68**
ϕ_R/λ_R		----	----	----	----	0.41	0.45	0.45
ϕ_R	$\beta = 2.33$	**0.28**	**0.22**	**0.23**	**0.25**	----	----	----
ϕ_R/λ_R		0.29	0.21	0.41	0.38	----	----	----
ϕ_R	$\beta = 3.00$	**0.19**	**0.14**	**0.17**	**0.17**	**0.42**	**0.48**	**0.48**
ϕ_R/λ_R		0.19	0.13	0.30	0.26	0.28	0.32	0.32

In terms of reliability, WBUZPILE and DRIVEN show significant lower reliability than Florida's static analysis methods. Regarding redundant piles ($\beta = 2.33$ for Alabama's method and $\beta = 2.25$ for Florida's method), the highest resistance factors from WBUZPILE (0.28) and DRIVEN (0.23) are 59% and 66% lower than the FORM resistance factor from FB-Deep method (0.68), respectively. Regarding non-redundant piles, the highest resistance factors from WBUZPILE (0.19) and DRIVEN (0.17) are 60% and 65% lower than the FORM resistance factor from FB-Deep method (0.48), respectively. These results indicate that WBUZPILE and DRIVEN are not as reliable as the static analysis methods provided in Florida.

In terms of efficiency, WBUZPILE and DRIVEN show lower efficiency than Florida's static analysis methods. Regarding redundant piles ($\beta = 2.33$ for Alabama's method and $\beta = 2.25$ for Florida's method), the highest efficiency factors from WBUZPILE (0.41) and DRIVEN (0.38) are 9% and 16% lower than the FORM efficiency factor from FB-Deep method (0.45), respectively. Regarding non-redundant

piles, the highest efficiency factors from WBUZPILE (0.30) and DRIVEN (0.26) are 6% and 23% lower than the FORM efficiency factor from FB-Deep method (0.32), respectively. These results indicate that WBUZPILE and DRIVEN are not as efficient as the static analysis methods provided in Florida.

In terms of consistency, WBUZPILE and DRIVEN show lower consistency than Florida's static analysis methods. WBUZPILE shows its best consistency with the concrete piles. However, its COV value is 3% larger than FB-Deep's COV. The case of DRIVEN shows its best consistency also with concrete piles. Nevertheless, its COV value is 12% larger than FB-Deep's COV. These results indicate that WBUZPILE and DRIVEN are not as consistent as Florida's static analysis methods.

In summary, according to the LRFD calibration performed, WBUZPILE and DRIVEN are not as reliable, efficient, and consistent as Florida's static analysis method.

10.1.4 Comparison of WBUZPILE and DRIVEN resistance factors with the state of Louisiana.

This section attempts to compare the resistance factors from WBUZPILE and DRIVEN with the resistance factors used by the state of Louisiana. The state of Louisiana is also on transition from ASD to LRFD. The section 1810 Deep Foundation of the 2015 Louisiana Building Code [54] just states that *Driven piles shall be designed and manufactured in accordance with accepted engineering practice to resist all stresses induced by handling, driving and service loads.* In other words, it still follows an ASD design methodology for driven piles. Nonetheless, researchers such as Abu-Farsakh [55] explored the incorporation of LRFD for piles driven in Louisiana Soils.

Abu-Farsakh [54] calibrated the resistance factors for driven piles using a 53 piles database using MCS and a dead-to-live ratio of 2. The design methods evaluated were the static method (α-method and Norlund method), three direct cone penetration test (CPT) design methods (Schmertmann methods, De Ruiter and Beringen method, and Bustamante and Gianseselli (LCPC) method), and the Case Pile Wave Analysis Program (CAPWAP) method. The calibration was performed following FOSM, FORM, and MCS

methodology with a target reliability index of 2.33. Abu-Farsakh [55] concludes that the De Ruiter method shows the highest resistance factor ($\phi_R = 0.73$), while the Schmertmann method presents the lowest resistance factor ($\phi_R = 0.49$),which is even lower than the AASHTO suggested resistance factor of 0.50.

The predominant soil type in Louisiana is silty clay. Thus, CPT design methods are popular. Nonetheless, CPT methods are not as popular in Alabama due to their inability to go through stiff soil layers. While the north portion of Alabama has shallow bedrock layers, the south portion shows deeper bedrock layers. It is clear that this factor limits the application of CPT methods in Alabama soils. However, the comparison is still developed because if specific cases of low to medium depth piles where the pile toe does not reach the bedrock are considered, the CPT methods can be used in Alabama soils. The two calibrations from Louisiana with the highest resistance factors are compared to the Alabama's resistance factors in Table 41.

Table 41: Comparison of the resistance factors from WBUZPILE and DRIVEN with the resistance factors from the state of Louisiana.

State	Alabama (2020)						Louisiana (2009)	
Case w/o Pile Type	All Piles		Steel-H Piles		Concrete Piles		All Piles	
Design method	WBUZPILE	DRIVEN	WBUZPILE	DRIVEN	WBUZPILE	DRIVEN	De Ruiter-Beringen method	Schmertmann method
Number of Piles	53	53	36	36	17	17	53	53
ϕ (β = 2.33)	**0.28**	**0.22**	**0.39**	**0.28**	**0.23**	**0.25**	**0.73**	**0.49**

In terms of reliability, WBUZPILE and DRIVEN show significant lower reliability than Louisiana's static analysis methods. Regarding redundant piles and if the highest resistance factors are considered, WBUZPILE and DRIVEN show 46% and 62% lower resistance factors than the De Ruiter-Beringen method (Louisiana), respectively. It is not possible to compare non-redundant resistance factors because they were not

available for the author. Nonetheless, it is still possible to conclude that WBUZPILE and DRIVEN are not as reliable as Louisiana's static analysis methods.

In summary, according to the LRFD calibration performed, WBUZPILE and DRIVEN are not as reliable as Louisiana's static analysis method. No quantitative comparison of the efficiency and consistency is possible due to the unavailability of data in Abu-Farsakh [54] . However, both can be considered implicit in the reliability comparison. Also, it should be noted that this specific comparison is the one that present the largest difference between resistance factors for static analysis methods.

10.1.5 Comparison of WBUZPILE and DRIVEN resistance factors with the state of Iowa.

This section attempts to compare the resistance factors from WBUZPILE and DRIVEN with the resistance factors used by the state of Iowa. The state of Iowa has already transitioned from ASD to LRFD. The Iowa DOT LRFD Bridge Design Manual [55] states that the pile section and contract length shall be determined by the load and resistance factor design (LRFD) method. Iowa DOT proposes resistance factors just for redundant piles considering different combinations for construction methods originally calibrated by AbdelSalam et al [22].

Firstly, the Iowa DOT LRFD Bridge Design Manual [56] lists resistance factors just for the Iowa Blue Book method as a static analysis method if the Iowa Dot ENR formula is used as driving criterion. In this way, the manual considers different resistance factors for cohesive, mixed, and non-cohesive soils.

Secondly, AbdelSalam et al [22] performed the LRFD calibration for driven piles considering Static Analysis Methods, Dynamic Analysis Methods, and Dynamic Formulas. For the case of the static analysis methods, AbdelSalam et al [22] used 25 tests for clay, 36 tests for sand, and 29 tests for mixed soils. The calibration was performed following lognormal data distribution and FOSM reliability approach.

In regards of static analysis methods, AbdelSalam et al [22] considered five methods: SPT-Meyerhof method, α-API, β-method, Nordlund method, and Blue Book method. They conclude that for redundant pile groups, the Blue Book method shows the

highest resistance factor for sand soils. The Blue Book method also shows the highest resistance factors for clay soils. In case of mixed soils, the SPT-Meyerhof has the highest resistance factors followed by the Blue Book method in second. For redundant piles, the resistance factors were reduced in 30%. Finally, AbdelSalam et al [22] recommends using the Iowa Blue Book method for all pile design due to its high efficiency and popularity in the state of Iowa.

A comparison between the resistance factors for WBUZPILE and DRIVEN method and the resistance factors for static analysis methods evaluated by Iowa DOT [56] is shown in Table 42. The case of mixed soils is considered because it is the most similar to Alabama's case.

Table 42: Comparison of the resistance factors WBUZPILE and DRIVEN with the resistance factors from the state of Iowa.

State		Alabama (2020)						Iowa (2012)	
Case w/o Pile Type		All Piles		Steel-H Piles		Concrete Piles		All Piles in cohesive and mixed soils	All Piles in non-cohesive soils
Design method		WBUZPILE	DRIVEN	WBUZPILE	DRIVEN	WBUZPILE	DRIVEN	Blue Book	Blue Book
ϕ_R	(β = 2.33)	**0.28**	**0.22**	**0.39**	**0.28**	**0.23**	**0.25**	**0.60**	**0.50**

In terms of reliability, WBUZPILE and DRIVEN show significantly lower reliability than the static analysis method listed by Iowa DOT. Regarding redundant piles, WBUZPILE and DRIVEN present lower resistance factors than the both cases of the Blue Book method provided by Iowa DOT. It is not possible to compare non-redundant piles since no non-redundant resistance factors are listed in Iowa DOT bridge manual [56].

In summary, according to the LRFD calibration performed, WBUZPILE and DRIVEN are not as reliable as Iowa's static analysis method provided by Iowa DOT

[55]. No quantitative comparison of the efficiency and consistency is possible due to the unavailability of data in Iowa DOT Bridge Design Manual [55]. However, both can be considered implicit in the reliability comparison.

10.1.6 Comparison of WBUZPILE and DRIVEN resistance factors with the state of Illinois.

This section attempts to compare the resistance factors from WBUZPILE and DRIVEN with the resistance factors used by the state of Illinois. The state of Illinois is still on transition from ASD to LRFD. The section 1810 Deep Foundations of the Building Code 2018 of Illinois [56] just states that *Driven piles shall be designed and manufactured in accordance with accepted engineering practice to resist all stresses induced by handling, driving and service loads.* In other words, it still follows an ASD design methodology for driven piles. Nonetheless, researchers such as Long et al. [58] explored the incorporation of LRFD for piles driven in Illinois Soils.

Long et al. [58] performed a LRFD Calibration of resistance factor for driven piles considering Static Analysis methods and Dynamic Analysis methods. For the case of the static analysis methods, Long et al. [58] used a collection of 26 load tests. The calibration was performed following lognormal data distribution and FORM reliability approach.

In regards of static analysis methods, Long et al. [58] considered five methods: The IDOT static (S-IDOT) method, the Kinematic IDOT (K-IDOT) method, the Imperial College Pile method, the Olson's method, and DRIVEN. The S-IDOT method uses SPT N-Values and undrained shear strength (if applicable) to determine the pile capacity. The K-IDOT method additionally considers whether the pile is plugged or unplugged. Basically, the piles are considered unplugged if the tip capacity is greater than the side capacity. On the other hand, if a H-Pile is found to be plugged, then it is considered a solid rectangular prism.

They conclude that the K-IDOT method is the one that better reflects the physical reality of a driven pile. It has the highest resistance and efficiency factors. In addition, it shows the best agreements with the dynamic formulae methods. A comparison of the

resistance factors from WBUZPILE and DRIVEN, and the FORM resistance factors for IDOT static analysis methods calibrated by Long et al. [58] is shown in Table 43. The dead-to-live load ratio considered by Illinois is 2 as considered in this study.

Table 43: Comparison of the resistance factors from WBUZPILE and DRIVEN with the resistance factors from the state of Illinois.

State		Alabama (2020)						Illinois (2009)		
Case w/o Pile Type		All Piles		Steel-H Piles		Concrete Piles		H-Piles		
Design method		WBUZPILE	DRIVEN	WBUZPILE	DRIVEN	WBUZPILE	DRIVEN	S-IDOT	Corrected S-IDOT	Corrected K-IDOT
Number of Piles		53	53	36	36	17	17	26	26	26
λ_R		0.979	1.049	1.175	1.230	0.564	0.664	1.110	0.970	1.090
COV_R		0.646	0.762	0.563	0.721	0.486	0.527	0.666	0.650	0.525
ϕ_R	(β = 2.33)	**0.28**	**0.22**	**0.39**	**0.28**	**0.23**	**0.25**	**0.29**	**0.26**	**0.40**
ϕ_R/λ_R		0.29	0.21	0.33	0.23	0.41	0.38	0.26	0.27	0.37
ϕ_R	(β = 3.00)	**0.19**	**0.14**	**0.26**	**0.20**	**0.11**	**0.17**	**0.19**	**0.18**	**0.28**
ϕ_R/λ_R		0.19	0.13	0.22	0.16*	0.30	0.26	0.17	0.19	0.26

In terms of reliability, WBUZPILE and DRIVEN show almost similar reliability to the static analysis methods from Illinois. It should be noted that the most reliable method provided by Illinois is the corrected K-IDOT method. In this way, regarding redundant piles and considering the highest resistance factors, WBUZPILE and DRIVEN shows 3% and 30% lower resistance factors than the corrected K-IDOT method, respectively. Regarding non-redundant piles and considering the highest resistance factors, WBUZPILE and DRIVEN shows 7% and 29% lower resistance factors than the corrected K-IDOT method, respectively. These results indicate that WBUZPILE and DRIVEN are as reliable as Iowa's static analysis methods.

In terms of efficiency, WBUZPILE and DRIVEN show almost similar efficiency to the static analysis methods from Illinois. It should be noted that the most efficient method provided by Iowa is the corrected K-IDOT method. In this way, regarding

redundant piles and considering the highest efficient factors, WBUZPILE shows 11% higher and DRIVEN shows 3% higher efficient factors than the corrected K-IDOT method. Regarding non-redundant piles and considering the highest efficient factors, WBUZPILE shows 15% higher and DRIVEN shows equal efficient factors than the corrected K-IDOT method. These results indicate that WBUZPILE and DRIVEN are slightly more efficient than Iowa's static analysis methods.

In terms of consistency, WBUZPILE and DRIVEN show almost similar consistency to static analysis methods used in Illinois. The average of the COV values from WBUZPILE (0.563) is just 8% smaller than the average COV values from Illinois' method (0.614). The average of the COV values from DRIVEN (0.667) is just 9% larger than the average COV values from Illinois' method (0.614). These results indicate that WBUZPILE are as consistent as the static analysis methods considered by Illinois.

In terms of consistency, WBUZPILE and DRIVEN show almost similar consistency to the static analysis methods from Illinois. It should be noted that the most consistency method provided by Iowa is the corrected K-IDOT method. In this way, if the most consistent cases are considered, WBUZPILE reveals a COV 7% lower and DRIVEN reveals a COV 0.2% larger than K-IDOT COV. These results indicate that WBUZPILE and DRIVEN are as consistent as Illinois's static analysis methods.

10.2 Comparison of Alabama Dynamic Load Testing resistance factors.

As previously mentioned, Dynamic Load Testing can be used as control field testing methods since they complement the static analysis methods. This section compares the calibrated DLT resistance factors with the resistance factors proposed by AASHTO, NCHRP 507, and specifications from other states.

10.2.1 Comparison of Alabama DLT resistance factors with AASHTO.

This section attempts to compare the resistance factors from Dynamic Load Testing in Alabama with the resistance factors provided by AASHTO [37] specifications. As stated before, AASHTO [37] presents resistance factors for static analysis methods and control construction methods. The resistance factor listed are mainly from Paikowsky et al. [6]. In regards of dynamic control construction methods, AASHTO [37] considers combinations between the prediction method and the number of tests performed. Table 44 compares Alabama's DLT resistance factors with the most similar cases from AASHTO [37]. It should be noted that AASHTO lists resistance factors for redundant piles. Nonetheless, its commentary suggests using an 80% of the redundant resistance factors for non-redundant piles.

Table 44: Comparison of the resistance factors from Alabama DLT with AASHTO specifications.

State	Alabama (2020)	AASHTO (2014)	
Pile Type	All Piles	Driving Criteria established by dynamic testing conducted on 100% of production piles	Driving Criteria established by dynamic testing, quality control by dynamic testing of at least two piles per site condition, but not less than 2% of the production piles
Design method	DLT (iCAP)	DLT with signal matching	DLT with signal matching
ϕ_R (β = 2.33)	**0.88**	**0.75**	**0.65**
ϕ_R (β = 3.00)	**0.70**	**0.60**	**0.52**

Table 44 shows that Alabama's DLT resistance factors are higher than the ones provided by AASHTO. In case of redundant and non-redundant piles piles, Alabama DLT's resistance factors are 17% larger than AASHTO DLT's resistance factors when conducted for 100% of the production piles, and 35% larger than AASHTO DLT's

resistance factors when conducted for 2% of the production piles. These larger factors indicate that the DLT is more reliable in Alabama Soils than when conducted in the soils evaluated by AASHTO [38].

In summary, it is found that Alabama's DLT have higher resistance factors than AASHTO's resistance factors. This fact indicates that DLT is more reliable when conducted in Alabama Soils than when conducted in the soils evaluated by AASHTO [38].

10.2.2 Comparison of Alabama DLT resistance factors with NCHRP 507.

This section attempts to compare the resistance factors from Dynamic Load Testing in Alabama with the resistance factors provided by the report 507 from National Cooperative Highway Research Program (NCHRP) [6]. The NCHRP 507 [6] specifications is a document developed by Paikowsky et al. in order to address issues and to provide resistance factors for the load and resistance factor design of deep foundations. In case of driven piles, the database is composed by 338 static analysis cases histories and 210 static and dynamic tested cases. The calibration methodology used is FOSM and FORM with 2.33 and 3.0 as reliability indices. All of the suggested resistance factors developed with both target reliability values can be found in the Tables 25 – 30 of his report.

Regarding control construction methods, Paikowsky et al. [6] studied Dynamic measurements, Dynamic Equations, and WEAP. Firstly, Dynamic Measurements include signal matching using CAPWAP and Energy Approach. Second, Dynamic Equations involve ENR, Gates, and FHWA modified method. Finally, WEAP is applied just to EOID. Table 45 shows the comparison between the resistance factors for Alabama's DLT and Dynamic Measurements and WEAP.

Table 45: Comparison of the resistance factors from Alabama DLT with the resistance factors from NCHRP 507.

State		Alabama (2020)	NCHRP 507 (2004)				
Pile Type / Case		All Piles	EOID	BOR	EOID	BOR	EOID
Design method		DLT (iCAP)	CAPWAP	CAPWAP	Energy Approach	Energy Approach	WEAP
ϕ_R	$\beta = 2.33$	**0.88**	**0.65**	**0.65**	**0.55**	**0.40**	**0.40**
ϕ_R/λ_R		0.55	0.40	0.56	0.49	0.52	0.24
ϕ_R	$\beta = 3.00$	**0.70**	**0.45**	**0.50**	**0.40**	**0.30**	**0.25**
ϕ_R/λ_R		0.44	0.28	0.44	0.37	0.41	0.15

As shown in table 45, Alabama DLT's resistance factors are significantly higher than the ones provided by NCHRP 507 [6]. While the highest resistance factors from NCHRP 507 [6] are from The CAPWAP signal matching method for EOID and BOR, the resistance factors from Alabama's DLT are even higher. In case of redundant piles, Alabama's DLT shows a 31% higher resistance factor than NCHRP CAPWAP for both EOID and BOR. In case of non-redundant piles, Alabama's DLT shows a 56% and 40% higher resistance factor than NCHRP CAPWAP for EOID and BOR, respectively.

In terms of efficiency, Alabama DLT's efficiency factor is generally higher than the NCHRP's resistance factors, with the exception of the CAPWAP applied to BOR methods, which shows the highest efficiency factor from NCHRP 507 [6]. In this specific case, Alabama's DLT shows almost similar efficiency factors to NCHRP 507 [6].

In summary, according to the data provided by ALDOT and the analysis performed, the calibrated resistance factors from Alabama's DLT are significantly larger than the ones from NCHRP 507 for redundant and non-redundant piles. In regards of efficiency, Alabama's DLT present similar efficiency to the NCHRP methods.

10.2.3 Comparison of the resistance factors from Alabama DLT with the state of Arkansas.

This section attempts to compare the resistance factors from Dynamic Load Testing in Alabama with the resistance factors used by the state of Arkansas. As stated before, the state of Arkansas is still on transition from ASD to LRFD. The section 1810 Deep Foundations of the Arkansas Fire Prevention Code Vol II Building [58] just states that *Driven piles shall be designed and manufactured in accordance with accepted engineering practice to resist all stresses induced by handling, driving and service loads.* In other words, it still follows an ASD design methodology for driven piles. Nonetheless, researchers such as Bostwick [40] explored the incorporation of LRFD for piles driven in Arkansas Soils for construction control methods.

Bostwick [40] performed different LRFD resistance factor calibrations through MCS using a 123 piles database size. The data is composed by SLT and DLT using CAPWAP as signal matching method. Bostwick [38] states that, on average, DLT value represent 60% of the SLT values. In other words, DLR tend to underpredict the pile capacity compared to SLT. 11 cases are studied, but just 7 show calibrated resistance factors including a Paikowsky et al [6]. database case, where 59 piles of their data were used to calibrated resistance factors. A comparison between the resistance factors for Alabama DLT method and the resistance factor for dynamic methods evaluated by Bostwick [40] is shown in Table 46.

Table 46: Comparison of the resistance factors from Alabama DLT with the resistance factors from the state of Arkansas.

State		Alabama (2020)	Arkansas (2014)						
Case w/o Pile Type		All Piles	All Piles EOID	H-Piles in Clay EOID	H-Piles in Sand EOID	PPC Piles in Clay EOID	PPC Piles in Sand EOID	All Piles BOR	Paikowsky Piles EOID
Design method		DLT (iCAP)	DLT (CAPWAP)	DLT (CAPWAP)	DLT (CAPWAP)	DLT (CAPWAP)	DLT (CAPWAP)	DLT (CAPWAP)	DLT (CAPWAP)
Number of Piles		18	123	18	32	28	20	37	59
λ_R		1.600	1.590	1.280	1.130	2.910	1.860	1.100	1.920
COV_R		0.352	0.630	0.550	0.400	0.820	1.130	0.320	0.590
ϕ_R	(β = 2.33)	**0.88**	**0.45**	**0.44**	**0.54**	**0.55**	**0.56**	**0.63**	**0.59**
ϕ_R/λ_R		0.55	0.28	0.34	0.48	0.19	0.30	0.57	0.31
ϕ_R	(β = 3.00)	**0.70**	**0.31**	**0.31**	**0.42**	**0.34**	**0.38**	**0.51**	**0.41**
ϕ_R/λ_R		0.44	0.19	0.24	0.37	0.12	0.20	0.46	0.21

In terms of reliability, Alabama DLT's resistance factors are significantly higher than the resistance factors provided by Bostwick [41]. The highest resistance factors from Bostwick [38] are the ones for the DLT (CAPWAP) method for all piles BOR. However, in case of redundant piles, Alabama DLT's resistance factor is 40% higher than All Piles BOR method's (Arkansas) resistance factor. In case of non-redundant 37% higher than All Piles BOR method's (Arkansas) resistance factor. This indicate that Alabama DLT is more reliable than the method evaluated by Bostwick [41] for Arkansas' soils.

In terms of efficiency, Alabama DLT's efficiency factors are slightly lower than the most efficient method evaluated in the state of Arkansas, which is the All Piles BOR method evaluated by Bostwick [41]. In case of redundant piles, Alabama DLT's efficiency factor is 3.5% lower than All Piles BOR method's efficiency factor. In case of non-redundant piles, Alabama DLT's efficiency factor is 5% lower than All Piles BOR method's efficiency factor. This indicate that Alabama DLT is slightly less efficient than the All Piles BOR method, which is most efficient method evaluated by Bostwick [41] for Arkansas' soils.

In terms of consistency, Alabama DLT is slightly more consistent than the most consistent method evaluated in the state of Arkansas, which is the All Piles BOR method evaluated by Bostwick [41]. Alabama DLT's COV is 10% larger than the All Piles BOR method's COV.

In summary, according to the LRFD calibration performed, the Alabama DLT method is generally more reliable, efficient, and consistent than the control construction methods evaluated by Bostwick [41] for Arkansas soils, with exception of the All Piles BOR method. The Alabama DLT method is more reliable, but less efficient and consistent than the All Piles BOR method.

10.2.4 Comparison of Alabama DLT resistance factors with the state of Iowa.

This section attempts to compare the resistance factors from Dynamic Load testing with the resistance factors used by the state of Iowa. As mentioned before, the state of Iowa has already transitioned from ASD to LRFD. The Iowa DOT LRFD Bridge Design Manual [56] states that the pile section and contract length shall be determined by the load and resistance factor design (LRFD) method. Iowa DOT proposes resistance factors just for redundant piles considering different combinations for construction methods originally calibrated by AbdelSalam et al [22]. In this section, the DLT resistance factors are compared the Iowa construction control resistance factors listed in Iowa DOT LRFD Bridge Design Manual and AbdelSalam et al [22] paper.

A comparison between the resistance factors for Alabama DLT method and the resistance factor for dynamic methods evaluated by Iowa DOT and AbdelSalam et al [22] is shown in Table 47. The case of mixed soils is considered because it is the most similar to Alabama's case.

Table 47: Comparison of the resistance factors from Alabama DLT with the resistance factors from the state of Iowa.

State		Alabama (2020)	Iowa		
Case w/o Pile Type		All Piles	All Piles in cohesive and mixed soils		
Design method		DLT (iCAP)	WEAP only (Blue Book based)	WEAP and PDA/CAPWAP (Blue Book based)	WEAP, PDA/CAPWAP, Planned Retap Test 3-days after EOID (Blue Book based)
ϕ_R	(β = 2.33)	**0.88**	**0.65**	**0.70**	**0.70**

In terms of reliability, Alabama DLT's resistance factors are significantly higher than the resistance factors provided Iowa DOT [56]. The highest resistance factors from Iowa DOT [55] are the ones for the WEAP and PDA/CAPWAP (Blue Book based) method and WEAP, PDA/CAPWAP, Planned Retap Test 3-days after EOID (Blue Book based) method. In case of redundant piles, the Alabama DLT's resistance factor is 26% higher than the resistance factors for both Iowa methods previously mentioned. This indicate that Alabama DLT is more reliable than the methods evaluated by Iowa DOT.

In summary, according to the LRFD calibration performed, the Alabama DLT method is generally more reliable than the three control construction methods provided by Iowa DOT. It is not possible compare the efficiency and consistency since no efficiency and COV values from Iowa DOT Bridge Design Manual [55] are available. However, they can be considered implicit in the resistance factors.

10.2.5 Comparison of Alabama DLT resistance factors with the state of Illinois.

This section attempts to compare the resistance factors from Dynamic Load testing with the resistance factors used by the state of Illinois. As stated before, the state

of Illinois is still on transition from ASD to LRFD. The section 1810 Deep Foundations of the Building Code 2018 of Illinois [57] just states that *Driven piles shall be designed and manufactured in accordance with accepted engineering practice to resist all stresses induced by handling, driving and service loads.* In other words, it still follows an ASD design methodology for driven piles. Nonetheless, researchers such as Long et al [57] explored the incorporation of LRFD for piles driven in Illinois Soils for construction control methods. This section attempts to compare the resistance factor from Alabama DLT with the resistance factors calibrated by Long et al. [58]. Table # shows a comparison between the preliminary resistance factors from Alabama and the resistance factors from Illinois using FORM and a dead-to-live ratio of 2

A comparison between the resistance factors for Alabama DLT method and the resistance factor for dynamic methods evaluated by Long et al. [58] is shown in Table 48.

Table 48: Comparison of the resistance factors from Alabama DLT with the resistance factors from the state of Illinois.

State		Alabama (2020)	Illinois (2009)		
Case w/o Pile Type		All Piles	H Piles and Pipe Piles		
Design method		DLT (iCAP)	FHWA-Gates	FHWA-UI	WS-DOT
Number of Piles		18	132	132	132
λ_R		1.600	1.020	1.150	1.050
COV_R		0.352	0.485	0.405	0.451
ϕ_R	(β = 2.33)	**0.88**	**0.47**	**0.61**	**0.47**
ϕ_R/λ_R		0.55	0.46	0.53	0.45
ϕ_R	(β = 3.00)	**0.70**	**0.30**	**0.42**	**0.34**
ϕ_R/λ_R		0.44	0.29	0.37	0.32

In terms of reliability, Alabama DLT's resistance factors are significantly higher than the resistance factors provided by Long et al. [58]. The highest resistance factors from Long et al. [58] are the ones FHWA-UI method. However, in case of redundant

piles, Alabama DLT's resistance factor is 44% higher than FHWA-UI method's resistance factor. In case of non-redundant piles, Alabama DLT's resistance factor is 67% higher than FHWA-UI method's resistance factor. This indicate that Alabama DLT is more reliable than the methods evaluated by Long et al. [58] for Illinois' soils.

In terms of efficiency, Alabama DLT's efficiency factors are slightly larger than the most efficient method evaluated in the state of Arkansas, which is the FHWA-UI method evaluated by Long et al. [58]. In case of redundant piles, Alabama DLT's efficiency factor is 3.8% lower than FHWA-UI method's efficiency factor. In case of non-redundant piles, Alabama DLT's efficiency factor is 19% larger than FHWA-UI method's efficiency factor. This indicate that Alabama DLT is slightly less efficient than the FHWA-UI method, which is most efficient method evaluated by Long et al [57] for Illinois' soils.

In terms of consistency, Alabama DLT is slightly more consistent than the most consistent method evaluated in the state of Illinois, which is the FHWA-UI method evaluated by Long et al. [58]. Alabama DLT's COV is 13% lower than the FHWA-UI method's COV.

In summary, according to the LRFD calibration performed, the Alabama DLT method is more reliable, efficient, and consistent than the control construction methods evaluated by Long et al. [58] for Illinois' soils. Even the most reliable, efficient, and consistent method from Illinois, which is the FHWA-UI method, shows lower performance than Alabama DLT method.

10.3 Summary of comparison of resistance factors with AASHTO, NCHRP 507, and other states.

This section attempts to summarize the comparison of the performance of the prediction methods used by ALDOT with prediction methods used by the federal government and other states. The parameters considered are the resistance factor and efficiency factor (not COV). ALDOT prediction methods are compared with the methods with the highest resistance and efficiency factor. It should be noted that, as seen in this chapter, specific comparisons are difficult due to the different cases considered by each

author. The different quality and quantity of data are the main factors to decide which cases can be studied. For instance, while other documents consider the soil type factor, this document considers just the type of pile due to the lack of data in specific soil types. Nevertheless, the comparison developed is useful to evaluate the performance of the prediction methods used by ALDOT.

Regarding static analysis methods and according to the comparison performed, WBUZPILE and DRIVEN present lower reliability and efficiency than the static analysis methods provide by the federal publications available such as AASHTO and NCHRP 507. In addition, this difference becomes even larger when comparing with Florida, Louisiana, and Iowa. The only state that shows consistent results with WBUZPILE and DRIVEN is Illinois. Apparently, this problem is cause by the limited data size from ALDOT. However, cases such as Louisiana, Iowa, and Illinois have similar or smaller data size than ALDOT. Florida has just 10 more piles than ALDOT and its results are significantly higher. Therefore, it can be concluded that the prediction method used by ALDOT (WBUZPILE) and DRIVEN is not as reliable for Alabama soils as the other static analysis methods considered in the comparison. For a better appreciation, Figures 58 to 61 show a comparison of WBUZPILE and DRIVEN resistance and efficiency factors with the static analysis methods with the highest resistance and efficiency factors found in this chapter for redundant and non-redundant piles.

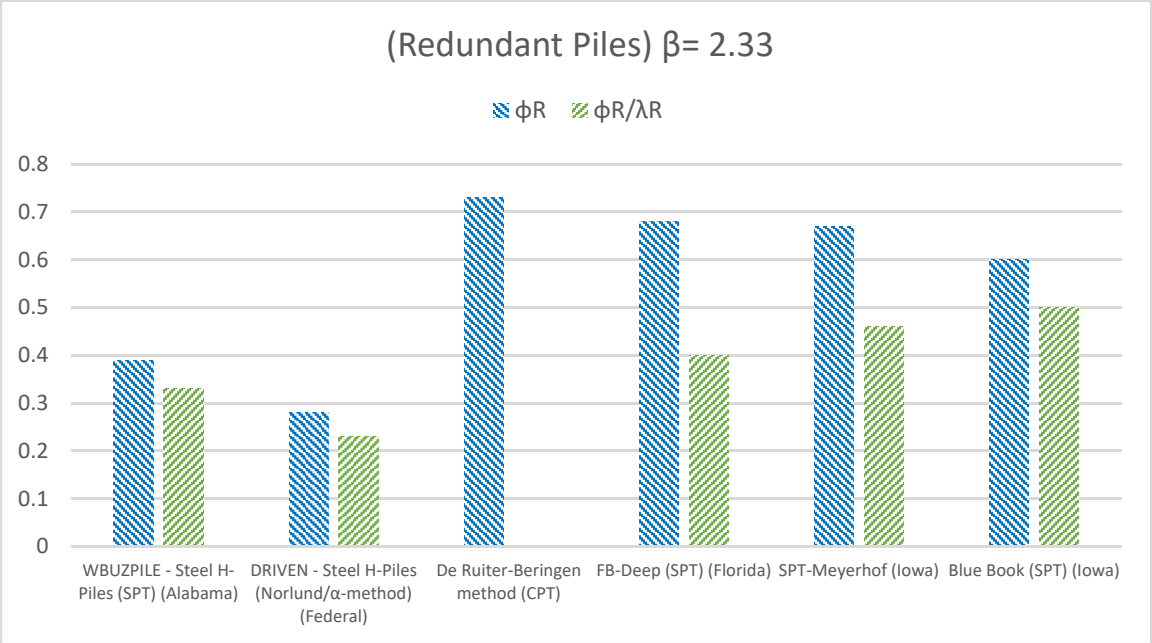

Figure 58: Static analysis methods with the highest ϕ_R for redundant piles.

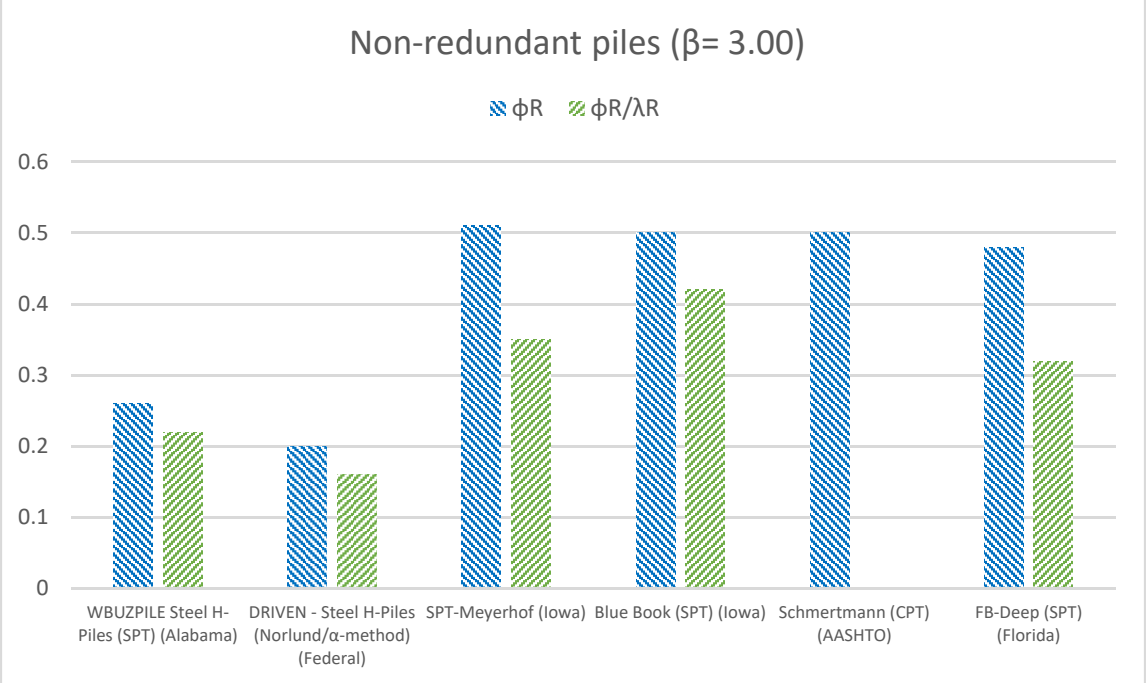

Figure 59: Static analysis methods the highest ϕ_R for non-redundant piles.

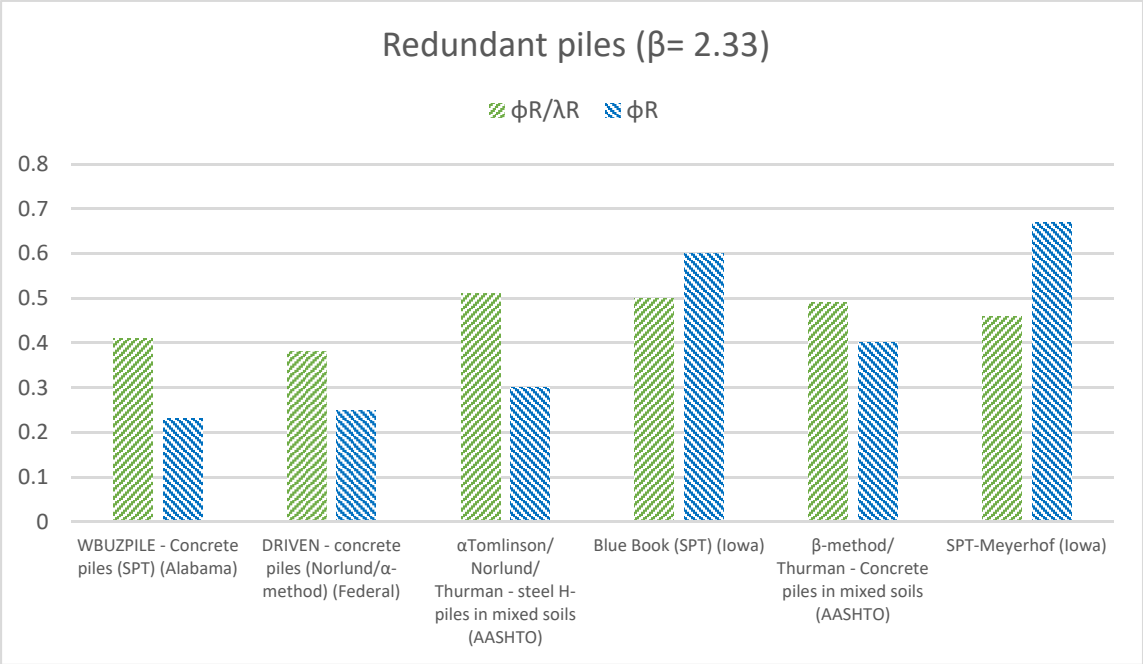

Figure 60: Static analysis methods with the highest ϕ_R/λ_R for redundant piles.

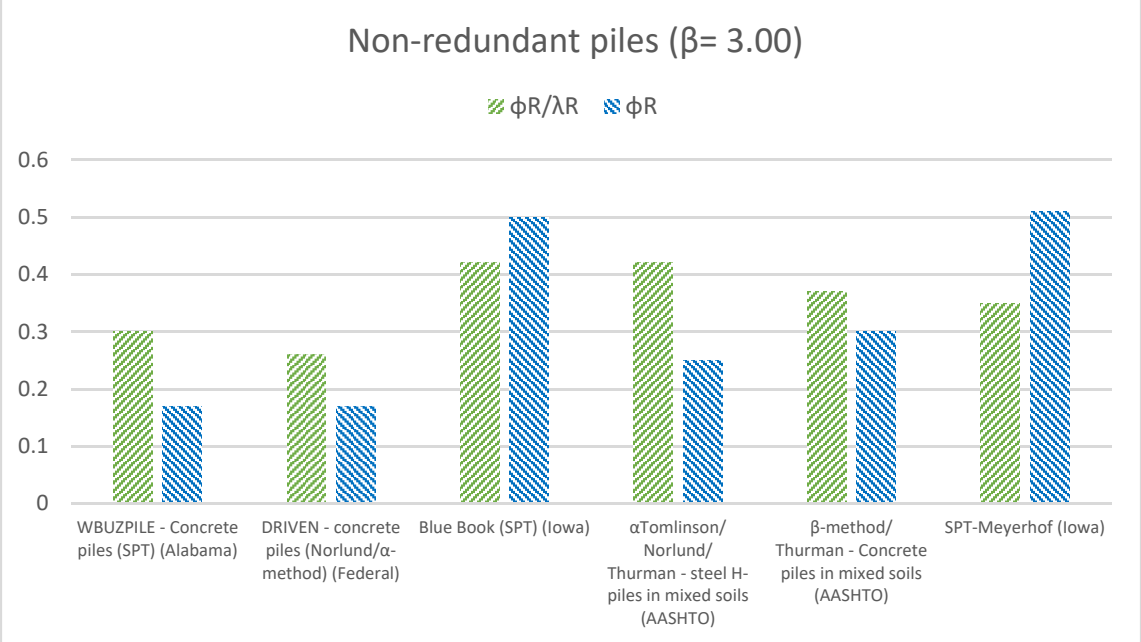

Figure 61: Static analysis methods with the highest ϕ_R/λ_R for non-redundant piles

Figures 58 and 60 show that, in regard on redundant piles, the Ruiter-Beringen method has the largest resistance factor and the αTomlinson/Norlund/Thurman method has the largest efficiency factor. Figures 59 and 61 show that, in regard of non-redundant piles, The SPT-Meyerhof method has the largest resistance factor, and the Blue Book and the αTomlinson/Norlund/Thurman method present the largest efficiency factors. These results indicate that the CPT, SPT, and some basic static analysis methods show high reliability and efficiency in other states. Nevertheless, this variety of results also indicates that a design program shall not be based on just one method. Therefore, it can be suggested to incorporate these models into an improved static analysis method for ALDOT. This improved ALDOT prediction method should consider at least three options. The first one can be based on CPT results and can be adapted from the Ruiter-Beringen method. The second alternative can be based on SPT results and can be adapted from the SPT-Meyerhof method (The Blue Book method can be considered as well). Finally, the third one can be based on the basic static analysis methods: αTomlinson, Norlund, and Thurman. The three results can be evaluated and considered according to the designer judgment.

Regarding control construction methods and according to the comparison performed, Alabama DLT method present higher reliability and almost similar efficiency to control construction methods provide by the federal publications available such us AASHTO and NCHRP 507. When comparing with other states, Alabama DLT has a higher reliability (higher resistance factors) than Arkansas, Illinois, and Iowa. However, Alabama DLT shows a slightly lower efficiency than Arkansas' methods and slightly larger than efficiency than Illinois's methods for non-redundant piles. It should be noted that even with a small data size (just 18 piles), Alabama DLT shows high reliability and acceptable efficiency. Calibrations performed for Arkansas and Illinois have larger data sizes, but they do not show as high reliability and efficiency. For a better understanding of the comparison, Figures 62 to 65 show a comparison of Alabama DLT resistance and efficiency factors with the control construction analysis methods with the highest resistance and efficiency factors found in this chapter for redundant and non-redundant piles.

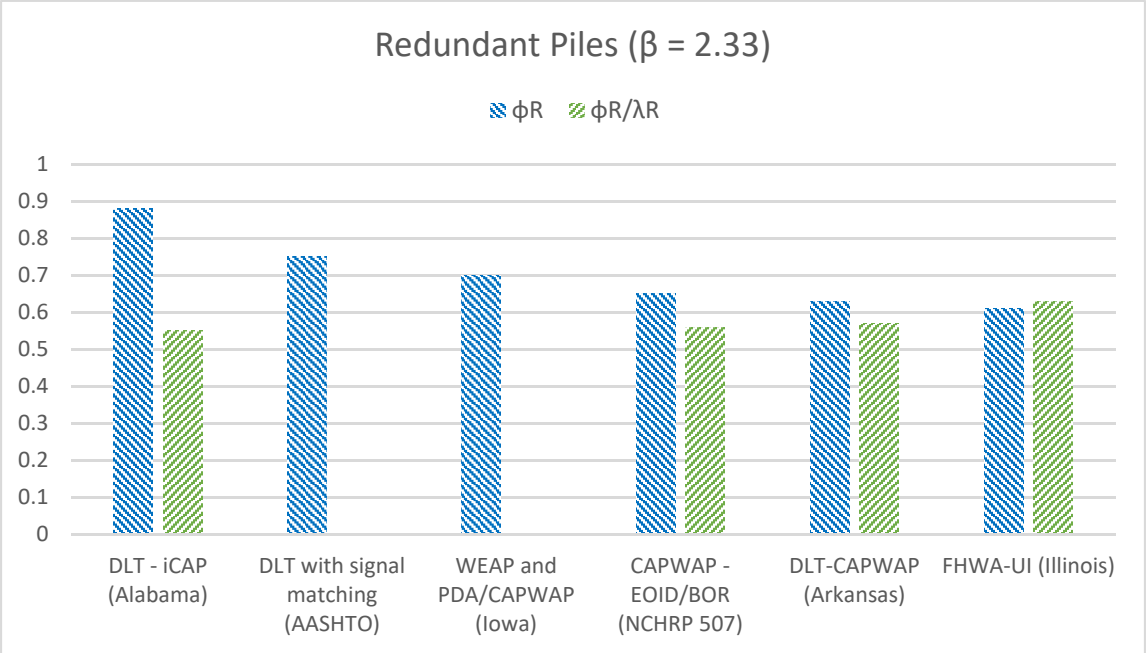

Figure 62: Control construction methods with the highest ϕ_R for redundant piles.

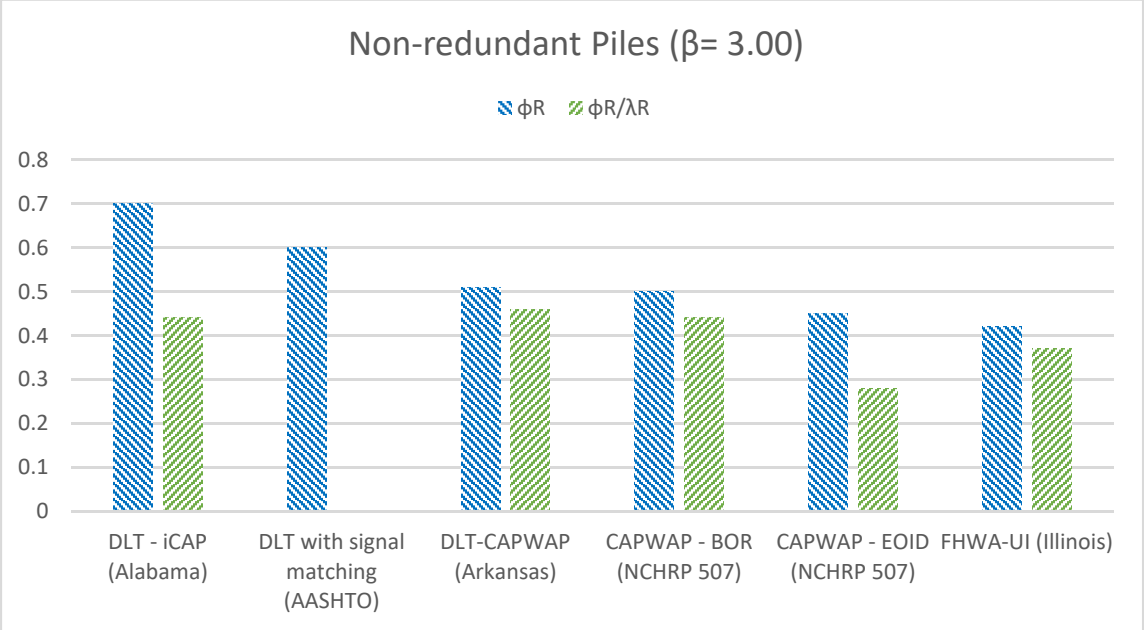

Figure 63: Control construction methods with the highest ϕ_R for non-redundant piles.

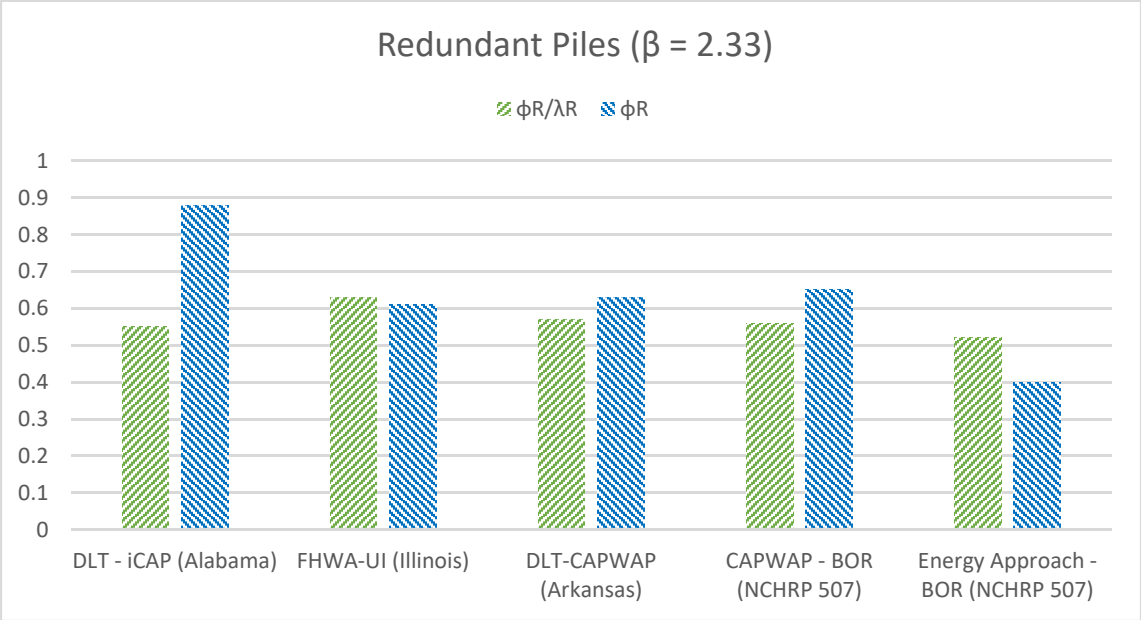

Figure 64: Control construction methods with the highest ϕ_R/λ_R for redundant piles.

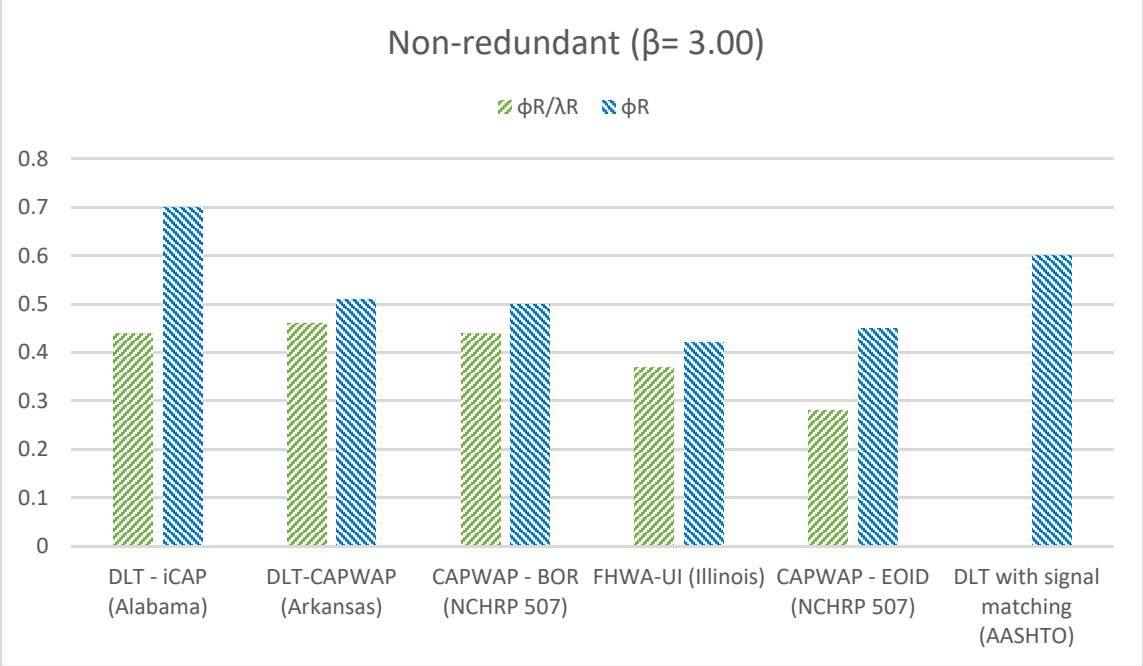

Figure 65: Control construction methods the highest to ϕ_R/λ_R for non-redundant piles.

Figures 62 and 64 show that, in regard on redundant piles, the DLT with signal matching method from AASHTO has the largest resistance factor (after Alabama DLT) and the FHWA-UI (Illinois) has the largest efficiency factor. Figures 43 and 45 show that, in regard of non-redundant piles, the DLT with signal matching method from AASHTO method has the largest resistance factor (after Alabama DLT), and the DLT with iCAP method presents the largest efficiency factors. These results indicate that DLT with signal matching is reliable and efficient control method for soils of Alabama and other states.

To put it briefly, the static analysis methods and the control construction method used by the state of Alabama show very different performances when compared to federal government and other states. On one hand, on average, the Alabama's static analysis methods are not as reliable, efficient, and consistent as the external studies considered in this chapter. On the other hand, the Alabama's control construction methods are more reliable, efficient, and consistent than the external studies considered in this chapter.

CHAPTER XI - DISCUSSION OF RESULTS AND COMPARISONS

As illustrated in the previous chapter, the LRFD resistance factors calibration, setup incorporation, and the comparison of resistance factors with bibliography from the federal government and other states are complex and very sensitive to the researcher judgment. Important considerations shall be taken before, during, and after performing the LRFD calibration. Therefore, this chapter shows the discussion and clarification related with the most important controversial facts involved within the present study.

The calibration methodology in this study consists of FOSM, FORM, and MCS. The definitive resistance factors shall be consistent with just one calibration method or the average between the three methods. Factors such as conservativeness (resistance factors and efficiency factors) and rigorousness are considered to decide which calibration method to consider. In terms of conservatism, the average bias efficiency factor and average resistance factor are evaluated and compared for each data case. The calibration for WBUZPILE and DRIVEN reveals that the data case A (entire data) shows that the most conservative method is FOSM with an average bias efficiency factor of 0.25 and average resistance factor of 0.22. For the same case, the least conservative method is MC with an average bias efficiency factor of 0.28 and average resistance factor of 0.24. The data case B (data without outliers identified by boxplot method) shows that the most conservative method is FOSM with an average bias efficiency factor of 0.30 and average resistance factor of 0.25. For the same case, the least conservative method is MC with an average bias efficiency factor of 0.33 and average resistance factor of 0.28. Finally, the data case C (data without outliers identified by two standard deviations method) shows that the most conservative method is FOSM with an average bias efficiency factor of 0.33 and average resistance factor of 0.26. For the same case, the least conservative method is MC with an average bias efficiency factor of 0.37 and average resistance factor of 0.29. Moreover, the calibration for DLT reveals that the data case A shows that the most conservative method is FOSM with an average bias efficiency factor of 0.44 and average resistance factor of 0.70. For the same case, the least conservative method is MC with an average bias efficiency factor of 0.50 and average resistance factor of 0.80. The data

cases B and C show that the most conservative method is FOSM with an average bias efficiency factor of 0.51 and average resistance factor of 0.70. For the same case, the least conservative method is MC with an average bias efficiency factor of 0.59 and average resistance factor of 0.90. These results indicate that MCS generates higher, and more efficient and less conservative resistance factors. In terms of rigorousness and from the author's perspective, FORM was the most rigorous method to use. FORM can be very rigorous to implement since it involves an iterative process, normal space and real space interaction, and basic geometry interpretation. Furthermore, the random variables are interacting with each other continuously. It is suggested to use software assistance to decrease the complexity FORM. MCS can be also rigorous because it also includes iteration and normal space variables. However, it is still understandable because each random variable is simulated individually and then incorporated to the limit equation together. In addition, MCS is based on numerical simulation assisted by software because performing it by hand would be extremely difficult and time consuming. FOSM is the least rigorous since the statistical characterization values are basically replaced in a simple equation. For these reasons MCS is considered for calibration of the definitive resistance factors in this study.

The data cases generate different resistance factors. The data case A, which include all values available, shows an average resistance factor of 0.23 and an average bias efficiency factor of 0.27. The data case B, which excludes statistical outliers (more than 1.5 times IQR), produces an average resistance factor of 0.27 and an average bias efficiency factor of 0.32. The data case C, which excludes outliers more apart than two standard deviations from the mean, produces an average resistance factor of 0.28 and an average bias efficiency factor of 0.35. If a comparison is performed, the data case B presents an average resistance factor increase of 17.4 % and an average increase efficiency factor increase of 18.5% with respect of data case A results. The data case C presents an average resistance factor increase of 21.7 % and an average increase efficiency factor increase of 29.6 % with respect of data case A results. Therefore, data cases B or C generate substantial improvement and efficiency in the resistance factors. Nevertheless, as mentioned before, the data case A is the only one that can be considered

for the definitive resistance factors because the data provided by ALDOT does not present actual proof to be subjected to outlier removal according to the guide provided by Allen et al [9]. In other words, Allen et al [9] stated 6 possible reasons to exclude outliers, but the data and documentation used in this study does not show any related case. Consequently, data case A, or not removing outliers, is considered as the definitive data case.

The setup incorporation in calibration purposes produced an important increase in the resistance factors. The evaluations at 30, 45, 60, and 90 days time interval showed that the larger the time, the higher increase of resistance factors. However, in actual projects, the time plays a very important role in its economy. In other words, it is not economically efficient to wait very long in order to gain more pile setup resistance because the project will have larger costs due to other aspects. In this way, it is important that the designer and the contractor establish an approximate time at which the piles will start to receive axial loads, before developing the final design.

As previously stated, the pile setup incorporation was possible due to the Skov and Denver [1] model. Even though, the predicted resistances (used as measured resistances) were reasonable, the ideal procedure is to actually perform field tests at several time intervals. Dynamic tests using analysis software (PDA) and signal matching, such as CAPWAP or iCAP, have a reasonable price and considerable time saving compared to static load testing. Pile capacity data at and after EOID is vital for a better understanding of pile setup and for a more accurate and economic design of driven piles.

The comparison of the LRFD resistance factors calibrated in this study with the LRFD resistance factors from AASHTO, NCHRP 507, and other states, showed that WBUZPILE and DRIVEN applied in Alabama soils show consistent resistance factors with the ones listed by AASHTO, NCHRP 507, Florida, Louisiana, Iowa, and Illinois regulations and studies. Nonetheless, both programs are still not as reliable, efficient, and consistent as the average design methods used by AASHTO, NCHRP 507, Florida, Louisiana, Iowa, and Illinois regulations and studies. Apparently, the main reason of this issue the limited sample size. However, studies developed in other states, such as Louisiana and Illinois, that data have similar or smaller sample size and show higher

better reliability, efficiency and consistency. In terms of reliability, Louisiana obtained LRFD resistance factors of 0.73 and 0.49 (Redundant all piles) for the De Ruiter-Beringen method and Schmertmann method, respectively, compared with 0.28 from WBUZPILE and 0.22 from DRIVEN, using a similar data size to this study (53 piles). Moreover, Illinois obtained a LRFD resistance factor of 0.40 (redundant steel H-piles) for the Corrected K-IDOT method compared to 0.39 from WBUZPILE and 0.28 from DRIVEN, using only 26 piles as data set. In terms of efficiency, NCHRP 507 [6] reported a efficiency factor of 0.51 (redundant steel H-Piles in mixed soils) compared to 0.33 from WBUZPILE and 0.24 from DRIVEN using only 20 piles as data set. In terms of consistency, the same case (redundant steel H-Piles in mixed soils) from NCHRP 507 [6] reported a COV of only 0.39 compared to 0.56 from WBUZPILE and 0.72 from DRIVEN using only 20 piles as data set. Consequently, it is encouraged to enhance the analysis methodology used by WBUZPILE. The author suggests that this enhanced method shall be developed based on at least 3 methods. The first one shall be based on CPT results and can be adapted from the Ruiter-Beringen method. The second alternative shall be based on SPT results and can be adapted from the SPT-Meyerhof method (The Blue Book method can be considered as well). Finally, the third one shall be based on the basic static analysis methods: αTomlinson, Nordlund, and Thurman. The three results can be evaluated and considered according to the judgement of the researcher or designer.

To put it briefly, the calibration of LRFD resistance factors involves complex and highly sensitive judgement of the researcher. Therefore, some considerations can be controversial and need to be discussed and clarified. The main considerations required to perform the LRFD calibrations adequately were described in this chapter. The topics discussed involve the calibration methodologies used in this study, the data cases evaluated, setup incorporation and its effects on the LRFD calibration, the data required for an ideal pile setup evaluation, and the comparison of the calibrated LRFD resistance factors from Alabama with bibliography from the federal government and other states.

CHAPTER XII - CONCLUSIONS AND RECOMMENDATIONS

12.1 Conclusions.

The primary objective of this study was to develop LRFD resistance factors unique to Alabama soils using FOSM, FORM, and MCS, to enhance accuracy and efficiency of pile design. The evaluated resistance determination methods were WBUZPILE, DRIVEN, and DLT. The second objective is to evaluate the performance of WBUZPILE and DRIVEN for pile design according to the relationships of the predicted capacity and the measured capacity. The third objective is to evaluate the performance of the Skov and Denver model for Alabama soils. The fourth objective was to evaluate the effect of pile setup on the calibrated LRFD resistance factors. Finally, the fifth objective was to compare the calibrated resistance factors with the recommended resistance factors from published studies from the federal government and other states in terms of reliability, consistency and efficiency. However, in addition to those objectives, the effect of data cases (filtering data from outliers) on the calibration resistance factors was evaluated as well as performance of WBUZPILE and DRIVEN according to the calibration results. The conclusions obtained from these objectives and analysis are described in the following paragraphs.

According to the data provided by ALDOT and the evaluation of the performance of WBUZPILE and DRIVEN based only on predicted and measured capacities, WBUZPILE predicts a 19% higher pile capacity than DRIVEN on average. Furthermore, WBUZPILE predicts 11% higher capacity for H-piles and 3% higher capacity for concrete piles when compared to DRIVEN. Both DRIVEN and WBUZPILE are better at predicting the capacity of H-piles. Moreover, it is shown in this study that for H-piles, WBUZPILE was least accurate at predicting the pile capacity for soil type 3, where the tip was in sand, and mixed soils were along the shaft. WBUZPILE was most accurate at predicting the pile capacity for soil type 6, where the tip was embedded in clay, and sand was along the pile shaft. For concrete piles, WBUZPILE was least accurate at predicting

pile capacity for soil type 6, where the tip was embedded in clay, and mixed soils were along the pile shaft. WBUZPILE was most accurate at predicting the pile capacity for soil type 2, where the tip was in sand, and clay was along the shaft, although there are limited data points to confirm these conclusions.

According to the data provided by ALDOT, the performance of the Skov and Denver model in Alabama soils was studied in two ways. The first way consists of using the model to predict the SLT resistance based on EOID field results. The second way consisted of using the model to predict the EOID resistance based on SLT field results. The results show that, for H-piles, the Skov and Denver method performs fairly accurately in both ways. For concrete piles, the Skov and Denver method is less accurate since it over-estimates the SLT capacity by 26.3% in the first analysis direction and under-estimates the EOID capacity by 14.5% in the second analysis direction.

According to the data provided by ALDOT and the evaluation of data cases performed, the data case A (entire data) presents the most conservative case for WBUZPILE, DRIVEN, and DLT. The calibration for WBUZPILE and DRIVEN shows data case A with an average resistance factor of 0.23 and average efficiency factor 0.27. The data case B (data without outliers identified by boxplot method) shows an average resistance factor of 0.27 and an average efficiency factor of 0.32, which represents a 17% and 19% of increase from data case A results, respectively. The data case C (data without outliers identified by two standard deviations method) shows an average resistance factor of 0.28 and an average efficiency factor of 0.35, which represents a 22% and a 30% of increase from data case A results, respectively. Data cases B and C shows very similar resistance and efficiency factors. The calibration for DLT shows the data case A average resistance factor of 0.76 and average efficiency factor 0.48. Data cases B and C shows equal resistance and efficiency factors since both cases use the same data. The data case B and C show an average resistance factor of 0.85 and an average efficiency factor of 0.56, which represents a 12% and 17% of increase from data case A results, respectively.

According to the data provided by ALDOT and the setup incorporation and calibration performed, the setup incorporation into the calibration of LRFD specifications

produces higher resistance factors, hence meaningful construction cost savings. Moreover, it was observed that the setup incorporation generally generates efficiency increase and unvarying consistency. The evaluation of WBUZPILE shows a resistance factor increase of between 0% to 27% for 30 days after EOID, 6% to 31% for 45 days after EOID, 9% to 35% for 60 days after EOID, 12% to 38% for 90 days after EOID. The evaluation of DRIVEN shows a resistance factor increase of between 4% to 29% for 30 days after EOID, 4% to 29% for 45 days after EOID, 8% to 35% for 60 days after EOID, 9% to 36% for 90 days after EOID. The evaluation of DLT shows a resistance factor increase of between 6% to 10% for 30 days after EOID, 7% to 13% for 45 days after EOID, 11% to 16% for 60 days after EOID, 16% to 20% for 90 days after EOID. It should be mentioned that more field tests are necessary to perform an ideal calibration of resistance factors considering pile setup.

According to the data provided by ALDOT and the comparison of calibrated resistance factors, it is concluded that WBUZPILE applied to pile design in Alabama soils shows consistent resistance factors with the ones listed by AASHTO, NCHRP 507, Florida, Louisiana, Iowa, and Illinois regulations and studies. Nonetheless, WBUZPILE is still not as reliable, efficient, and consistent as the average design methods listed in the compared bibliography. In case of general piles, it underestimates the actual resistance by 2%. In case of steel H-Piles, it overestimates the actual resistance by 18%. In case of concrete piles, it underestimates the actual resistance by 44%. In terms of consistency, WBUZPILE generates relatively large COV values (0.486 or larger). For these reasons, WBUZPILE produces resistance factors between 0.17 and 0.39.

According to the data provided by ALDOT and the comparison of calibrated resistance factors performed, it is concluded that DRIVEN applied to pile design in Alabama Soils shows consistent resistance factors with the ones listed by AASHTO, NCHRP 507, Florida, Louisiana, Iowa, and Illinois regulations and studies. Nonetheless, DRIVEN is still not as reliable, efficient, and consistent as the average design methods listed in the compared bibliography. In case of general piles, it overestimates the actual resistance by 5%. In case of steel H-Piles, it overestimates the actual resistance by 23%. In case of concrete piles, it underestimates the actual resistance by 34%. In terms of

consistency, DRIVEN generates large COV values (0.527 or larger). For these reasons, DRIVEN produces resistance factors between 0.15 and 0.28.

According to the data provided by ALDOT and the analysis performed, it is concluded that WBUZPILE is slightly more efficient and consistent than DRIVEN for general piles and steel H-piles. However, DRIVEN is slightly more efficient and consistent than WBUZPILE for concrete piles.

According to the data provided by ALDOT and the analysis performed, it is concluded that DLT applied to pile design in Alabama soils shows consistent resistance factors with AASHTO, FHWA, and other states. Furthermore, DLT is still more reliable, efficient, and consistent as the average design methods used by AASHTO, FHWA, and other states. DLT tends to underestimate the actual resistance by 38%. In terms of consistency, DLT generates a relatively small COV value (0.352). For these reasons, DLT produces resistance factors between 0.70 and 0.88.

According to the data provided by ALDOT and the calibration performed, it is concluded to consider the results of the Monte Carlo calibration method and the data case A, which includes all data available, as the definitive resistance factors. The final recommended resistance factors for WBUZPILE, DRIVEN, and dynamic load testing are shown in Table 49. The resistance factors from AASHTO specifications [37] are also listed in Table 49 to show whether this study calibrated higher or lower resistance factors.

Table 49: Recommended resistance factors for driven piles

Condition	Pile type	Resistance Determination or Construction control method	Resistance factor ϕR	ϕR from AASHTO (2014)
Nominal axial bearing resistance of non-redundant pile (4 piles or less)	All piles	WBUZPILE	**0.19**	0.71*
		DRIVEN	**0.14**	0.36 or 0.28
		PDA/iCAP	**0.70**	0.60
	Steel H-piles	WBUZPILE	**0.26**	0.71*
		DRIVEN	**0.20**	0.36 or 0.28
		PDA/iCAP	**0.70**	0.60
	Concrete piles	WBUZPILE	**0.17**	0.71*
		DRIVEN	**0.23**	0.36 or 0.28
		PDA/iCAP	**0.70**	0.60
Nominal axial bearing resistance of redundant pile (5 piles or more)	All piles	WBUZPILE	**0.28**	0.71*
		DRIVEN	**0.22**	0.45 or 0.35
		PDA/iCAP	**0.88**	0.75
	Steel H-piles	WBUZPILE	**0.39**	0.71*
		DRIVEN	**0.28**	0.45 or 0.35
		PDA/iCAP	**0.88**	0.75
	Concrete piles	WBUZPILE	**0.17**	0.71*
		DRIVEN	**0.25**	0.45 or 0.35
		PDA/iCAP	**0.88**	0.75

* = Obtained by fitting Factor of Safety (ASD).

12.2 Recommendations.

As shown in the conclusions chapter, several meaningful information and facts are provided by this study. However, this study also revealed that the LRFD calibration for driven piles in Alabama soils can be enhanced in the future by applying novel concepts and enlarge the data set available. Thus, this section describes some recommendations for future research as well as recommendations for the University of South Alabama and ALDOT.

12.2.1 Recommendation for future research.

This section provides three recommendations to improve the results from future research related to LRFD calibration within geotechnical engineering.

First, it is recommended that if more pile tests are available, the calibration can be performed more specifically to calibrate higher resistance factors. In other words, the piles can be categorized by shaft soil type, toe soil type, length, material, and geologic zones. This categorization would reduce the effect of external variables not considered and, hence reduce the COV of the samples and increase the resistance factors.

Second, it is recommended to incorporate the concept of lower-bound capacities for future calibration purposes. According to Reddy and Stuedlein [45], for piles in compression, the consideration of lower-bound limit results in a 20%-150% increase in the calibrated resistance factors and would represent a substantial increase in usable pile capacity.

Third, it is recommended to incorporate the concept of The Bayesian Update in case of new pile load test information arrives. As mentioned by Jabo [49], the implementation of The Bayesian Theorem makes the new information more valuable in the process of coupling new and existing data than just feeding a new entry into the database. In this way, new high-quality data and the Bayesian update are capable of generating higher resistance factors.

12.2.2 Recommendations for ALDOT and The University of South Alabama.

This section provides four recommendations for the University of South Alabama and ALDOT with the objective of establishing better sources, data, and tools for engineers and researchers concerned about LRFD calibration for Alabama soils.

First, it is recommended to test a larger number of piles in Alabama. More data available is necessary to generate more accurate models to predict the ultimate pile resistance. It was shown than the COV of the resistance bias values has a strong impact on the final resistance factor. In this way, in general, an effective way to reduce COV is by increasing the size of the sample.

Second, it is recommended to perform more field tests after EOID at standard intervals of time. In this way, pile setup can be better evaluated and produce higher resistance factors. This paper incorporated pile setup using the model from Skov and Denver [1] and Haque and Steward [29] for calculating the measured resistance at 30, 60, and 90 days. However, the ideal way would be to have actual measured data from restrike tests.

Third, it is recommended to establish a database system for piles in Alabama. The number and availability of pile information and test results can have a significant positive impact on the calibration of resistance factors. Experiences such as PILOT in Iowa, represent a useful tool for the federal and local governments, universities, and researchers.

Fourth, it is encouraged to enhance the analysis methodology used by WBUZPILE. The comparison chapter demonstrates that the current data size from ALDOT is capable of generating a prediction method as reliable, efficient, and consistent as the methods listed by AASHTO, NCHRP 507, Florida, Louisiana, Iowa, and Illinois regulations and studies. The author suggests that this enhanced method shall be developed based on at least 3 methods. The first one shall be based on CPT results and can be adapted from the Ruiter-Beringen method. The second alternative shall be based on SPT results and can be adapted from the SPT-Meyerhof method (The Blue Book method can be considered as well). Finally, the third one shall be based on the basic static analysis methods: αTomlinson, Nordlund, and Thurman. The three results can be evaluated and considered according to the judgment and experience of the researcher or designer.

REFERENCES

[1] R. Skov and H. Denver, "Time-dependence of bearing capacity of piles," BiTech Publishers, Vancouver, Canada, 1988.

[2] B. J. Pement, "Evaluation of WBUZPILE design methodology and the development of a LRFD driven pile resistance factor for Alabama soils," The University of South Alabama, Mobile, 2017.

[3] R. Luna, "Evaluation of Pile Load Tests for use in Missouri LRFD Guidelines," Missouri Department of transportation, Jefferson City, 2014.

[4] J. DiMaggio, T. Saad, T. Allen, R. Barry, Al Dimillio, G. Goble , P. Passe, T. Shike and G. Person, "FHWA International Technology Exchange Program, report number FHWA-PL-99-013," FHWA, 1999.

[5] E. D. Prado Villegas., "Development of LRFD driven pile resistance factor by first order second moment method in Alabama soils," University of South Alabama, Mobile, AL, 2015.

[6] S. G. Paikowsky, B. Birgisson, M. McVay, T. Nguyen, C. Kuo, G. Beacher, B. Ayyub, K. Stenersen, K. O'Malley, L. Chernauskas and M. O'Neill, Load and Resistance Factor Design (LFRD) for deep foundations - NCHRP report 507, Washington D.C.: Transportation Research Board of The National Academies, 2004.

[7] M. A. Styler, "Development and implementation of the Diggs format to perform LRFD resistance factor calibration of driven concrete piles in Florida," University of Florida, Florida, 2006.

[8] M. N. Haque and Abu-Farsakh, "Estimation of Pile Setup and Incorporation of resistance factor in Load Resistance Factor Design Framework," ASCE, 2018.

[9] T. M. Allen, S. A. Nowak and R. J. Bathurst, "Calibration to Determine Load and Resistance factors for Geotechnical and Structural Design," Transport Research Board, Washington D.C., 2005.

[10] A. Vesic, Design of Pile Foundations, Washington D.C.: Transportation Research Board, 1977.

[11] Federal Highway Administration, "Design and Construction of Driven Pile Foundations - Lesson learned on the Central Artery/Tunnel Project," Georgetown Pike, 2006.

[12] Federal Highway Administration, Geotechnical Engineering Circular No. 12 - Volume I: Design and Construction of Driven Pile Foundations, Washington DC: National Higghway Institute/ U.S. Department of Transportation, July, 2016.

[13] American Association of State Highwat and Transportation Officials (AASHTO), AASHTO LRFD Bridge Design Specifications, US Customary Units, Seventh Edition, with 2015 Interim Revisions., Washington D.C.: American Association of State Highwat and Transportation Officials, 2014.

[14] M. Ashour, A. Helal and H. Ardalan, "Upgrade of Axially Loaded Pile-Soul Modeling with the implementation of LRFD Design procedure," University of Alabama, Huntsville, Huntsville, 2012.

[15] F. H. Kulhawy and P. W. Mayne, Manual on estimating soil properties for foundation design. Rpt. EL-6800, Palo Alto, CA: Electric Power Res. Inst., 1990.

[16] A. Caquot and J. Kerisel, Tables for the calculation of passive pressure, Active pressure and bearing capacity of foundations, Paris: Gauthier-Villars, 1948.

[17] A. Caquot and J. Kerisel, "Tables for the calculationof passive pressure, Active pressure and bearing capacitu of foundations," Gauther-Villars, Paris, 1948.

[18] M. W. O'Neill and L. C. Reese, "Drilled shafts: Construction Procedures and Design Methods, Publication FHWA-IF-99-025," FHWA, Washington D.C., 1999.

[19] P. J. Hannigan, F. Rausche, G. Likins, B. Robinson and M. Becker, Design and Construction of Driven Pile Foundations - Volumes I and II, Washington D.C.: Federal Highway Administration, 2016.

[20] E. J. Steward, J. Cleary, A. Gillis, R. Jones and E. Prado, "Investigation of Pile Setup (Freeze) in Alabama. Development of a Setup Prediction Method and Implementation into LRFD Driven Pile Design," University of South Alabama, Mobile, AL, 2015.

[21] Federal Highway Administration, "Load and Resistance Factor Design (LRFD) for HIghway Bridge Substructures," U.S. Department of transportation, 2001.

[22] S. S. AbdelSalam, S. Sritharan, M. T. Suleiman and M. Roling, "Development of LRFD Procedures for Bridge Pile Foundations in Iowa - Volume III: Recommended Resistance Factors with Consideration of Construction Control and Setup," Iowa State University, Ames, IA, 2012.

[23] Federal Highway Administration, "Geotechnical Engineering Circular No. 12 - Volume II: Design and Construction of Driven Pile Foundations," Washington DC, National Higghway Institute/ U.S. Department of Transportation, July, 2016.

[24] Alabama Department of Transportation, "Standard Specifications for Highway Construction," Alabama Department of Transportation, Montgomery, 2002.

[25] ASTM D1143-07, "Standard Test Methods for Deep Foundations Under Static Axial Compressive Load. Book of ASTM Standards," ASTM International, West Conshohocken,, 2014.

[26] D. P. Coduto, Foundation Design: Principles and Practices, Englewood Cliffs, NJ: Prentice-Hall Inc., 2001.

[27] E. A. Smith, "Pile-Driving Analysis by the Wave Equation, Journal of the Soil Mechanics and Foundation Division," ASCE, 1962.

[28] G. Likins, L. Liang and T. Hyatt, "Development of Automatic Signal Matching Procedure - iCAP," Proceedings from Testin and Design Methods for Deep Foundations, 2012.

[29] M. N. Haque and E. J. Steward, "Evaluation of Pile Setup Phenomenon for Driven Piles in Alabama," ALDOT and University of South Alabama, 2019.

[30] F. Rausche, G. Likins and H. Hussein M, "Analysis of post-installation dynamic load test data for capacity evaluation of deep foundations," Proc. from Research In Practice in Geotechnical Engineering (Geo-Concgres 2008), Lousiana, 2008.

[31] M. C. McVay, L. B. Birgisson, L. Zhang, A. Perez and S. Putcha , "Load and resistance factor desifn (LRFD) for driven piles using dynamic methods-A Florida Perspective," Geotechnial Testing Journal, 2000, 2000.

[32] J. H. Schmertmann, "The mechanical aging of soils," J. Geotech. Engineering Vol. 117 (9) pp. 1288-1330, 1991.

[33] L. Yang and R. Liang, "Incorporating setup into reliability-based design of driven piles in clay," Can. Geotech. Journal 43 (9): pp 946-955, 2006.

[34] AASHTO, "LRFD bridge design specifications, 3rd ed.," AASHTO, Washington D.C., 2004.

[35] M. Revell, «ALDOT Pile Design,» 2016.

[36] A. S. Nowak and K. R. Collins, Reliability of Structures, Second Edition, Boca raton: CRC Press, 2007.

[37] S. Songwon, "A Review and Comparison of Methods for Detecting Outliers in Univariate Data Sets," University of Pittsburgh, Pittsburgh, 2006.

[38] AASHTO, "LRFD Bridge Design Specifications (7th edition)," American Association of State Highway and Transporation Officials, Washington D.C., 2014.

[39] L. B. Scott and R. Salgado, "Evaluation of load factors for use in geotechnical design. Journal of Geotechnial and Geoenvironmental Engineering," ASCE, 2003.

[40] E. Rosenblueth and L. Esteva, "Reliability Bases for some Mexican Codes. ACI Publication SP-31," American Concrete Institute, Detroit, MI, 1972.

[41] D. A. Bostwick, "Calibration of Resistance Factos for Driven Piles using Static and Dynamic Test," University of Arkansas, Fayetteville, 2014.

[42] R. C. Patev, "Risk Technology Workshop: Engineering Reliability Concepts, Introduction to Engineering Reliability," United States Army Corps of Engineers, 2010.

[43] C. A. Cornell, "Structural safety specifications based on secondmoment reliability," Symposium Int. Association Bridges and Structural Engineering, London, 1969.

[44] N. C. Lind, "Consistent partial safety factors," Journal of Structural Engineering, 1971.

[45] K.-K. Phoon, F. H. Kulhawy and M. D. Grigoriu, "Development of a Reliability-Based Design Framework for Transmission Line Structure Foundations," Journal of Geotechnical and Geoenvironmental Engineering, ASCE, 2003.

[46] S. C. Reddy and A. W. Stuedlein, "Ultimate limit state reliability-based design of augered cast-in-place piles considering lower-bound capacities," Canadian Geotechnical Journa, NCR Research Press, 2017.

[47] AASHTO, "LRFD bridge design specifications, 3rd edition.," American Association of State Highway and Transportation Officials (AASHTO), Washington D.C., 2007.

[48] R. J. Bathurst, B. Q. Huang and T. M. Allen, "LRFD Calibration of steel reinforced soil walls," In Proceedings of Geo-Frontiers 2011, 2011.

[49] A. W. Stuedlein, W. J. Neely and T. M. Gurtowski, "Reliabilty-based design of augered cast-in-place in granular soils.," Journal of Geotechnical and Geoenvironmental Engineering., 2012.

[50] J. Jabo, "Reliability-Basd Design and Acceptance Protocol for Driven Piles," University of Arkansas, Arkansas, May, 2014.

[51] M. C. McVay, V. Alvarez, L. Zhang, A. Perez and A. Gibsen, "Estimating driven pile capacities during construction," 2002.

[52] S. AbdelSalam, S. Sritharan and M. Suleiman, "Current Design and Construction Practices of Bridge Pile Foundations with Emphasis on implementation of LRFD. Journal of Bridge Engineering 2010 15(6): 749-758," American Society of Civil Engineers, 2010.

[53] International Code Council, Florida Building Code - Building, Sixth edition, ICC, 2017.

[54] Lousiana State Governing Body, Building Code 2015 of Lousiana, IBC, 2015.

[55] M. Y. Abu-Farsakh, "Calibration of Resistance Factors needed in the LRFD Design of Driven Piles," Louisiana Transportation Research Center, 2009.

[56] Iowa DOT - Office of Bridges and Structures, LRFD Bridge Design Manual, Iowa DOT.

[57] International Building Council, Building Code 2018 of Illinois, IBC, 2018.

[58] J. H. Long, J. Hendrix and A. Baratta, "Evaluation/Modification od IDOT Foundation Piling Design and Construction Policy," Illinois Department of Transportation, Urbana, IL, 209.

[59] International Building Council, Arkansas Fire Prevention Code Vol II Building, IBC, 2012.